

Comparison of the Cox proportional hazards model and Random Survival Forest algorithm for predicting patient-specific survival probabilities in clinical trial data

Ricarda Graf^{1*}, Susan Todd² and M. Fazil Baksh²

¹Institute of Mathematics, University of Augsburg, Augsburg, 86159, Germany.

²Department of Mathematics and Statistics, University of Reading, Reading, RG6 6AX, UK.

*Corresponding author(s). E-mail(s): ricarda.graf@math.uni-augsburg.de;
Contributing authors: s.c.todd@reading.ac.uk; m.f.baksh@reading.ac.uk;

Abstract

The Cox proportional hazards model is often used for model development in data from randomized controlled trials (RCT) with time-to-event outcomes. Random survival forests (RSF) is a machine-learning algorithm known for its high predictive performance. We conduct a comprehensive neutral comparison study to compare the predictive performance of Cox regression and RSF in real-world as well as simulated data. Performance is compared using multiple performance measures according to recommendations for the comparison of prognostic prediction models. We found that while the RSF usually outperforms the Cox model when using the C index, Cox model predictions may be better calibrated. With respect to overall performance, the Cox model often exceeds the RSF in nonproportional hazards settings, while otherwise the RSF typically performs better especially for smaller sample sizes. Overall performance of the RSF is more affected by higher censoring rates, while overall performance of the Cox model suffers more from smaller sample sizes.

Keywords: Cox regression, Machine-learning prediction, Proportional hazards, Random survival forest, Randomized controlled trials, Simulation study, Survival analysis

1 Introduction

Prognostic prediction models (also clinical prediction models, or risk scores) are used to estimate an individual's probability based on multiple risk factors that a disease or outcome will occur in a specific period of time. They are most often used at time of diagnosis or start of treatment to support physicians in early detection, diagnosis, treatment decision, and prognosis, and to inform patients about their risks (Moons et al., 2012). They are applied in the medical field in general, and in particular in the field of cancer treatment and research, the field of diabetes and the cardiovascular field (Moons et al., 2012; Goldstein et al., 2017). Clinical decision tools such as “ClinicalPath” (Elsevier, 2022) for cancer treatment or the Framingham Risk Score (Wilson et al., 1998) for coronary heart disease, are examples of prognostic prediction models.

Cox regression (Cox, 1972) is most widely used for developing prognostic models in medical time-to-event data (Goldstein et al., 2017; Collins et al., 2011, 2014; Mahar et al., 2017; Mallett et al., 2010; Steyerberg et al., 2013; Wynants et al., 2019; Phung et al., 2019; Hueting

et al., 2022). These models are based on, among others, patient and disease characteristics, laboratory measurements, and medical tests to estimate an individual's risk of experiencing the outcome. Cox regression provides estimates of the hazard ratios for each explanatory variable. In the context of clinical trials, the treatment effect hazard ratio is of particular interest, i.e. the relative likelihood of the outcome in patients receiving a specific treatment compared to a control (Mallett et al., 2010). As a semi-parametric model, it is assumed that at least 10 events have to be observed per predictor variable included in the Cox model to obtain reasonable results (Peduzzi et al., 1995; Vittinghoff and McCulloch, 2006), so it cannot be used in high-dimensional settings with a large number of potential predictor variables compared to the number of individuals. During model development, researchers often have to decide on a fraction of available predictors to be included in the final model (Moons et al., 2012). Even if there are many potential uncorrelated candidate variables, a decision for a limited set has to be made. Cox regression requires prespecification of a model, including possible (higher order) interaction terms and variable transformations in case of nonlinear relationships of continuous covariates with the survival outcome. Moreover, it makes the assumption of proportional hazards which means that it assumes the hazard ratio of any two patients to be constant over the period of follow-up. In cases where the new treatment only shows an advantage at an early or later stage, respectively, interpretation of its results may not be meaningful. Especially in long-term studies, this assumption may be violated (Hilsenbeck et al., 1998). On the other hand, the Cox model provides corresponding measures of uncertainty (confidence intervals for the hazard ratios), which generally form the basis for clinical decision making, is easy to use and has short computational times. When using the Cox model for predictions, the specification of a baseline survival distribution is required (Therneau and Grambsch, 2000). In comparison, the Random survival forest (RSF) algorithm (Ishwaran et al., 2008) is a nonparametric machine-learning approach. It is suitable for the same variable types as the Cox model, i.e. continuous right-censored survival time outcomes and continuous as well as categorical predictor variables. In contrast, it does not require an explicit specification of a model but is able to detect and incorporate even complex interactions between the covariates and the survival outcome as well as nonlinear relationships. It is also suitable for a large number of covariates, although it is advisable not to include variables that are already suspected not to be meaningful in order to not unnecessarily increase computational complexity. It also seems suitable for dependent censoring (Zhou and Mcardle, 2015). Moreover, it does not require the proportional hazard assumption. However, since the RSF does not make parametric assumptions regarding the data, it also does not provide uncertainty measures such as confidence intervals for its estimates which are important for the analysis of clinical trial data. Machine-learning methods such as random forests have proven to increase predictive accuracy in prognostic studies (Murmu and Györfy, 2024), especially in high-dimensional data such as genetic, protein or imaging biomarkers (Cohen et al., 2018; Zhang et al., 2020; Kawakami et al., 2019; Lin et al., 2022; Ruyssinck et al., 2016). For example, a prognostic model for glioblastoma widely used for more than two decades and most recently adapted to incorporate further relevant covariates (Bell et al., 2017), is based on a survival tree method. The RSF may help predicting patient outcomes and survival rates more accurately. Therefore the current work aims to explore the potential application of the RSF to data from randomized controlled trials (RCT) by comparing its predictive performance to the Cox proportional hazards (Cox-PH) model.

Previous studies compared the performance of Cox regression and RSF in observational clinical data, more specifically real-world datasets (e.g. Guo et al., 2023; Sarica et al., 2023; Chowdhury et al., 2023; Moncada-Torres et al., 2021; Farhadian et al., 2021; Miao et al., 2015; Spooner et al., 2020; Qiu et al., 2020; Kim et al., 2019; Datema et al., 2012; Omurlu et al., 2009; Du et al., 2020). The predominantly used performance measure in these studies is Harrell's C index (Harrell et al., 1982, 1996), a rank-based measure of discrimination, used in combination with cross-validation. Very rarely, calibration, or overall performance are assessed. Only the study by Du et al. (2020) considered all three types of performance measures. In their systematic review and meta-analysis of 52 studies predicting hypertension, Chowdhury et al. (2022) compared the performance of regression approaches (including Cox regression) and various machine-learning methods (RSF was not applied in any of the studies). These authors too found that performance comparison based on the C index was common in contrast to comparisons based on calibration. Most of the above mentioned studies aiming

to compare the performance of the Cox and RSF model stated an at least slightly better performance of the RSF model with respect to the C index.

To the best of our knowledge, only one study compared the two approaches (among other approaches) based on data simulations (Baralou et al., 2022). In the particularly extensive simulation study by Baralou et al. (2022), the reference data is taken from an observational study. Apart from simulating data with different characteristics, another difference to most of the before-mentioned studies is, that their comparison is not only based on the default log-rank splitting rule for the RSF, but includes two further splitting rules. Moreover, they compare the approaches based on a measure of discrimination (time-dependent area under the curve, AUC) as well as a measure of overall performance (Integrated Brier score, IBS (Graf et al., 1999)). Most notably, they found that the RSF outperformed the Cox-PH model in scenarios with lower censoring rates in the presence of covariate interactions. However, they do not examine the performance for data from randomized controlled trials (including factors specific to RCTs such as different sizes of treatment effect, the absence/presence of treatment-covariate interactions, and smaller sample sizes less than 500), the influence of violation of the proportional hazard assumption, other splitting rules available for the RSF, and measures of calibration.

The TRIPOD (Transparent Reporting of a multivariable prediction model for Individual Prognosis or Diagnosis) recommendations (Moons et al., 2015) state that prognostic models should be compared with respect to discrimination (e.g. Harrell’s C index, time-dependent AUC for time-to-event data), calibration, and overall performance (e.g. Integrated Brier score). These three aspects of model performance are also described in Steyerberg et al. (2010) and McLernon et al. (2023), for example. In this paper, we will use Harrell’s C index, calibration curves, and the Integrated Brier score, which will be described in Section 2.3.

Responsible integration of machine learning algorithms in any step of a clinical trial may help overcome some of the challenges in its design, conduct, and analysis, e.g. with respect to patient recruitment, or the planning of treatment interventions (Miller et al., 2023; Weissler et al., 2021). Evidence is needed where machine learning algorithms can be applied in order to gain an advantage such as more precise predictions free from parametric assumptions on the data structure. To the best of our knowledge, this is the first simulation study comparing the performance of the Cox-PH and RSF model for clinical trial settings. The aim of this paper is to evaluate the predictive accuracy of both methods, the Cox regression model and the RSF algorithm, in predicting patient-specific survival probabilities in right-censored clinical trial data. We considered two possible scenarios, where treatment-covariate interactions in the data are either absent or present. For this purpose, two publicly available clinical trial datasets (University of Massachusetts, 1980; Byar and Green, 1980) without and with known treatment-covariate interactions serve as a reference for data simulations. In contrast to previous studies, we compared the performance of all six RSF splitting rules (currently available in the most commonly used R packages `randomForestSRC` (Ishwaran and Kogalur, 2023) and `ranger` (Wright et al., 2023)), and based the evaluation on measures of discrimination, calibration, and overall performance for a more detailed comparison. Values for censoring rate, sample sizes, and size of treatment effect are varied.

2 Materials and methods

2.1 Reference datasets

Two clinical trial datasets serve as a reference for data simulations, where one dataset does not have any known treatment-covariate interactions (Section 2.1.1), and the other comprises multiple treatment-covariate interactions (Section 2.1.2). More details are given in the following sections.

2.1.1 Data without treatment-covariate interactions: Randomized Controlled Trial (RCT) in primary biliary cirrhosis

An RCT conducted by the Mayo Clinic between 1974 and 1984 (University of Massachusetts, 1980) investigates the effect of D-penicillamine on survival times in 312 patients with primary biliary cirrhosis (PBC), with time to the occurrence of death, or liver transplantation, respectively, as the event of interest. A total of 16 prognostic factors were recorded of which ten were

continuous and six were categorical variables. The median follow-up time is about five years. Table 1a shows more detailed summary statistics. We replaced missing values in three of the continuous covariates by their column means, i.e. incomplete data are included for estimating the correlation structure and fitting univariate parametric distributions to the data.

	Median	Mean (SE)	Minimum	Maximum	# missing values
Survival time					
Time of follow-up [Days]	1839.5	2006.4 (1123.3)	41	4556	–
Continuous prognostic factors					
Age [Years]	49.8	50 (10.6)	26.3	78.4	–
Serum bilirubin [mg/dl]	1.4	3.3 (4.5)	0.3	28	–
Serum cholesterol [mg/dl]	322	369.6 (221.3)	120	1775	–
Albumin [gm/dl]	3.5	3.5 (0.4)	2	4.6	–
Urine copper [mg/day]	73	97.6 (85.6)	4	588	2
Alkaline phosphatase [U/liter]	1259	1982.7 (2140.4)	289	13862.4	–
Aspartate aminotransferase - SGOT [U/ml]	114.7	122.6 (56.7)	26.4	457.2	–
Triglycerides [mg/dl]	108	124.7 (65.1)	33	598	30
Platelet count [# platelets per $m^3/1000$]	257	261.9 (95.6)	62	563	4
Prothrombin time [sec]	10.6	10.7 (1)	9	17.1	–
			Levels		# missing values
Event indicator, treatment code					
Event indicator [0: censored, 1: death]	0: 59.9%	1: 40.1%			–
Treatment code [1: DPA, 2: placebo]	1: 50.6%	2: 49.4%			–
Categorical prognostic factors					
Sex [0: male, 1: female]	0: 11.5%	1: 88.5%			–
Presence of ascites [0: no, 1: yes]	0: 92.3%	1: 0.07%			–
Presence of hepatomegaly [0: no, 1: yes]	0: 48.7%	1: 51.3%			–
Presence of spiders [0: no, 1: yes]	0: 71.2%	1: 28.8%			–
Presence of edema ¹⁾	0: 84.3%	0.5: 9.3%	1: 6.4%		–
Histologic state of disease [grade]	1: 5.1%	2: 21.5%	3: 38.5%	4: 34.9%	–

Table 1a: Randomized controlled trial in primary biliary cirrhosis: summary statistics of baseline measurements in 312 patients in the study conducted by the Mayo Clinic.

¹⁾ 0 = no edema and no diuretic therapy for edema; 0.5 = edema present for which no diuretic therapy was given or edema resolved with diuretic therapy; 1 = edema despite diuretic therapy.

Abbreviations: DPA - D-penicillamine, SGOT - serum glutamic-oxaloacetic transaminase

Performance comparison of the Cox model to a non-parametric alternative such as the RSF is motivated by the violation of the proportional hazard assumption in some datasets on which Cox regression is based. For instance, in this RCT dataset, the overall assumption of proportional hazards would be violated ($\chi^2 = 20.86$, $df = 8$, $p = 0.0075$, test by Grambsch and Therneau (Grambsch and Therneau, 1994) implemented in the function `cox.zph` from the R package `survival` (Therneau and Lumley, 2024) after variable selection based on findings in the literature and the statistical measures AIC (Akaike information criterion) and BIC (Bayesian information criterion), an approach a researcher examining these data would typically follow. Model selection was done as follows: in the literature, the GLOBE score (Lammers et al., 2015), the Mayo score (Dickson et al., 1989), and the UK-PBC score (Carbone et al., 2015) are suggested as prognostic risk scores for prediction of survival in patients with primary biliary cirrhosis (Goet et al., 2021). According to these, the variables age, bilirubin, alkaline phosphatase, platelet count, and prothrombin time are relevant and were therefore included in the model. The histologic stage of disease has also been determined as a relevant factor (Scheuer, 1989) and is therefore included. Other available variables were dropped from the analysis. More specifically, urine copper levels in patients suffering from primary biliary cirrhosis were usually within a normal range (Carey, 1980; Salaspuro et al., 1981). In addition, aspartase aminotransferase (AST)/SGOT is not a disease-specific indicator because values may be increased in patients with cirrhosis in general (Sebastiani and Alberti, 2006), and found to be normal or only modestly increased in other studies in primary biliary cirrhosis patients (Zhang et al., 2002; Nguyen et al., 2014; Poupon, 1991). Models fulfilling the before mentioned conditions

were then compared based on AIC and BIC. The final dataset, in which the proportional hazards assumption was tested, consequently included the variables age, serum bilirubin, albumin, alkaline phosphatase, platelet count, prothrombin time, and histologic stage of disease.

2.1.2 Data with treatment-covariate interactions: Randomized Controlled Trial (RCT) in prostate cancer patients

The second dataset considered comprises 474 patients with advanced prostate cancer for whom complete data are available in the RCT examining the effect of the synthetic oestrogen drug diethyl stilboestrol on survival time. The placebo group comprises patients receiving either placebo or the lowest dose level, the treatment group comprises patients receiving one of two higher dose levels (Byar and Green, 1980). Table 1b gives an overview of the data structure. For data simulations, we removed the binary variable cancer stage due to multicollinearity. Based on findings in the literature (Byar and Green, 1980; Royston and Sauerbrei, 2004), we included relevant interaction terms between treatment and the variables age, presence of bone metastases, and serum acid phosphatase, respectively. Again, in a model comprising all main effects and these three interaction terms, for example, the proportional hazard assumption would not be fulfilled ($\chi^2 = 22.2$, $df = 12$, $p = 0.0355$, test by Grambsch and Therneau (Grambsch and Therneau, 1994)), therefore comparing the performance of the Cox-PH model to a model not based on this assumption such as the RSF may be interesting.

	Median	Mean (SE)	Minimum	Maximum	# missing values
Survival time					
Time of follow-up	33.5	36.3 (23.2)	0.5	76.5	–
Continuous prognostic factors					
Age [Years]	73	71.6 (6.9)	48	89	–
Standardized weight	98	99 (13.3)	69	152	–
Systolic blood pressure	14	14.4 (2.4)	8	30	–
Diastolic blood pressure	8	8.2 (1.5)	4	18	–
Size of primary tumour [cm ²]	10	14.3 (12.2)	0	69	–
Serum (prostatic) acid phosphatase [King Armstrong units]	7	125.7 (638.5)	1	9999	–
Haemoglobin [g/100 ml]	137	134.2 (19.4)	59	182	–
Gleason stage-grade category [mg/dl]	10	10.3 (2)	5	15	–
	Levels				# missing values
Event indicator, treatment code					
Event indicator [0: censored, 1: death]	0: 28.8%	1: 71.2%	–		
Treatment code [0: lowest dose of diethyl stilboestrol (placebo), 1: higher doses]	0: 49.9%	1: 50.1%	–		
Binary prognostic factors					
Performance status	0: 90.1%	1: 9.9%	–		
History of cardiovascular disease [0: no, 1: yes]	0: 56.6%	1: 43.4%	–		
Presence of bone metastases [0: no, 1: yes]	0: 83.8%	1: 16.2%	–		
Abnormal electrocardiogram [0: normal, 1: abnormal]	0: 34.1%	1: 65.9%	–		

Table 1b: Randomized controlled trial in prostate cancer patients: summary statistics of baseline measurements in 474 patients in the prostate cancer dataset.

2.2 Methods for performance comparison

Methods were first compared using the bootstrap technique by Wahl et al. (2016) which is based on the work by Jiang et al. (2008), an internal validation technique based on the real data. It uses bootstrap samples to obtain point estimates of the performance measures and corresponding CIs. It is described in Section 2.2.1. A second approach then uses data simulations. Simulations facilitate manipulations of properties of the data but at the same time require specification of data-generating mechanisms, i.e. underlying parametric distributions for variables are assumed. The approach is described in Section 2.2.2.

2 .2.1 Comparison in real-world data: nonparametric bootstrap approach

The nonparametric bootstrap approach for point estimates by Wahl et al. (2016) is an extension of the algorithm by Jiang et al. (2008) and based on the .632+ bootstrap method (Efron and Tibshirani, 1997), and thus assumes independence of observations. It estimates the .632+ bootstrap estimate ($\hat{\theta}^{.632+}$) of the respective performance measure including a 95% confidence interval.

The bootstrap estimate $\hat{\theta}^{.632+}$ is computed as a weighted average of the apparent performance $\hat{\theta}^{orig,orig}$ (training and test data given by the original dataset) and the average “out-of-bag” (OOB) performance $\hat{\theta}^{bootstrap,OOB} = \sum_{b=1}^B \hat{\theta}_b^{bootstrap,OOB}$ computed from B bootstrap datasets (training data given by the bootstrap dataset, and test data given by the samples not present in the bootstrap dataset). The formula is:

$$\hat{\theta}^{.632+} = (1 - w) \cdot \hat{\theta}^{orig,orig} + w \cdot \hat{\theta}^{bootstrap,OOB},$$

where $w = \frac{0.632}{1 - 0.368 \cdot R}$ and $R = \frac{\hat{\theta}^{bootstrap,OOB} - \hat{\theta}^{orig,orig}}{\theta^{noinfo} - \hat{\theta}^{orig,orig}}$. In case of the C index, $\theta^{noinfo} = 0.5$. For the Brier score, $\theta^{noinfo} = 0.75$. Then each bootstrap dataset is assigned a weight $w_b = \frac{\hat{\theta}_b^{bootstrap,bootstrap} - \hat{\theta}^{orig,orig}}{\hat{\theta}_b^{bootstrap,bootstrap} - \hat{\theta}^{orig,orig}}$, where $\hat{\theta}_b^{bootstrap,bootstrap}$ is the value of the performance measure, when the bootstrap dataset $b \in \{1, \dots, B\}$ is used as training as well as test dataset. The $\frac{\alpha}{2}$ and $1 - \frac{\alpha}{2}$ percentiles of the empirical distribution of these weights, $\xi_{\frac{\alpha}{2}}$ and $\xi_{1-\frac{\alpha}{2}}$, give the CI of $\hat{\theta}^{.632+}$:

$$[\hat{\theta}^{.632+} - \xi_{1-\frac{\alpha}{2}}, \hat{\theta}^{.632+} + \xi_{\frac{\alpha}{2}}]$$

2 .2.2 Comparison in data with differing properties: data simulations

For data simulations, we generated covariate data similar to the reference data by using copula models. The specific distributions and corresponding parameters we used can be found in the Supplementary Material A (Table A.1a, Table A.1b, Table A.2a, Table A.2b, Fig. A.1, Fig. A.2). Covariate-dependent survival times were generated from a Weibull(λ, γ) distribution according to the cumulative hazard inversion method by Bender et al. (2005) implemented in the R package `simSurv` (Brilleman and Gasparini, 2022). Scale parameters λ were fixed at the value estimated from the respective reference dataset ($\lambda = 2241.74$ for the primary biliary cirrhosis dataset, $\lambda = 39.2$ for the prostate cancer dataset), shape parameters γ were varied in order to create scenarios with decreasing ($\gamma = 0.8$), constant ($\gamma = 1$), increasing ($\gamma = 2$), and non-proportional hazards, i.e. different values per treatment group ($\gamma_0 = 2, \gamma_1 = 5$). Random censoring times were generated from a uniform distribution $U_{[0,b]}$ such that censoring percentages of 30% and 60%, respectively, corresponding to the actual censoring rates in the two reference datasets, were obtained. For this, we used the approach by Ramos et al. (2024), but in some cases had to manually adjust the values of the distribution parameter b . We considered total sample sizes $N \in \{100, 200, 400\}$ for the $n_{sim} = 500$ training datasets. For the $n_{sim} = 500$ independent test datasets, the total sample size is $N = 500$. Moreover, we considered different values of the treatment effect when generating the data ($\beta_{treatment} \in \{0, 0.8, -0.4\}$) corresponding to different hazard ratios of the treatment effect. For the RSF, all available splitting rules are included in the method comparison (overview in Table A.3).

For both scenarios, the scenario without treatment-covariate interactions (primary biliary cirrhosis dataset) and the scenario with multiple treatment-covariate interactions (prostate cancer dataset) all variables (main effects) are included in the model. Interaction terms are not included since usually the presence of interactions is unknown due to limited sample size. For the Cox model, backward variable selection is done based on the Akaike information criterion (as implemented in the R function `stepAIC` from the MASS package (Ripley et al., 2024)) in order to determine which main effects will be included. The RSF does intrinsic variable selection: for each split in the tree a random subset of splitting variables among the available variables is selected, and data are partitioned based on the splitting value which yields the optimal result with respect to the splitting rule, i.e. which results in highest heterogeneity between the two respective subsets.

Application of the RSF requires specification of some hyperparameter values, which can be done using grid search. This means that multiple values around the recommended defaults are

specified, and for each combination the error rate ($1 - C$ index) is computed in those data which were not used to build a particular tree model, i.e. the “out-of-bag” data. The RSF does work reasonably well even without extensive hyperparameter tuning (Boehmke and Greenwell, 2019). According to Boehmke and Greenwell (Boehmke and Greenwell, 2019), the number of trees and the number of randomly chosen variables considered for data splitting in a node (m_{try}) are the most important hyperparameters. They recommend to use 10 times the number of variables (covariates) present in the model as the number of trees. They mention the default which equals the square root of the number of covariates rounded down to the nearest integer ($m_{\text{try}} = \lfloor \sqrt{\#\text{covariates}} \rfloor$) for the number of randomly chosen splitting variables per node, and which is used in both R packages, `randomForestSRC` (Ishwaran and Kogalur, 2023) and `ranger` (Wright et al., 2023). Boehmke and Greenwell (Boehmke and Greenwell, 2019) recommend to consider five evenly spaced values around this default during grid search. In order to prevent overfitting, early-stopping criteria can be used with both R functions, either the maximum tree depth or a minimum number of samples per terminal/leaf node can be specified. In `randomForestSRC` (Ishwaran and Kogalur, 2023) the default for the minimum number of samples in a terminal node is set to 15 observations. In our grid search, we considered five, ten and 15 times the number of covariates for the number of trees, 15, 30, and 45 for the number of observations in terminal nodes, and three, four, and five for the value of m_{try} . We chose less than the recommended five values for m_{try} because these RCT datasets consist of a rather small number of covariates compared to other applications of the RSF. We measured computational times per algorithm including variable selection (for the Cox model) and hyperparameter tuning (for the RSF model), respectively.

2.3 Performance measures

According to recommendations (Moons et al., 2015; Steyerberg et al., 2010; McLernon et al., 2023), we based comparisons of the algorithms’ performance on performance metrics measuring discrimination, calibration, and overall performance. In the context of survival analysis, discrimination refers to the model’s ability to distinguish between patients with higher and lower risk of the outcome. Calibration compares predicted survival probabilities to the observed event frequencies in a given time interval. Overall performance encompasses both discrimination as well as calibration of the model. Some performance measures have been extended for use with survival outcomes.

2.3.1 Measure of discrimination: Harrell’s C index

The C index was originally developed for binary outcomes (Greenberg and Sen, 1985), and its modification for the use in data with survival outcomes has been subject to criticism (Hartman et al., 2023). For each pair of patients, the C index compares whether the one with the shorter event time also has the higher predicted risk of suffering the event. These rank-based comparisons may favour the model with the more inaccurate predictions (Vickers and Cronin, 2010), and may not adequately reflect the influence different sets of covariates have on the outcome (Cook, 2007), such that its interpretation may be misleading and not clinically meaningful for survival outcomes. Information on how the C index is calculated for the Cox and RSF model can be found in Supplementary Material C. Computation of the C index is implemented in the function `cindex` in the R package `pec` (Gerds) for the Cox model, and in the function `get.cindex` in the R package `randomForestSRC` (Ishwaran and Kogalur, 2023) for the RSF.

2.3.2 Measure of calibration: Calibration curves

A calibration plot of observed on predicted probabilities of mortality indicates deviation from perfect prediction the more the slope deviates from the ideal diagonal line (Van Calster et al., 2019). It quantifies the agreement between the actual and predicted outcome within a specified duration of time. Austin et al. (2020) describe and implement an approach for estimating calibration curves for survival outcomes. We used their calibration curve which is estimated based on Cox regression using restricted cubic splines.

2.3.3 Measure of overall performance: Integrated Brier score

The Integrated Brier score (Graf et al., 1999) summarizes the Brier scores over time, i.e. it is a time range performance measure. The Brier score calculates the difference between predicted and actual survival at a given time point, and thus values indicate better overall performance the closer they are to zero. It is implemented in the function `integrated_brier_score` in the R package `survex` (Spytek et al., 2024).

3 Results

3.1 Results of the bootstrap approach

Table 3 and Table 4 show the bootstrap estimates of the C index and Integrated Brier score, respectively, when applying the bootstrap approach for point estimates (Jiang et al., 2008; Wahl et al., 2016) to both reference datasets. The same results are shown in Figure 1 (primary biliary cirrhosis dataset) and Figure 2 (prostate cancer dataset). The first impression is that the point estimates $\hat{\theta}^{.632+}$ alone indicate a potentially better performance of most RSF models compared to the Cox-PH model but their confidence intervals are often much wider and mostly include the $\hat{\theta}^{.632+}$ estimate of the Cox-PH model. This is the case for both reference datasets, either without or including treatment-covariate interactions. For the PBC data (Figure 1), confidence intervals of the RSF with splitting rules “log-rank test”, “log-rank score test”, and “extremely randomized trees” do not include the $\hat{\theta}^{.632+}$ estimate of the C index of the Cox-PH model, with completely separate confidence intervals for the “extremely randomized trees” splitting rule. For the $\hat{\theta}^{.632+}$ estimates of the Integrated Brier score, all confidence intervals corresponding to RSF models contain the respective $\hat{\theta}^{.632+}$ estimate of the Cox model, although the point estimates $\hat{\theta}^{.632+}$ of the RSF indicate a somewhat better overall performance (except for the log-rank score test splitting rule). Regarding the prostate cancer dataset (Figure 2), all confidence intervals of the $\hat{\theta}^{.632+}$ C index estimates of the RSF models contain the $\hat{\theta}^{.632+}$ estimate of the Cox model. Only the confidence interval of the $\hat{\theta}^{.632+}$ Integrated Brier score estimates of the RSF with the log-rank splitting rule does not contain the respective estimate of the Cox model, but the confidence intervals still slightly overlap.

In summary, the RSF (“log-rank test”) seems to have an advantage over the Cox model when comparing overall performance in both datasets, because its point estimates are the lowest and the corresponding confidence intervals have the smallest overlap. With respect to the C index, the RSF (“extremely randomized trees”) performs better in the data without treatment-covariate interactions (primary biliary cirrhosis dataset). For the prostate cancer dataset, RSF may have better performance concluded from the point estimates alone, but confidence intervals of the Cox and RSF models completely overlap such that no clear conclusion can be made.

Table 3: Bootstrap estimates $\hat{\theta}^{.632+}$ (95% confidence interval) of the C index and Integrated Brier score in the RCT data without treatment-covariate interactions (primary biliary cirrhosis dataset). Predictions are based on $n_{\text{sim}} = 1000$ bootstrap datasets.

	Cox-PH	Random survival forest					
		Log-rank test	Log-rank score	Gradient-based Brier score	Harrell's C	Extremely randomized trees	Maximally selected rank statistics
C index	0.776 (0.735,0.817)	0.855 (0.778,0.932)	0.847 (0.815,0.88)	0.856 (0.768,0.944)	0.858 (0.764,0.953)	0.844 (0.819,0.869)	0.868 (0.698,1)
Integrated Brier score	0.131 (0.124,0.161)	0.116 (0.106,0.146)	0.148 (0.118,0.197)	0.12 (0.112,0.151)	0.117 (0.109,0.147)	0.129 (0.126,0.152)	0.121 (0.108,0.147)

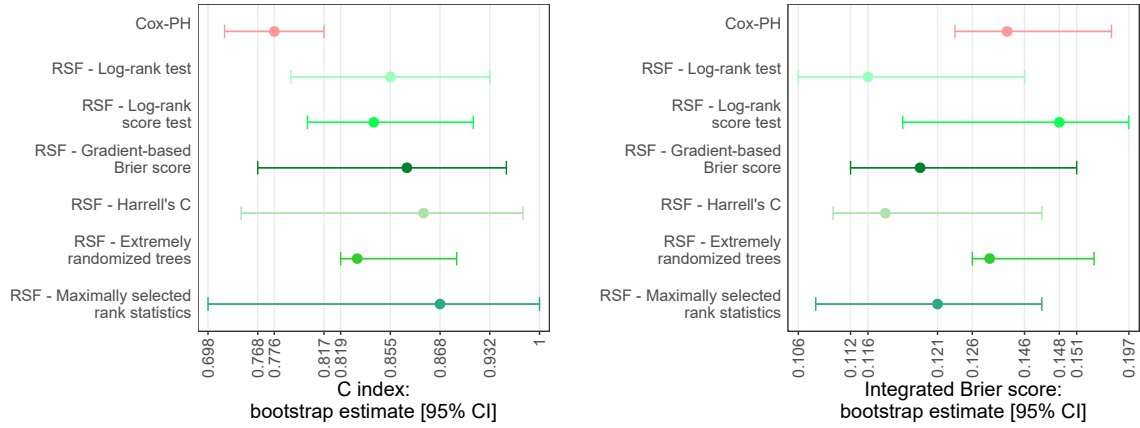


Fig. 1: Bootstrap estimate $\hat{\theta}^{.632+}$ (95% confidence interval) of the C index (right) and Integrated Brier score (left) for the RCT in primary biliary cirrhosis patients.

Abbreviations: Cox-PH - Cox proportional hazards model, RSF - Random survival forest.

Table 4: Bootstrap estimates $\hat{\theta}^{.632+}$ (95% confidence interval) of the C index and Integrated Brier score data with three treatment-covariate interactions (prostate cancer dataset). Predictions are based on $n_{\text{sim}} = 1000$ bootstrap datasets.

	Cox-PH	Random survival forest					
		Log-rank test	Log-rank score	Gradient-based Brier score	Harrell's C	Extremely randomized trees	Maximally selected rank statistics
C index	0.521 (0.513,0.53)	0.66 (0.438,0.881)	0.642 (0.462,0.821)	0.653 (0.456,0.85)	0.657 (0.432,0.881)	0.645 (0.498,0.792)	0.663 (0.413,0.913)
Integrated Brier score	0.201 (0.194,0.211)	0.17 (0.158,0.199)	0.183 (0.177,0.205)	0.176 (0.165,0.206)	0.172 (0.155,0.206)	0.179 (0.175,0.204)	0.172 (0.13,0.23)

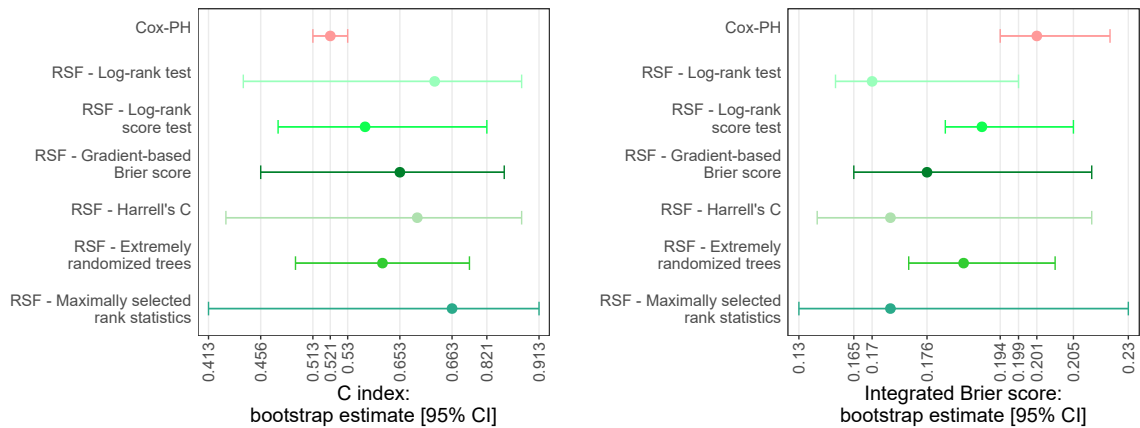


Fig. 2: Bootstrap estimate $\hat{\theta}^{.632+}$ (95% confidence interval) of the C index (left) and Integrated Brier score (right) for the RCT in prostate cancer patients.

Abbreviations: Cox-PH - Cox proportional hazards model, RSF - Random survival forest.

3.2 Simulation study results

In this section, the simulation study results for one of the treatment effects considered in the simulation study ($\beta_{\text{treatment}} = -0.4$) are presented and discussed. The results for other values of the treatment effect ($\beta_{\text{treatment}} \in \{0, 0.8\}$) are similar and can be found in the Supplementary Material. Varying the size of the treatment effect only seems to have a minor influence on the methods' performance. Moreover, we only show the results for the algorithms that are of most interest, which are the Cox model and the RSF using the standard log-rank test splitting rule. Additionally, the results of the RSF based on other splitting rules are shown if they outperform these two methods with respect to the median result. Only the best performing one among them is shown in case there are multiple better performing alternatives. Results for the remaining RSF splitting rules are shown in the Supplementary Material.

The C index estimates, which correspond to the models' discriminative performance, are shown in Figure 3 (30% censoring rate) and Figure 4 (60% censoring rate). Results for the RCT data without treatment-covariate interactions (PBC dataset) are shown in Figure 3(a) and Figure 4(a). For a censoring rate of 30%, varying hazards, and sample sizes, the RSF based on the log-rank test splitting rule performs best. For a censoring rate of 60%, the Cox model performs best in the nonproportional hazards setting independent of sample size, and otherwise the RSF performs best. In this case (censoring rate of 60%), for a total sample size of $N = 100$, the RSF using the "maximally selected rank statistics" splitting rule (slightly) outperforms the standard log-rank test splitting rule in the scenarios assuming a decreasing and constant hazard. Otherwise the log-rank test splitting rule gives the best results. Results for the RCT data with multiple treatment-covariate interactions (prostate cancer dataset) are shown in Figure 3(b) and Figure 4(b). Here, the RSF based on the "extremely randomized trees" splitting rule performs best for both censoring rates, the considered total sample sizes of $N \in \{100, 200, 400\}$ and the varying properties of the hazard. The difference to the standard RSF using the log-rank splitting rule is more evident with a proportion of approximately up to 50% for the nonoverlapping parts of the boxes although the difference is less clear in the nonproportional hazards setting.

The Integrated Brier score estimates, which correspond to the models' overall performance (encompassing both, the models' discrimination and calibration) are shown in Figure 5 (30% censoring rate) and Figure 6 (60% censoring rate). Results for the RCT data without treatment-covariate interactions (PBC dataset) are shown in Figure 5(a) and Figure 6(a). The Cox model has clearly the best overall performance in the nonproportional hazards settings. It also (very slightly) outperforms the RSF in the scenario with increasing hazard when either $N = 400$ for a censoring rate of 30% or when $N \in \{200, 400\}$ for a censoring rate of 60%. Otherwise, the RSF performs better. The difference is even more evident when the total sample size becomes smaller. For decreasing and constant hazards, the "Gradient-based Brier score" splitting rule slightly outperforms the "log-rank test" splitting rule for the RSF for both censoring rates and all sample sizes. Results for the RCT data with multiple treatment-covariate interactions (prostate cancer dataset) are shown in Figure 5(b) and Figure 6(b). From these results, it can be suspected that the Cox model's performance in comparison to the RSF increases for larger sample sizes and higher censoring rates. While the Cox model only slightly outperforms the RSF for decreasing and constant hazards in case $N = 400$ when the censoring rate is 30%, it does so more clearly for a censoring rate of 60%, where it additionally clearly outperforms the RSF in the nonproportional hazards settings. Overall, the gap in performance between both models becomes smaller for the higher censoring percentage. For all other scenarios the RSF using the "extremely randomized trees" splitting rule performs best (with one exception where the log-rank splitting rule works better: $N = 100$ with decreasing hazard and 30% censoring) although the difference to the log-rank test splitting rule is marginal.

Some calibration curves at median survival time for the RCT data without treatment-covariate interactions (PBC dataset) are shown in Figure B.5a and Figure B.5b. Calibration curves for a proportional and nonproportional hazards setting are compared. Calibration curves for the respective scenarios for the RCT data with multiple treatment-covariate interactions (prostate cancer dataset) are shown in Figure B.6a and Figure B.6b. Calibration of the Cox model improves with increasing sample size while for the RSF this is at least less evident. Especially in the nonproportional hazards setting and absence of treatment-covariate interactions, the Cox model's results are better calibrated compared to the RSF (Figure B.5b). In contrast,

the difference in calibration between the two models is less obvious for the nonproportional hazards setting in case treatment-covariate interactions are present in the data (Figure B.6b). Judged by the percentiles shown as dashed lines, calibration generally varies less in the Cox model results than in the RSF results. Deviation from perfect calibration of the RSF results is caused by a too narrow range of predictions compared to the true values, resulting in calibration curves that are too steep.

Computational complexity of the methods is compared in Figure 11. It includes the variable selection step for the Cox model, and the grid search for finding the optimal combination of hyperparameters for the RSF. Computational times are the lowest for the Cox model, although the RSF still has relatively low computational times for total sample sizes of $N = 100$, and even for the larger sample sizes when the RSF splitting rules “log-rank test”, “extremely randomized trees”, or “maximally selected rank statistics” are used. In contrast, computational time considerably increases for larger sample sizes as well as larger number of covariates for the RSF splitting rules “log-rank score test”, “gradient-based Brier score”, and “Harrell’s C ”. Complete simulation study results can be found in Supplementary Material B.1 (C index), B.2 (Integrated Brier score), and B.3 (calibration curves).

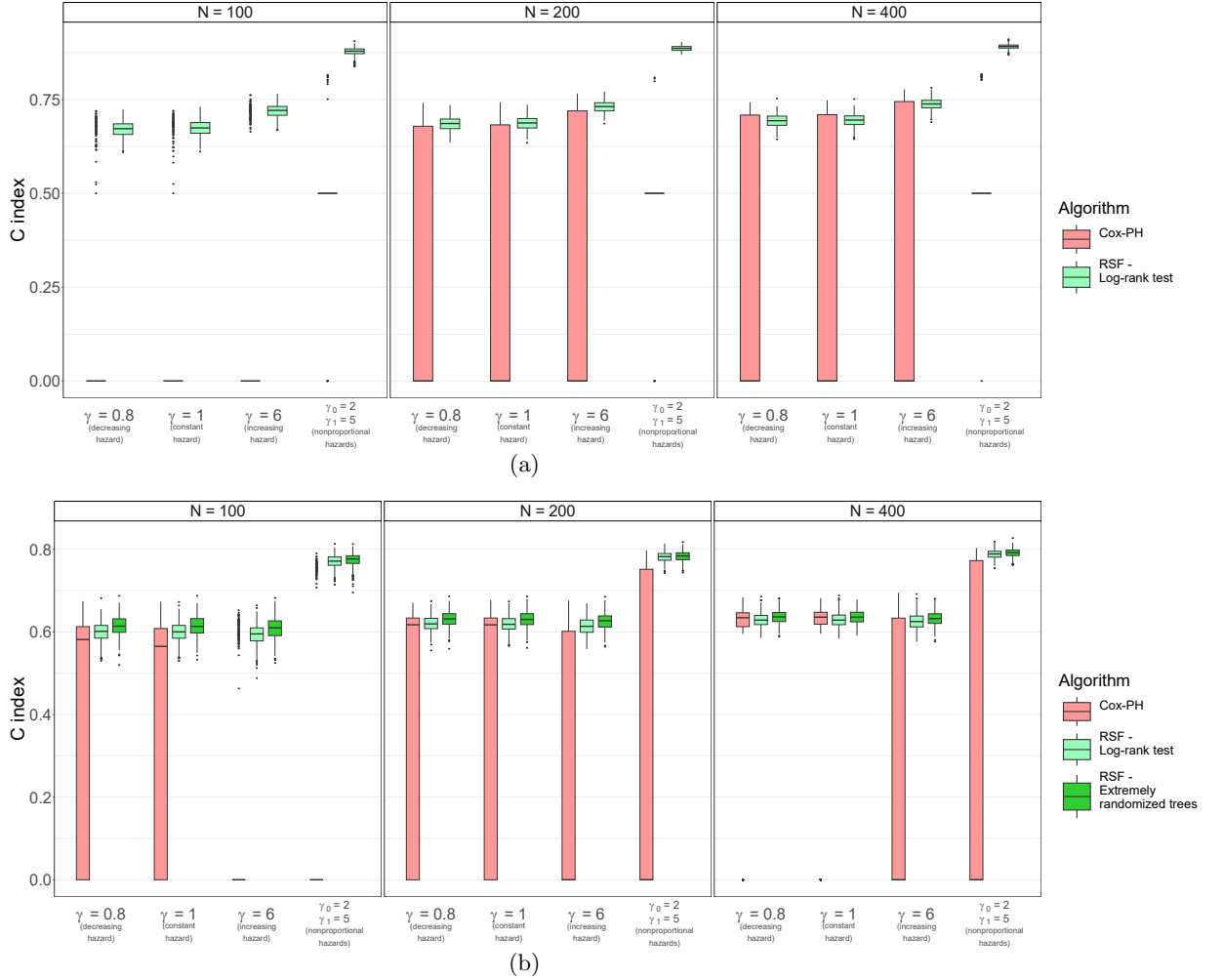


Fig. 3: C index estimates in the simulation scenario assuming 30% censoring and a treatment effect of $\beta_{\text{treatment}} = -0.4$ for the RCT in primary biliary cirrhosis (a) and in prostate cancer patients (b). Survival times are generated from a Weibull distribution with scale parameters estimated from the respective reference dataset, shape parameters (γ) vary in order to examine the impact of differing hazards, and the violation of the proportional hazards assumption. Results are shown for different total sample sizes N .

Abbreviations: Cox-PH - Cox proportional hazards model, RSF - Random survival forest.

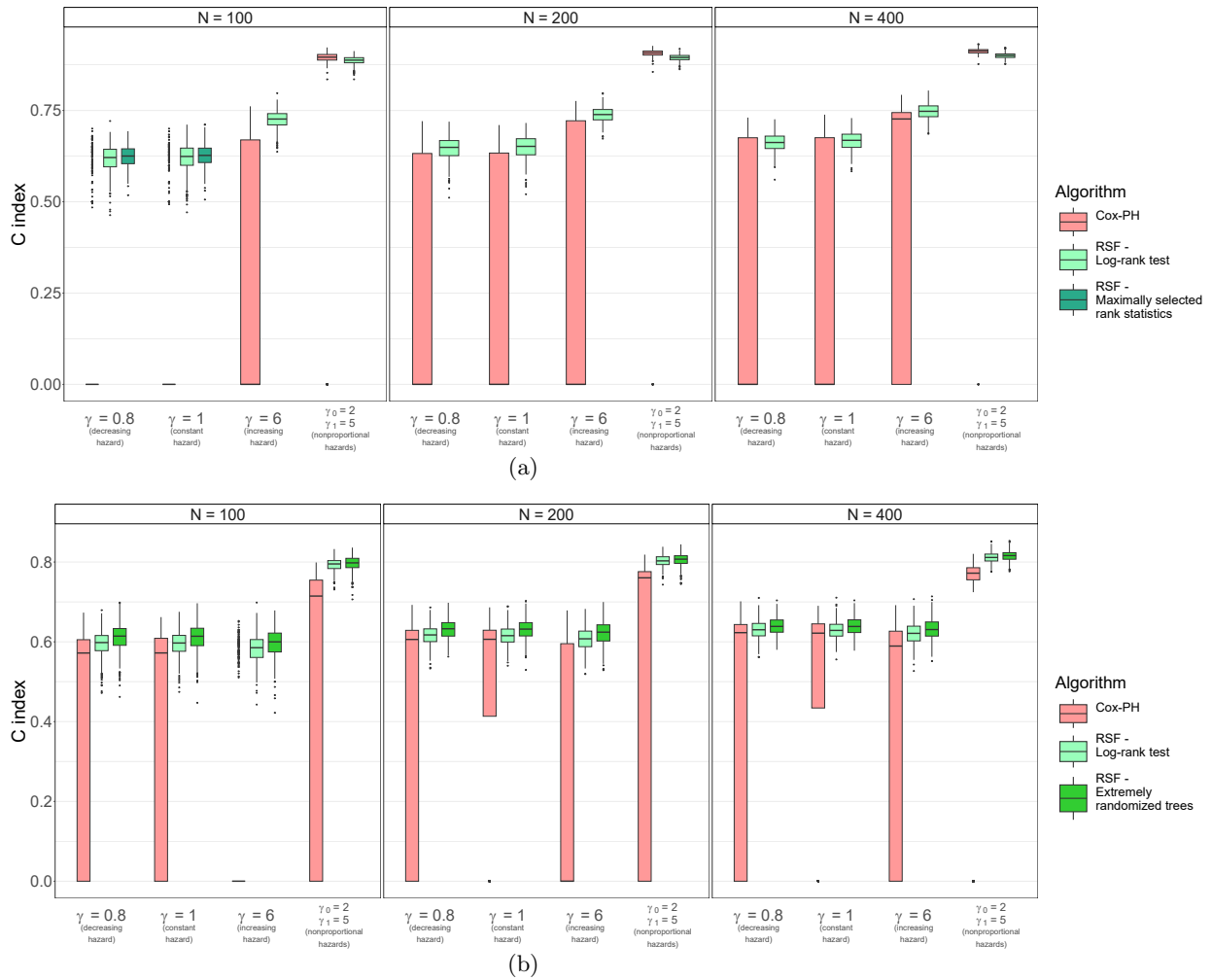


Fig. 4: C index estimates in the simulation scenario assuming 60% censoring and a treatment effect of $\beta_{\text{treatment}} = -0.4$ for the RCT in primary biliary cirrhosis (a) and in prostate cancer patients (b). Survival times are generated from a Weibull distribution with scale parameters estimated from the respective reference dataset, shape parameters (γ) vary in order to examine the impact of differing hazards, and the violation of the proportional hazards assumption. Results are shown for different total sample sizes N .

Abbreviations: Cox-PH - Cox proportional hazards model, RSF - Random survival forest.

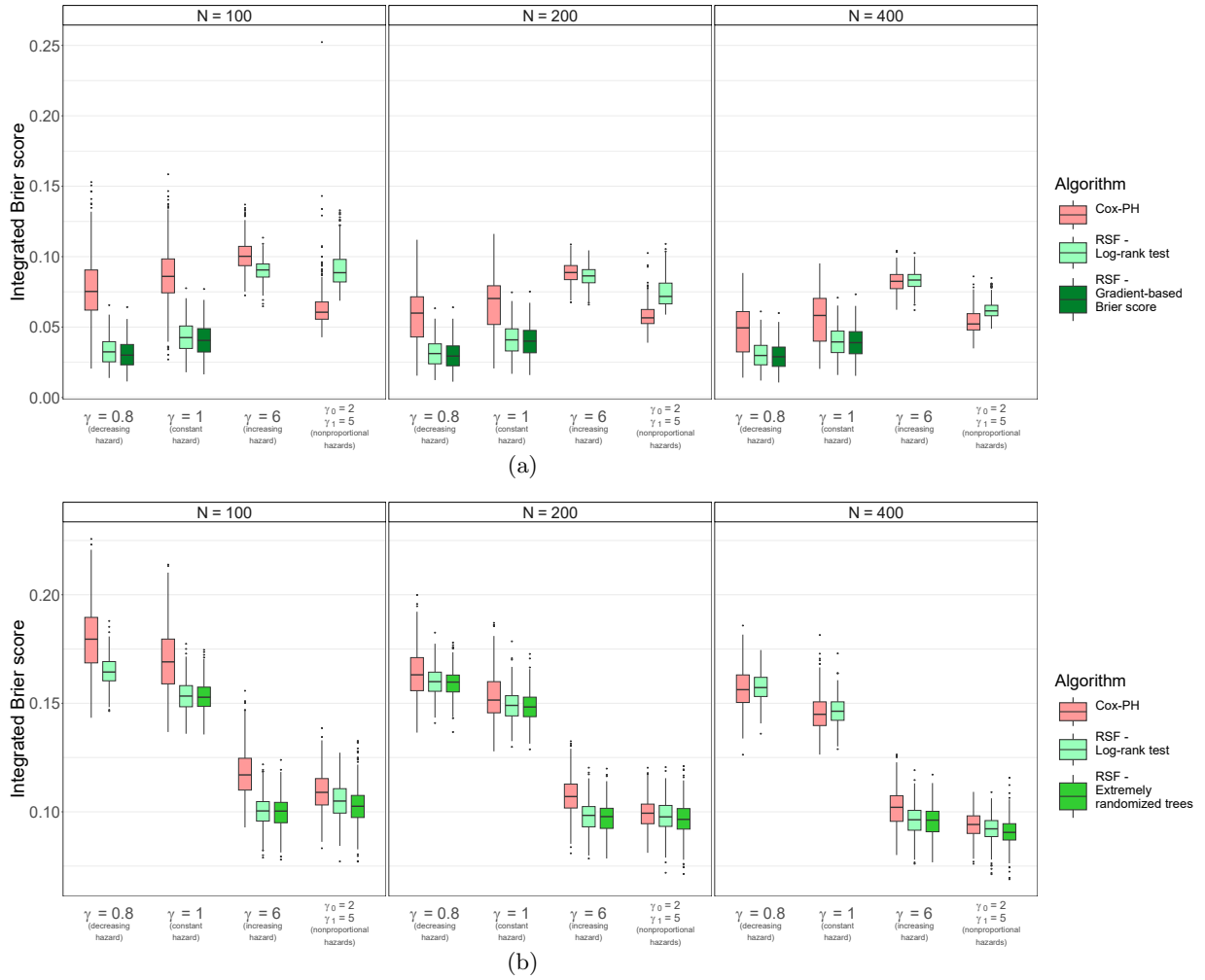


Fig. 5: Integrated Brier score (IBS) estimates in the simulation scenario assuming 30% censoring and a treatment effect of $\beta_{\text{treatment}} = -0.4$ for the RCT in primary biliary cirrhosis (a) and in prostate cancer patients (b). Survival times are generated from a Weibull distribution with scale parameters estimated from the respective reference dataset, shape parameters (γ) vary in order to examine the impact of differing hazards, and the violation of the proportional hazards assumption. Results are shown for different total sample sizes N .

Abbreviations: Cox-PH - Cox proportional hazards model, RSF - Random survival forest.

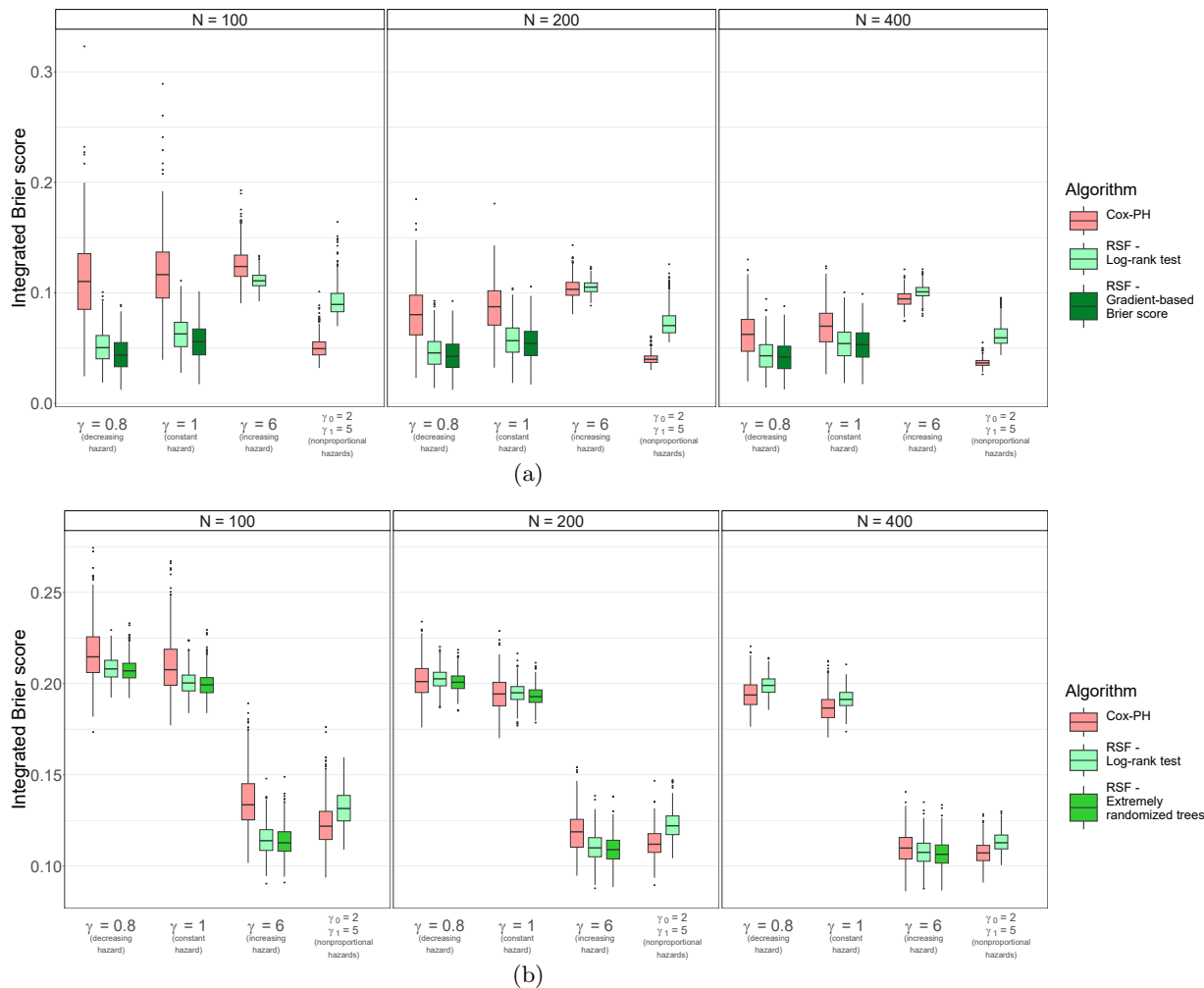


Fig. 6: Integrated Brier score (IBS) estimates in the simulation scenario assuming 60% censoring and a treatment effect of $\beta_{\text{treatment}} = -0.4$ for the RCT in primary biliary cirrhosis (a) and in prostate cancer patients (b). Survival times are generated from a Weibull distribution with scale parameters estimated from the respective reference dataset, shape parameters (γ) vary in order to examine the impact of differing hazards, and the violation of the proportional hazards assumption. Results are shown for different total sample sizes N .

Abbreviations: Cox-PH - Cox proportional hazards model, RSF - Random survival forest.

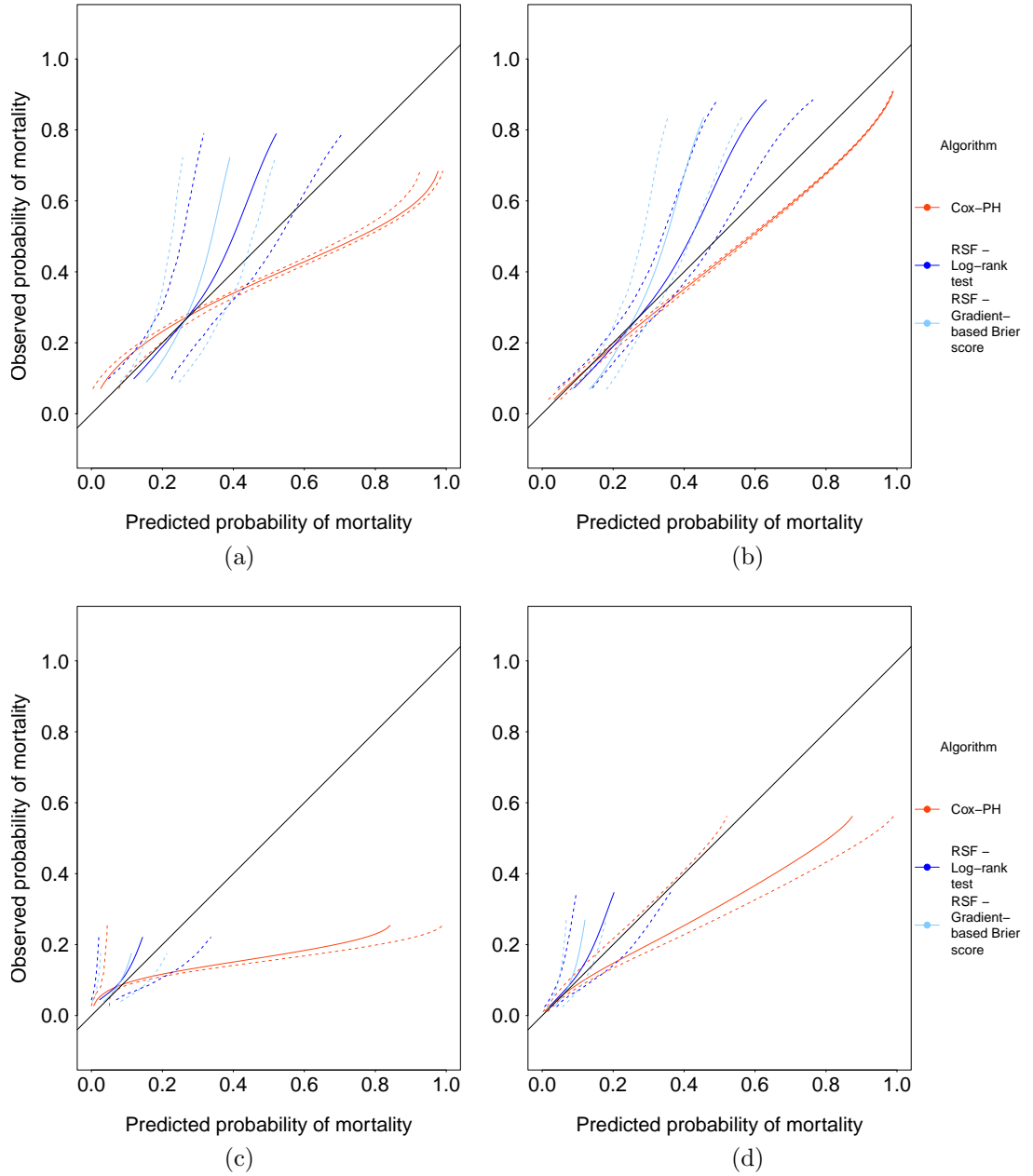


Fig. 7: Calibration curves for a proportional hazards scenario (primary biliary cirrhosis dataset). Calibration curves at the median (50% quantile) survival time for a proportional hazards setting (Weibull survival time distribution $W(\lambda = 2241.74, \gamma = 1)$), $\beta_{\text{treatment}} = -0.4$, and $n_{\text{sim}} = 500$ simulated datasets based on data without treatment-covariate interactions (primary biliary cirrhosis dataset). The solid line represents the mean calibration curve, the outer dotted lines represent the 2.5th and 97.5th percentile of the calibration curve. The black diagonal line corresponds to perfect calibration.

(a) 30% censoring, $N = 100$, (b) 30% censoring, $N = 400$,

(c) 60% censoring, $N = 100$, (d) 60% censoring, $N = 400$.

Abbreviations: Cox-PH - Cox proportional hazards model, RSF - Random survival forest.

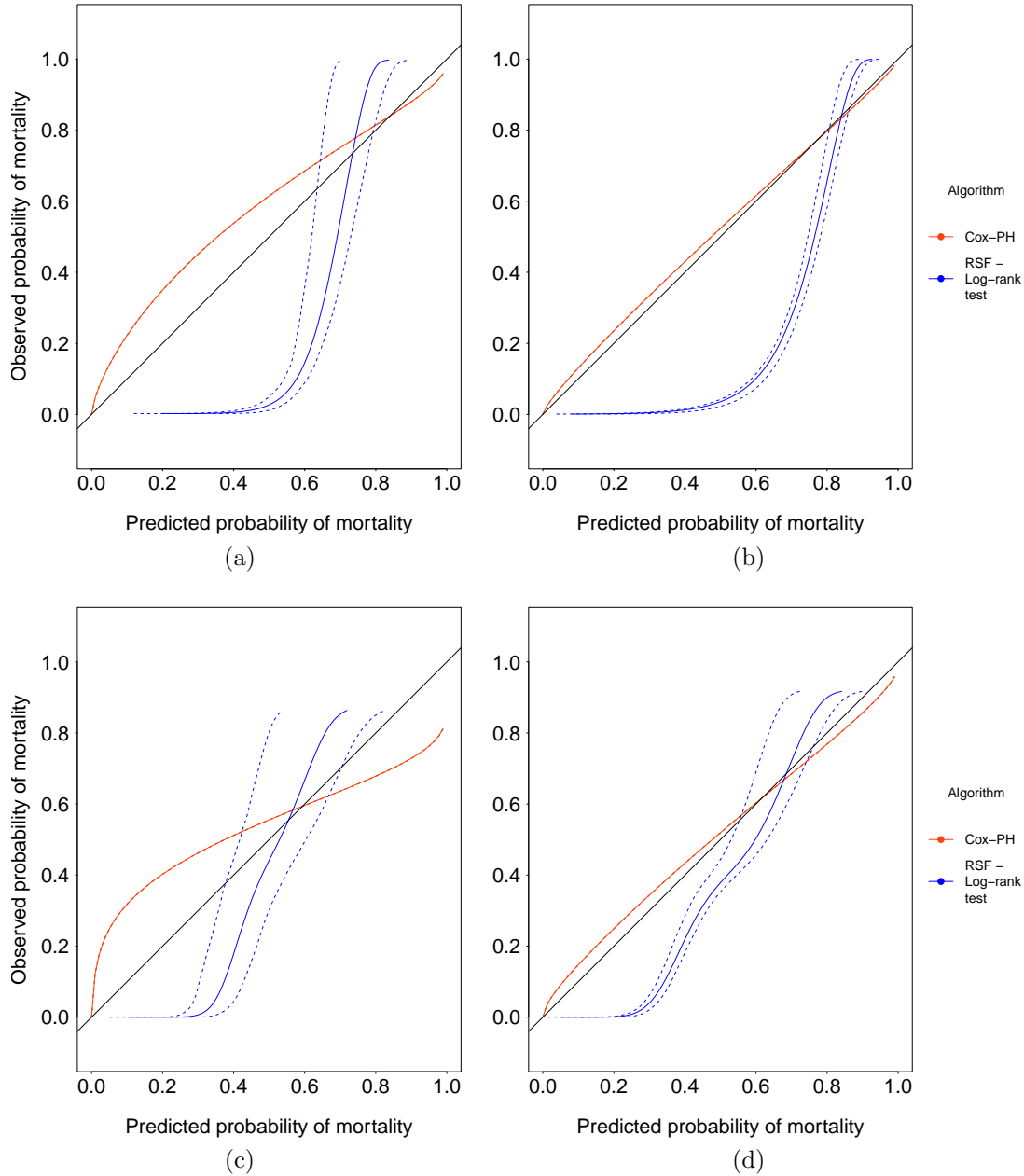


Fig. 8: Calibration curves for a nonproportional hazards setting (primary biliary cirrhosis dataset). Calibration curves at the median (50% quantile) survival time for a nonproportional hazards setting (Weibull survival time distribution $W(\lambda = 2241.74, \gamma \in \{2, 5\})$), $\beta_{\text{treatment}} = -0.4$, and $n_{\text{sim}} = 500$ simulated datasets based on data without treatment-covariate interactions (primary biliary cirrhosis dataset). The solid line represents the mean calibration curve, the outer dotted lines represent the 2.5th and 97.5th percentile of the calibration curve. The black diagonal line corresponds to perfect calibration.

(a) 30% censoring, $N = 100$, (b) 30% censoring, $N = 400$,

(c) 60% censoring, $N = 100$, (d) 60% censoring, $N = 400$.

Abbreviations: Cox-PH - Cox proportional hazards model, RSF - Random survival forest.

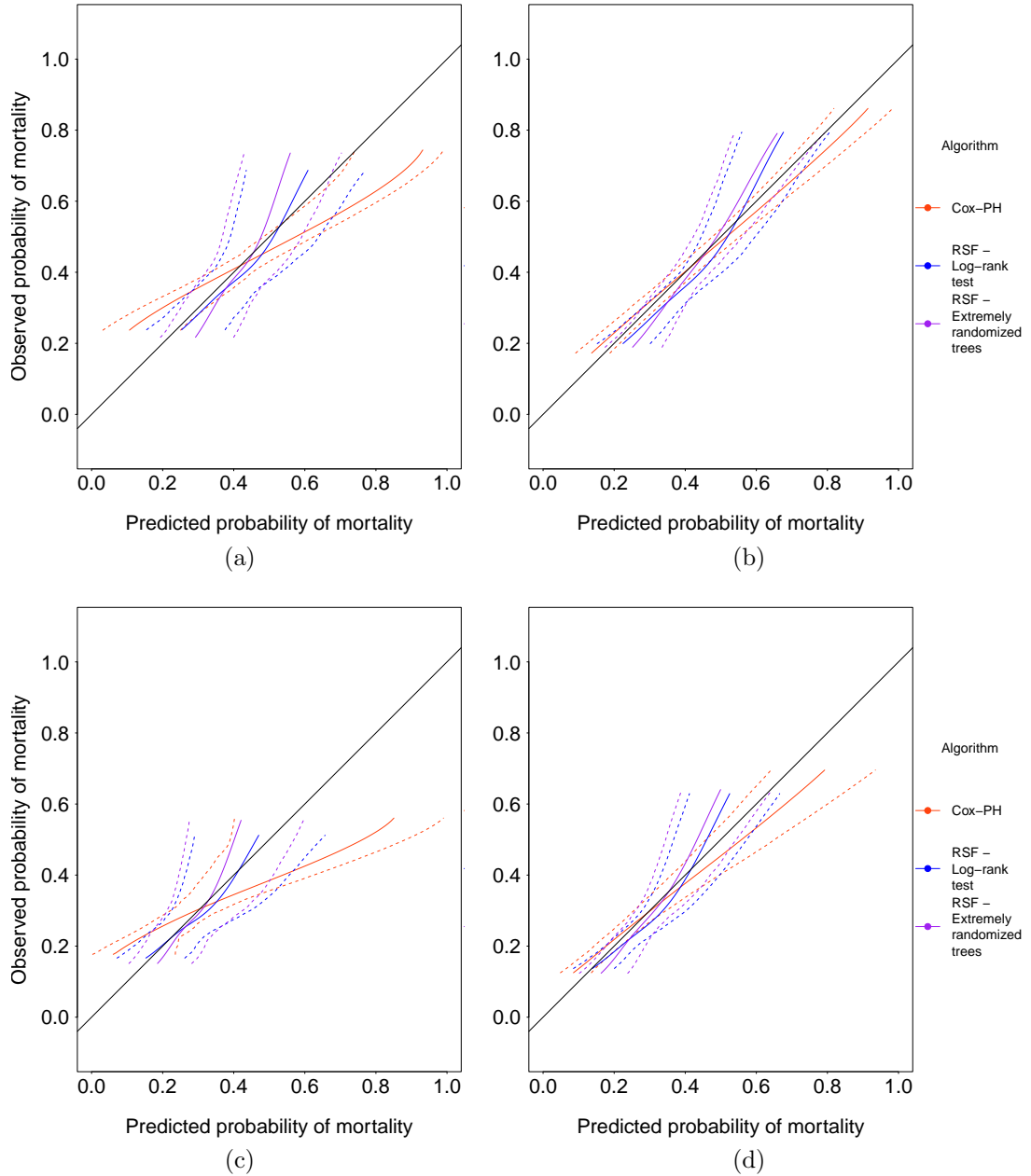


Fig. 9: Calibration curves for a proportional hazards setting (prostate cancer dataset). Calibration curves at the median (50% quantile) survival time for a proportional hazards setting (Weibull survival time distribution $W(\lambda = 2241.74, \gamma = 1)$), $\beta_{\text{treatment}} = -0.4$, and $n_{\text{sim}} = 500$ simulated datasets based on data with three treatment-covariate interactions (prostate cancer dataset). The solid line represents the mean calibration curve, the outer dotted lines represent the 2.5th and 97.5th percentile of the calibration curve. The black diagonal line corresponds to perfect calibration. (a) 30% censoring, $N = 100$, (b) 30% censoring, $N = 400$, (c) 60% censoring, $N = 100$, (d) 60% censoring, $N = 400$.

Abbreviations: Cox-PH - Cox proportional hazards model, RSF - Random survival forest.

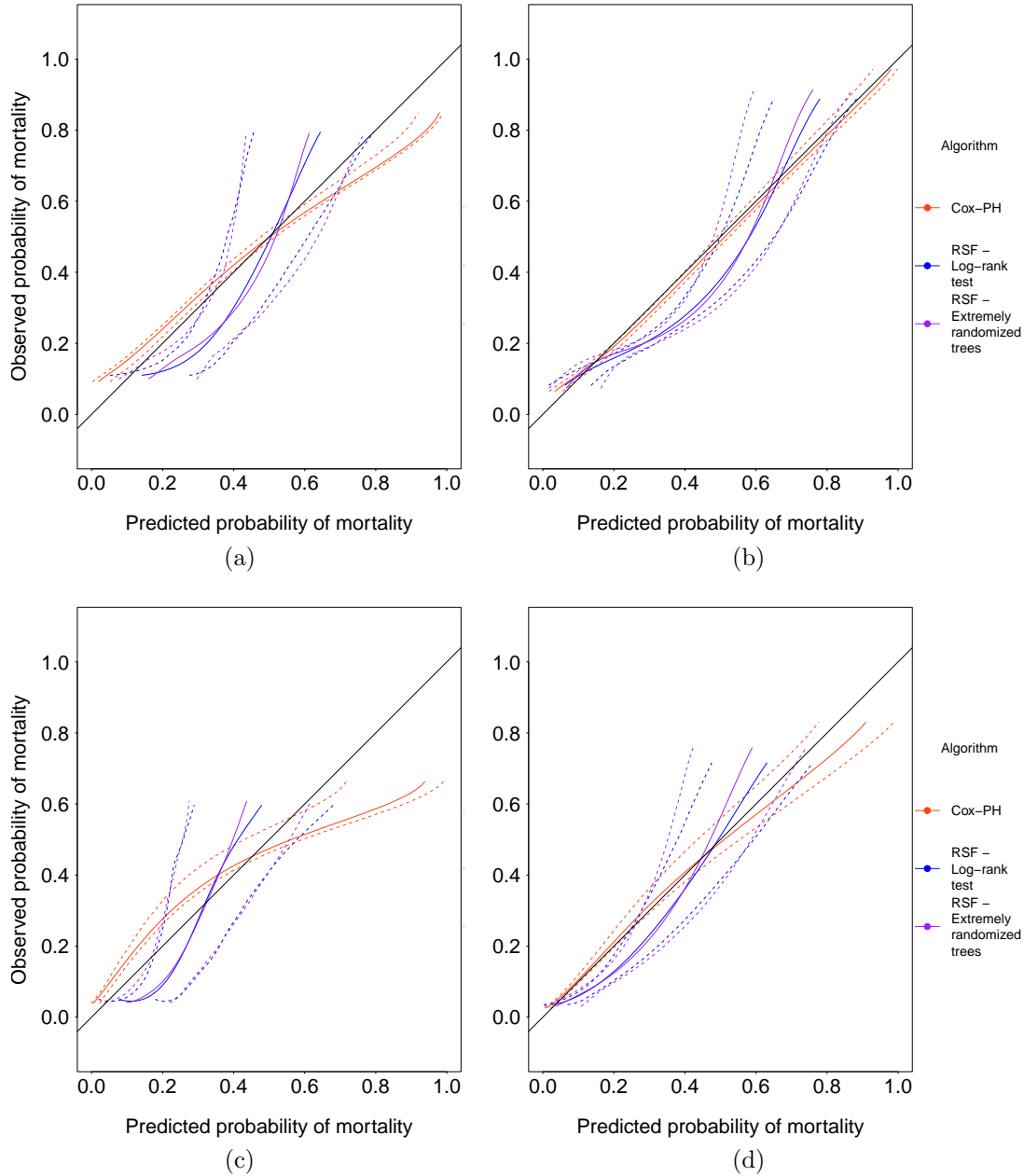


Fig. 10: Calibration curves for a nonproportional hazards setting (prostate cancer dataset). Calibration curves at the median (50% quantile) survival time for a nonproportional hazard setting (Weibull survival time distribution $W(\lambda = 39.2, \gamma \in \{2, 5\})$), $\beta_{\text{treatment}} = -0.4$, and $n_{\text{sim}} = 500$ simulated datasets based on data with three treatment-covariate interactions (prostate cancer dataset). The solid line represents the mean calibration curve, the outer dotted lines represent the 2.5th and 97.5th percentile of the calibration curve. The black diagonal line corresponds to perfect calibration.

(a) 30% censoring, $N = 100$, (b) 30% censoring, $N = 400$,

(c) 60% censoring, $N = 100$, (d) 60% censoring, $N = 400$.

Abbreviations: Cox-PH - Cox proportional hazards model, RSF - Random survival forest.

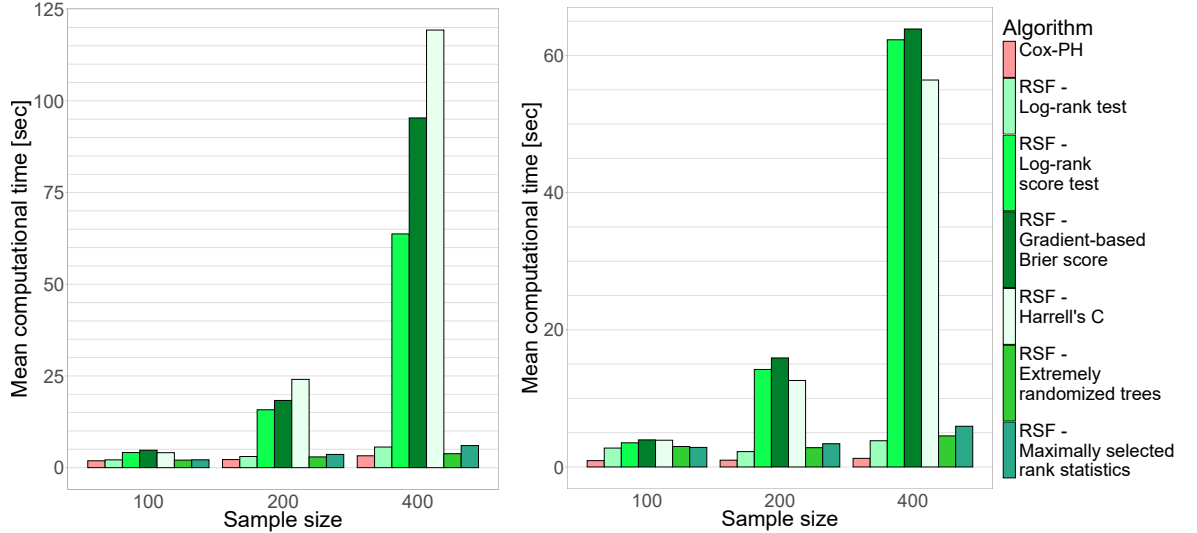


Fig. 11: Mean computational times for the RCT data without treatment-covariate interactions (primary biliary cirrhosis dataset, left), and for the RCT data with three treatment-covariate interactions (prostate cancer dataset, right).

Abbreviations: Cox-PH - Cox proportional hazards model, RSF - Random survival forest.

4 Discussion

We performed an extensive simulation study in order to perform neutral comparison of the Cox regression model and the RSF model when predicting survival probabilities in RCT data, in which we included all currently available splitting rules for the RSF implemented in two widely used R packages, `randomForestSRC` (Ishwaran et al., 2021) and `ranger` (Wright et al., 2023). We followed recommendations for neutral comparison studies (Weber et al., 2019; Morris et al., 2019) to ensure an objective evaluation of the results.

We considered a variety of settings. We used two publicly available RCT datasets as a reference for data simulations, where one dataset is characterized by the absence of treatment-covariate interactions (University of Massachusetts, 1980, biliary cirrhosis dataset) and the other by two significant and one weak treatment-covariate interaction (Byar and Green, 1980, prostate cancer dataset). In each case, we considered different total sample sizes, values of the treatment effect, censoring rates, and properties of the hazard that may occur in other real-world datasets. Comparisons are based on measures of discrimination, calibration, and overall performance as recommended in the literature (Moons et al., 2015; Steyerberg et al., 2010; McLernon et al., 2023).

Depending on the research question, different aspects of the algorithm’s performance may be more important. With respect to discrimination measured by the C index, the RSF predictions are usually more accurate, with only one exception for the data without treatment-covariate interactions and nonproportional hazards with 60% censoring. Many researchers who compared the performance of the Cox and RSF models in (real-world) observational medical data, have based their conclusions on the C index estimates, but some methodologists oppose its extension and application to time-to-event medical data. In the data without treatment-covariate interactions the standard “log-rank test” RSF splitting rule performed best, while for the data with multiple treatment-covariate interactions, the “extremely randomized trees” splitting rule performed better than the standard RSF (which still performed better than the Cox model). With respect to overall performance measured by the IBS, the Cox model performs considerably better in the nonproportional hazards settings for both censoring rates (30%, 60%) in the data without treatment-covariate interactions, and for 60% censoring in the data with multiple treatment-covariate interactions. We therefore assume that deviation from the proportional hazards assumption may not always affect the Cox models performance. Moreover, higher censoring rates may affect the RSF’s overall performance to a greater extent than the Cox model’s overall performance. This conclusion has also been made by Baralou et al. (2022). In the other

scenarios, the performance gap between both models tends to increase with decreasing sample size, which may be due to the RSF’s better ability for reasonable predictions even in higher dimensional settings. The Cox model benefits more from larger sample sizes. For the largest considered total sample size ($N = 400$) for the data with multiple treatment-covariate interactions, the Cox model additionally outperformed the RSF in all but the increasing hazard scenario. In the data without treatment-covariate interactions, the “gradient-based Brier score” may perform better than the standard “log-rank test” RSF splitting rule. In the data with multiple treatment-covariate interactions, again the “extremely randomized trees” splitting rule performs better identical to the comparisons based on the C index. It may be worthwhile to try the “extremely randomized trees” splitting rule in data where treatment-covariate interactions are assumed.

Calibration, a measure of agreement between (estimated) true and predicted outcomes, seems to be worse for the RSF compared to the Cox model in many cases. Calibration of RSF predictions varies to a higher extent, and the difference between both models is in some cases very evident. It is unclear whether the results could be influenced by the approach of estimating the calibration curves itself which is based on Cox model predictions to approximate the true outcome.

The results are affected by the size of the treatment effect only to a minor degree.

Limitations of our simulation study are that only a limited number of datasets and scenarios, as well as a limited number of performance measures can be considered. Moreover, we only considered the combination of Weibull distributed survival times and uniformly distributed censoring times. There also exist further RSF splitting rules (Ishwaran et al., 2008) that are not currently implemented in the R packages `randomForestSRC` (Ishwaran et al., 2021) and `ranger` (Wright et al., 2023), which we did not include in the method comparison.

We found that overall performance measures such as the IBS may be more suitable for drawing general conclusions about the superiority of one method over the other for predictions in RCT data based on some publications in the methodological literature as well as the simulation study results which include many outliers suggesting a poor performance of the Cox model when considering the C index, a conclusion that is less obvious or even reversed when considering the IBS. Regarding different RSF splitting rules, the “log-rank test” performed reasonably well. In some cases other splitting rules perform better based on the median result, most remarkably the “extremely randomized trees” splitting rule in the presence of treatment-covariate interactions. Computational times of some RSF splitting rules such as the standard “log-rank test” or the “extremely randomized trees” splitting rule do not extremely exceed those of the Cox model.

5 Conclusions

The RSF may help predicting patient outcomes more accurately. Different aspects of performance may be interesting depending on the research question.

In terms of discrimination, the RSF will most likely outperform the Cox regression model in many settings. This is in accordance with method comparisons in different real-world datasets (Guo et al., 2023; Sarica et al., 2023; Chowdhury et al., 2023; Moncada-Torres et al., 2021; Farhadian et al., 2021; Miao et al., 2015; Spooner et al., 2020; Qiu et al., 2020; Kim et al., 2019; Datema et al., 2012; Omurlu et al., 2009; Du et al., 2020). The performance in our reference datasets suggests that the RSF tends to perform better but the confidence intervals are still overlapping, not allowing a definitive conclusion. Only the RSF based on the “extremely randomized trees” splitting rule can be said to definitively perform better than Cox regression in the data without treatment-covariate interactions. In our simulations, the RSF based on “log-rank test” splitting usually performs best for the data without interactions, only in the data with 60% censoring, Cox regression performs better in the non-proportional hazards settings. In their simulations, Baralou et al. (2022) also found that performance of the RSF may suffer with higher censoring rates. The RSF based on “extremely randomized trees” splitting always performs best in data with treatment-covariate interactions for the lower and higher censoring proportion.

With respect to overall performance, simulation results of both models are more comparable, although performance in the reference datasets still suggests that the RSF tends to perform better but without clear evidence due to overlapping confidence intervals. In the simulations

based on data without treatment-covariate interactions, the Cox model performs best in non-proportional hazards settings, and may perform better in case of increasing hazards for higher sample sizes and higher censoring rates, respectively. Otherwise, especially for smaller sample sizes, the RSF based on “log-rank test” splitting performs better. The RSF based on “Gradient-based Brier score” splitting may have a slight advantage compared to the standard splitting rule for decreasing and constant hazards. For simulated data with treatment-covariate interactions, the Cox model outperforms the RSF especially for the higher censoring rate in the nonproportional hazards settings or higher sample sizes ($N = 400$), respectively. Otherwise, the RSF based on the “extremely randomized trees” splitting rule performs best. Calibration of the Cox model seems to be visibly better in the nonproportional hazards settings.

Acknowledgments

We would like to thank Prof. Dr. Sarah Friedrich, Chair for Mathematical Statistics and Artificial Intelligence in Medicine, Institute for Mathematics, University of Augsburg, Germany, for her support.

The authors gratefully acknowledge the resources on the LiCCA HPC cluster of the University of Augsburg, co-funded by the Deutsche Forschungsgemeinschaft (DFG, German Research Foundation) –Project-ID 499211671.

Funding sources

The authors are grateful for financial support of the Young Researchers Travel Scholarship Program of the University of Augsburg, and for the financial support of The International Dimension of ERASMUS+ during Ricarda Graf’s research visit to the University of Reading. The sponsors had no role in study design, collection, analysis and interpretation of data, writing of the report and decision to submit the article for publication.

Data availability statement

The two datasets used as references for data simulations are publicly available: the RCT in primary biliary cirrhosis patients is available from a number of sources, for example from the Vanderbilt Department of Biostatistics ([Vanderbilt Department of Biostatistics](#)), from the book by Fleming and Harrington ([Fleming, Thomas R. and Harrington, David P., 2005](#)), from kaggle ([fedesoriano](#)), and from the website of the University of Massachusetts ([University of Massachusetts, 1980](#)), and the RCT in prostate cancer patients is available in the R package `subtee` ([Ballarini et al., 2021](#)). The R code for reproducing the results of the simulation study is available on Figshare ().

Supplementary Material A: Parameters used for data simulation

In this section, details regarding data simulations from copula models are given, i.e. correlation matrices and parametric distributions. Comparisons of the true covariate distributions and the fitted distributions are also shown.

Table A.1a: Correlation matrix of the variables in the primary biliary cirrhosis dataset used in the copula model.

	Age	Sex	Presence of ascites	Presence of hepatomegaly	Presence of spiders	Presence of edema	Serum bilirubin	Serum cholesterol	Albumin	Urine copper	Alkaline phosphatase	SGOT	Triglycerides	Platelet count	Prothrombin time	Histologic stage of disease
Age	1	-0.1931	0.216	0.0862	-0.0529	0.1966	0.0386	-0.1493	-0.1953	0.0613	-0.0472	-0.1499	0.0209	-0.1384	0.1963	0.1297
Sex	-0.1931	1	0.0087	0.0509	0.14	0.0371	-0.0385	0.0053	-0.0653	-0.2301	0.0043	-0.0184	-0.0874	0.0855	-0.1211	-0.0268
Presence of ascites	0.216	0.0087	1	0.159	0.1593	0.4257	0.3756	-0.1071	-0.3574	0.218	0.0326	0.0887	0.1348	-0.2184	0.3214	0.3683
Presence of hepatomegaly	0.0862	0.0509	0.159	1	0.283	0.1714	0.4109	0.0957	-0.3083	0.283	0.1686	0.1621	0.1564	-0.2062	0.2144	0.4953
Presence of spiders	-0.0529	0.14	0.1593	0.283	1	0.2427	0.3673	-0.006	-0.2348	0.2704	0.0948	0.1565	0.0091	-0.1588	0.2566	0.3298
Presence of edema	0.1966	0.0371	0.4257	0.1714	0.2427	1	0.3863	-0.1294	-0.3237	0.2124	0.0389	0.106	0.0652	-0.2126	0.3403	0.2814
Serum bilirubin	0.0386	-0.0385	0.3756	0.4109	0.3673	0.3863	1	0.3806	-0.3346	0.4565	0.117	0.4417	0.4185	-0.0868	0.3617	0.3049
Serum cholesterol	-0.1493	0.0053	-0.1071	0.0957	-0.006	-0.1294	0.3806	1	-0.064	0.123	0.1401	0.3372	0.2768	0.178	-0.0294	-0.004
Albumin	-0.1953	-0.0653	-0.3574	-0.3083	-0.2348	-0.3237	-0.3346	-0.064	1	-0.2643	-0.1015	-0.22	-0.0947	0.203	-0.234	-0.2684
Urine copper	0.0613	-0.2301	0.218	0.283	0.2704	0.2124	0.4565	0.123	-0.2643	1	0.1873	0.2936	0.2723	-0.0641	0.2179	0.23
Alkaline phosphatase	-0.0472	0.0043	0.0326	0.1686	0.0948	0.0389	0.117	0.1401	-0.1015	0.1873	1	0.1122	0.1687	0.1428	0.0894	0.0992
SGOT	-0.1499	-0.0184	0.0887	0.1621	0.1565	0.106	0.4417	0.3372	-0.22	0.2936	0.1122	1	0.1194	-0.1195	0.1122	0.1455
Triglycerides	0.0209	-0.0874	0.1348	0.1564	0.0091	0.0652	0.4185	0.2768	-0.0947	0.2723	0.1687	0.1194	1	0.0948	0.0192	0.0749
Platelet count	-0.1384	0.0855	-0.2184	-0.2062	-0.1588	-0.2126	-0.0868	0.178	0.203	-0.0641	0.1428	-0.1195	0.0948	1	-0.2213	-0.1984
Prothrombin time	0.1963	-0.1211	0.3214	0.2144	0.2566	0.3403	0.3617	-0.0294	-0.234	0.2179	0.0894	0.1122	0.0192	-0.2213	1	0.2572
Histologic stage of disease	0.1297	-0.0268	0.3683	0.4953	0.3298	0.2814	0.3049	-0.004	-0.2684	0.23	0.0992	0.1455	0.0749	-0.1984	0.2572	1

Table A.1b: Correlation matrix of the variables in the RCT in prostate cancer patients used in the copula model.

	Age	Standardized weight	Systolic blood pressure	Diastolic blood pressure	Size of primary tumour	Serum prostatic acid phosphatase	Haemoglobin	Gleason stage-grade	Performance status	History of cardiovascular disease	Presence of bone metastases	Prostate cancer stage	Abnormal electrocardiogram
Age	1	-0.0761	0.0863	-0.0727	0.0137	-0.0628	-0.0842	-0.0518	0.0529	0.1699	-0.0717	-0.0125	0.1658
Standardized weight	-0.0761	1	0.1911	0.2265	-0.0440	-0.0654	0.2612	-0.0864	-0.0940	0.0558	-0.1827	-0.0792	0.0148
Systolic blood pressure	0.0863	0.1911	1	0.6289	0.0451	-0.0532	0.0608	-0.0283	0.0538	0.1231	-0.0424	-0.0067	0.1080
Diastolic blood pressure	-0.0727	0.2265	0.6289	1	-0.0474	-0.0605	0.1437	-0.0731	-0.0225	0.0362	-0.0825	-0.0227	0.0775
Size of primary tumour	0.0137	-0.0440	0.0451	-0.0474	1	0.0895	-0.1375	0.3748	0.0704	-0.0876	0.2538	0.2190	0.0183
Serum prostatic acid phosphatase	-0.0628	-0.0654	-0.0532	-0.0605	0.0895	1	-0.1355	0.1531	0.0999	-0.0335	0.3061	0.6594	-0.0122
Haemoglobin	-0.0842	0.2612	0.0608	0.1437	-0.1375	-0.1355	1	-0.1396	-0.1409	0.0108	-0.3004	-0.1241	-0.0245
Gleason stage-grade	-0.0518	-0.0864	-0.0283	-0.0731	0.3748	0.1531	-0.1396	1	0.1277	-0.1474	0.3873	0.6509	-0.0203
Performance status	0.0529	-0.0940	0.0538	-0.0225	0.0704	0.0999	-0.1409	0.1277	1	-0.0653	-0.1919	0.127	-0.0565
History of cardiovascular disease	0.1699	0.0558	0.1231	0.0362	-0.0876	-0.0335	0.0108	-0.1474	-0.0653	1	0.0576	0.0946	0.1849
Presence of bone metastases	-0.0717	-0.1827	-0.0424	-0.0825	0.2538	0.3061	-0.3004	0.3873	-0.1919	0.0576	1	-0.6679	0.0745
Prostate cancer stage	-0.0125	-0.0792	-0.0067	-0.0227	0.2190	0.6594	-0.1241	0.6509	0.127	0.0946	-0.6679	1	-0.0303
Abnormal electrocardiogram	0.1658	0.0148	0.108	0.0775	0.0183	-0.0122	-0.0245	-0.0203	-0.0565	0.1849	0.0745	-0.0303	1

Table A.2a: Univariate distributions from which covariate values are simulated (primary biliary cirrhosis dataset).

Variable	Description	Distribution
Z_2	Age [Years]	$Z_2 \sim \mathcal{TN}(\mu = 50.02, \sigma = 10.58, a = 26.28, b = 78.44)$
Z_3	Sex [0: male, 1: female]	$Z_3 \sim \text{Ber}(p = 0.88)$
Z_4	Presence of ascites [0: no, 1: yes]	$Z_4 \sim \text{Ber}(p = 0.08)$
Z_5	Presence of hepatomegaly [0: no, 1: yes]	$Z_5 \sim \text{Ber}(p = 0.51)$
Z_6	Presence of spiders [0: no, 1: yes]	$Z_6 \sim \text{Ber}(p = 0.29)$
Z_7	Presence of edema ¹⁾	$Z_7 \sim \mathcal{TN}(\mu = 0.11, \sigma = 0.27, a = 0, b = 1)$
Z_8	Serum bilirubin [mg/dl]	$Z_8 \sim \mathcal{TLN}(\log(\mu) = 0.58, \log(\sigma) = 1.03, a = 0.3, b = 28)$
Z_9	Serum cholesterol [mg/dl]	$Z_9 \sim \mathcal{TLN}(\log(\mu) = 5.81, \log(\sigma) = 0.42, a = 120, b = 1775)$
Z_{10}	Albumin [gm/dl]	$Z_{10} \sim \mathcal{TN}(\mu = 3.52, \sigma = 0.42, a = 1.96, b = 4.64)$
Z_{11}	Urine copper [mg/day]	$Z_{11} \sim \mathcal{TEXP}(\lambda = 0.01, b = 488)$
Z_{12}	Alkaline phosphatase [U/liter]	$Z_{12} \sim \mathcal{TLN}(\log(\mu) = 7.27, \log(\sigma) = 0.72, a = 289, b = 13862.4)$
Z_{13}	Aspartate aminotransferase - SGOT [U/ml]	$Z_{13} \sim \mathcal{TLN}(\log(\mu) = 4.71, \log(\sigma) = 0.45, a = 26.35, b = 457.25)$
Z_{14}	Triglycerides [mg/dl]	$Z_{14} \sim \mathcal{TLN}(\log(\mu) = 4.73, \log(\sigma) = 0.43, a = 33, b = 598)$
Z_{15}	Platelet count [# platelets per $m^3/1000$]	$Z_{15} \sim \mathcal{TN}(\mu = 261.94, \sigma = 95.0, a = 62, b = 563)$
Z_{16}	Prothrombin time [sec]	$Z_{16} \sim \mathcal{TLN}(\log(\mu) = 2.37, \log(\sigma) = 0.09, a = 9, b = 17.1)$
Z_{17}	Histologic stage of disease [grade]	$Z_{17} \sim \mathcal{TN}(\mu = 3.03, \sigma = 0.88, a = 1, b = 4)$

Table A.2b: Univariate distributions from which covariate values are simulated (RCT in prostate cancer patients).

Variable	Description	Distribution
AGE	Age [Years]	$\text{AGE} \sim \mathcal{TN}(\mu = 71.56, \sigma = 6.9, a = 48, b = 89)$
WT	Standardized weight	$\text{WT} \sim \mathcal{TLN}(\log(\mu) = 4.58, \log(\sigma) = 0.13, a = 69, b = 152)$
SBP	Systolic blood pressure	$\text{SBP} \sim \mathcal{TLN}(\log(\mu) = 2.65, \log(\sigma) = 0.16, a = 8, b = 30)$
DBP	Diastolic blood pressure	$\text{DBP} \sim \mathcal{TLN}(\log(\mu) = 2.08, \log(\sigma) = 0.18, a = 4, b = 18)$
SZ	Size of primary tumour [centimeters squared]	$\text{SZ} \sim \mathcal{TEXP}(\lambda = 0.07, b = 69)$
AP	Serum (prostatic) acid phosphatase [King-Armstrong units]	$\text{AP} \sim \mathcal{TLN}(\log(\mu) = 2.64, \log(\sigma) = 1.63, a = 1, b = 9999)$
HG	Haemoglobin [g/100ml]	$\text{HG} \sim \mathcal{TN}(\mu = 134.2, \sigma = 19.36, a = 59, b = 182)$
SG	Gleason stage-grade category	$\text{SG} \sim \mathcal{TN}(\mu = 10.3, \sigma = 2.02, a = 5, b = 15)$
PF	Performance status	$\text{PF} \sim \mathcal{B}(p = 0.1)$
HX	History of cardiovascular disease [0: no, 1: yes]	$\text{HX} \sim \mathcal{B}(p = 0.43)$
BM	Presence of bone metastases [0: no, 1: yes]	$\text{BM} \sim \mathcal{B}(p = 0.16)$
EKG	Abnormal electrocardiogram [0: normal, 1: abnormal]	$\text{EKG} \sim \mathcal{B}(p = 0.66)$

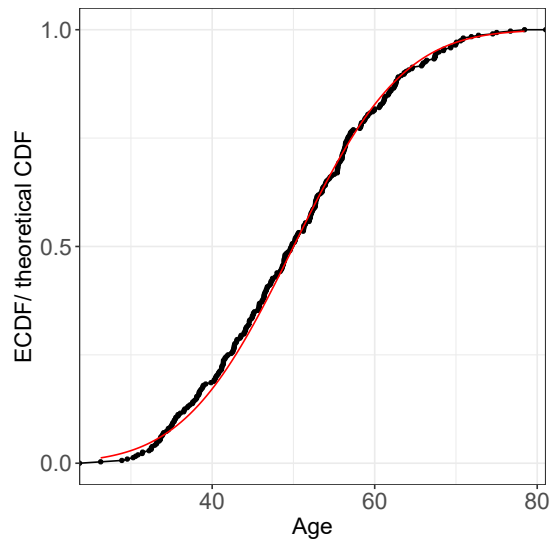
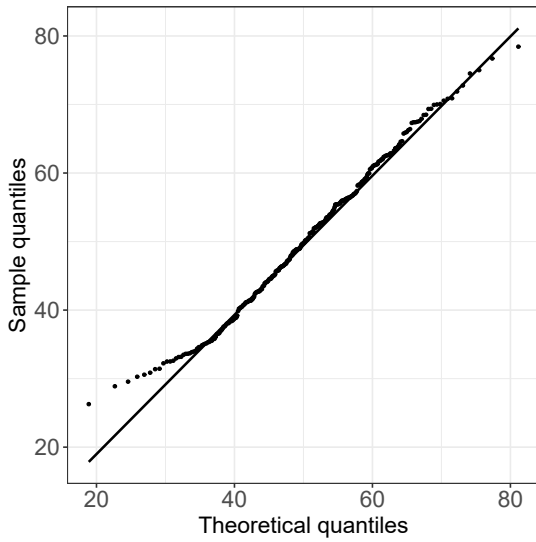


Fig. A.1a Distribution of age compared to the truncated normal distribution with $\mu = 50.02$, and $\sigma = 10.58$.

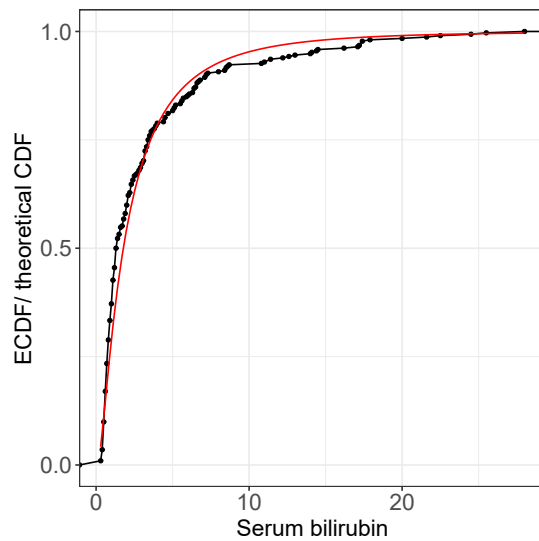
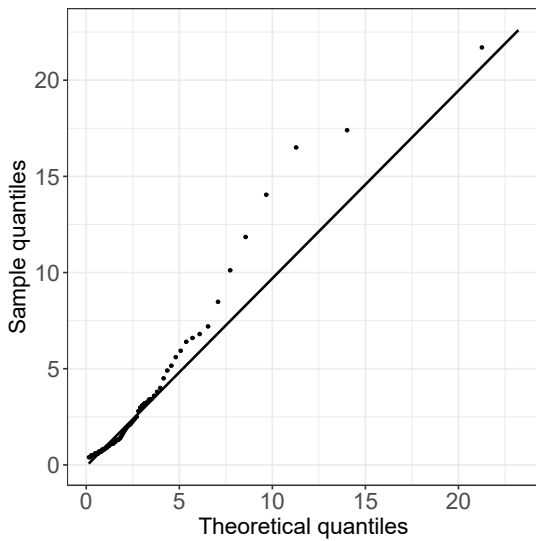


Fig. A.1b Distribution of serum bilirubin compared to the truncated log-normal distribution with $\log(\mu) = 0.58$, and $\log(\sigma) = 1.03$.

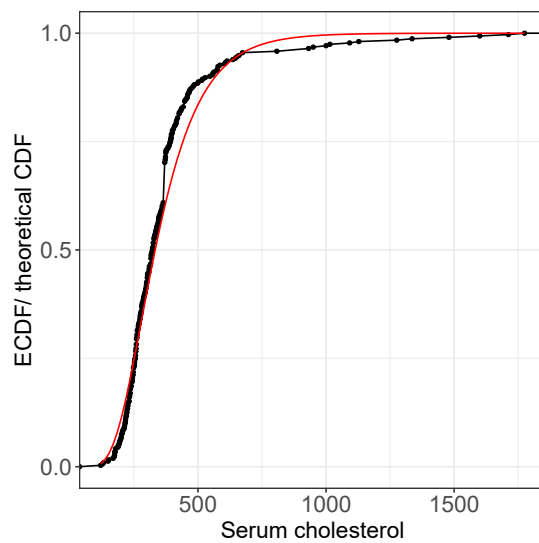
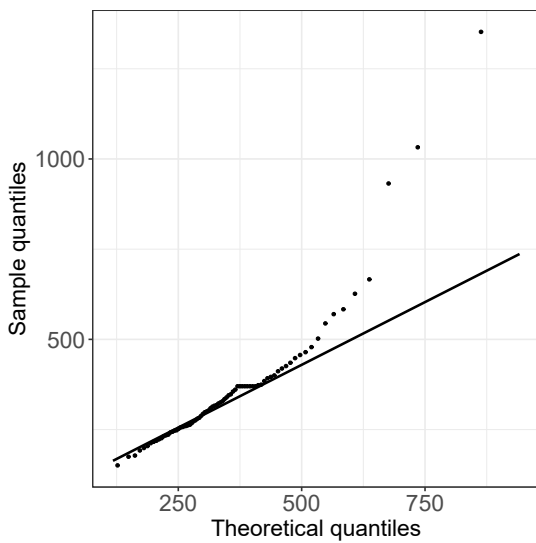


Fig. A.1c Distribution of serum cholesterol compared to the truncated log-normal distribution with $\log(\mu) = 5.81$, and $\log(\sigma) = 0.42$.

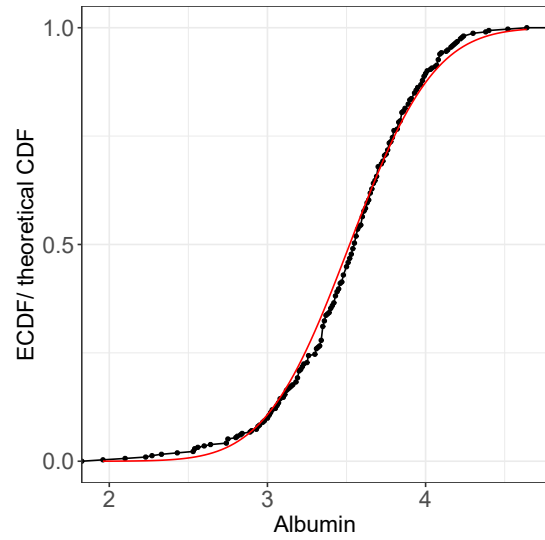
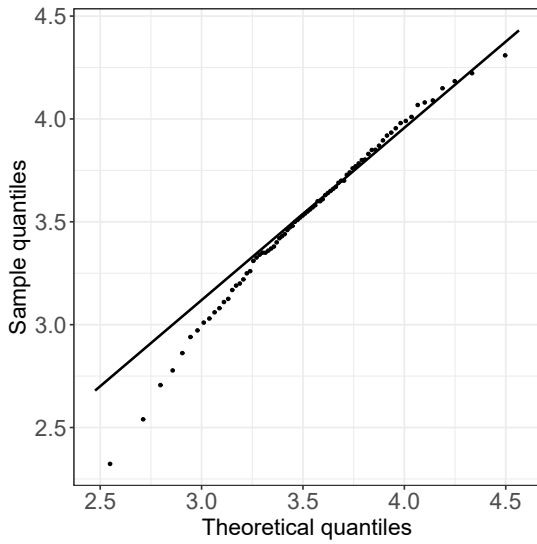


Fig. A.1d Distribution of triglycerides compared to the truncated normal distribution with $\mu = 3.52$, and $\sigma = 0.42$.

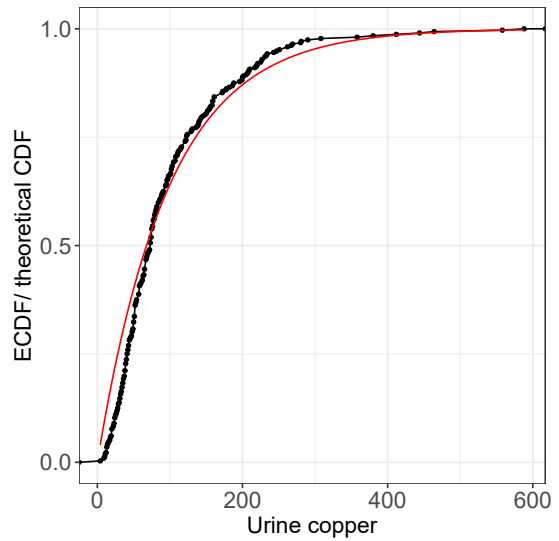
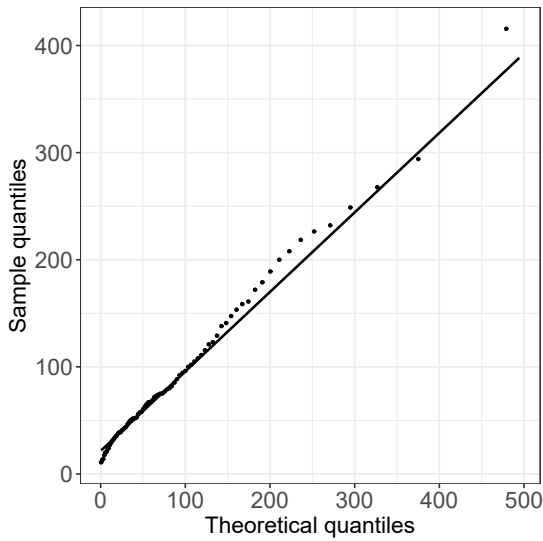


Fig. A.1e Distribution of urine copper compared to the truncated exponential distribution with $\lambda = 0.01$.

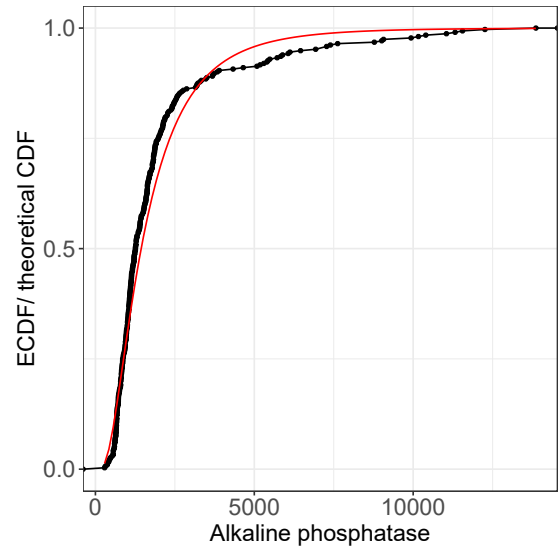
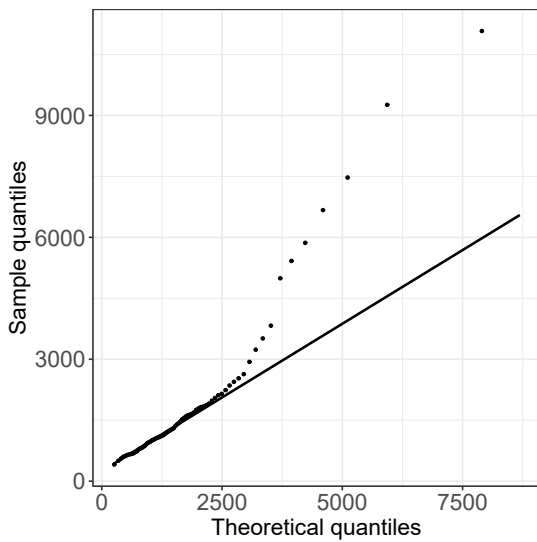


Fig. A.1f Distribution of alkaline phosphatase compared to the truncated log-normal distribution with $\log(\mu) = 7.27$, and $\log(\sigma) = 0.72$.

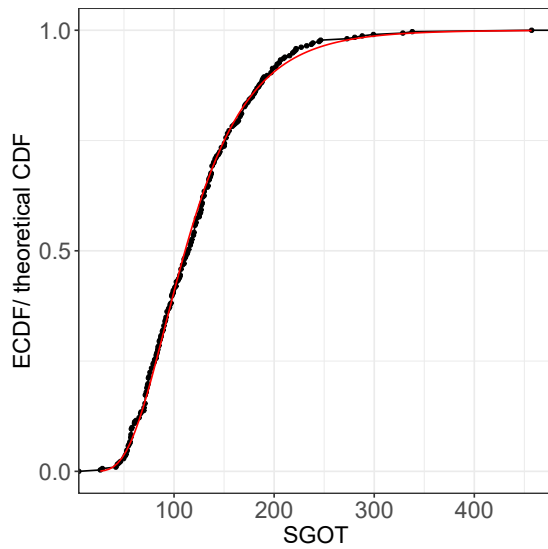
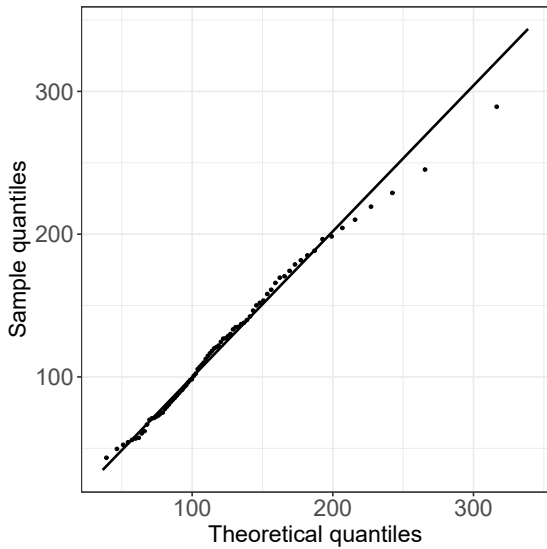


Fig. A.1g Distribution of SGOT compared to the truncated log-normal distribution with $\log(\mu) = 4.71$, and $\log(\sigma) = 0.45$.

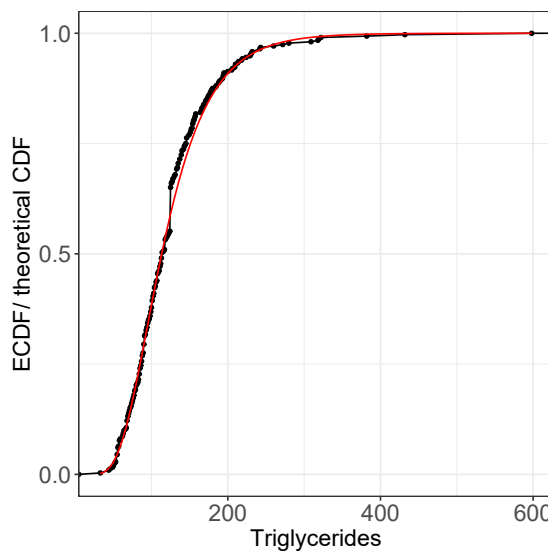
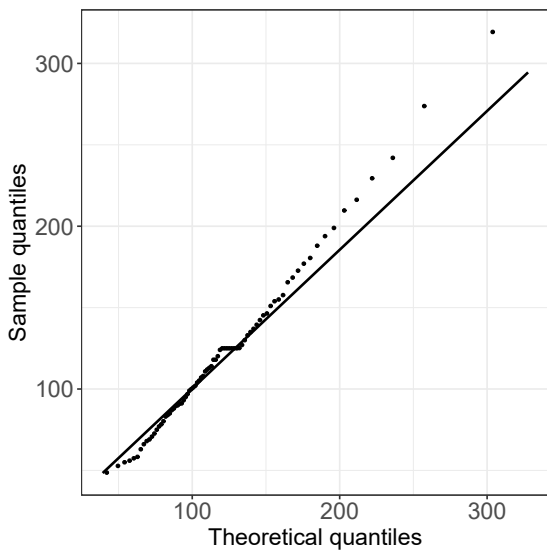


Fig. A.1h Distribution of triglycerides compared to the truncated log-normal distribution with $\log(\mu) = 4.73$, and $\log(\sigma) = 0.43$.

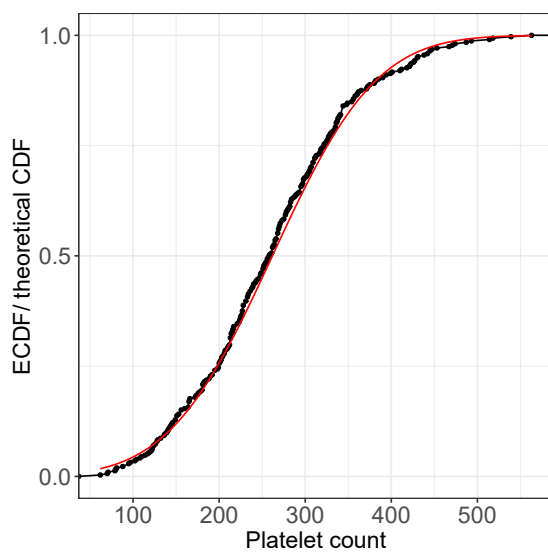
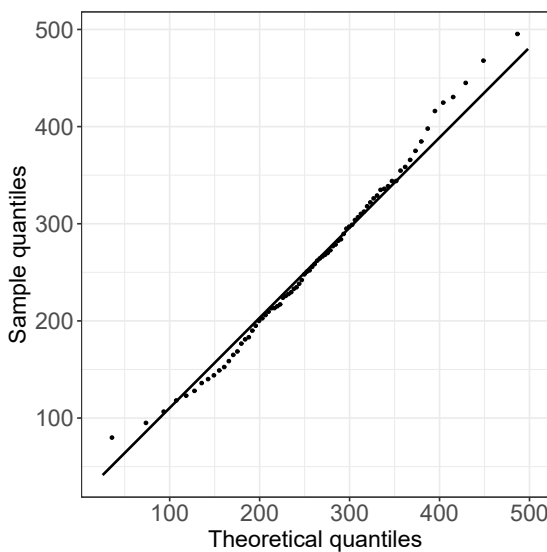


Fig. A.1i: Distribution of platelet count compared to the truncated normal distribution with $\mu = 261.94$, and $\sigma = 95.0$.

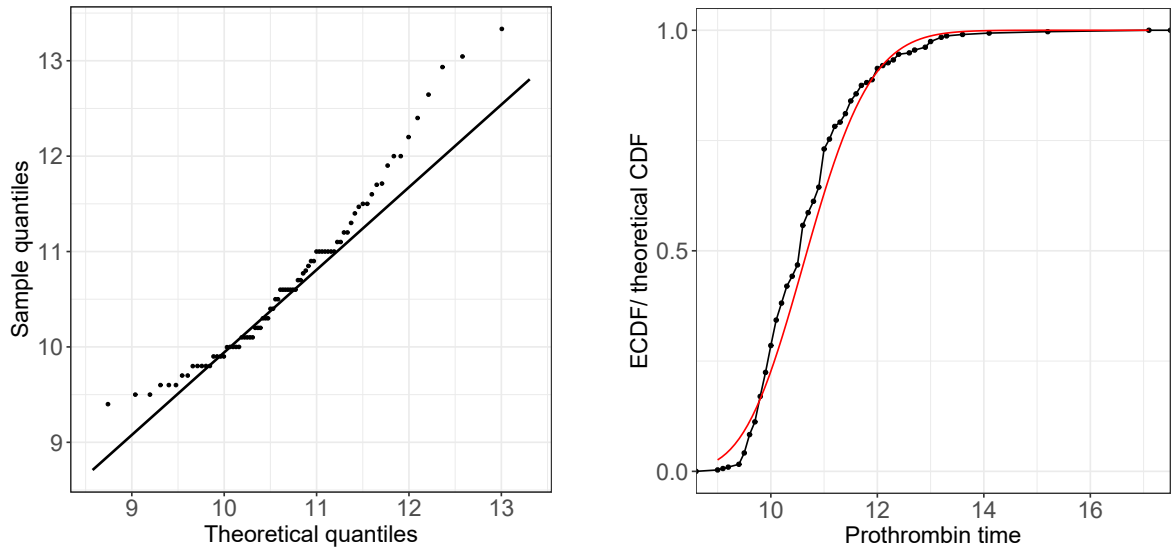


Fig. A.1j: Distribution of prothrombin time compared to the truncated log-normal distribution with $\log(\mu) = 2.37$, and $\log(\sigma) = 0.09$.

A.1: Comparison of the true covariate distribution with the distribution used in the copula model (biliary cirrhosis dataset). QQ-plot (left) and plot comparing the theoretical and empirical cumulative distribution functions (right) based on maximum likelihood estimates of the respective distributional parameters for each continuous variable in the primary biliary cirrhosis dataset. Truncated distributions were fitted with lower and upper limits corresponding to the minimum and maximum value of the variable.

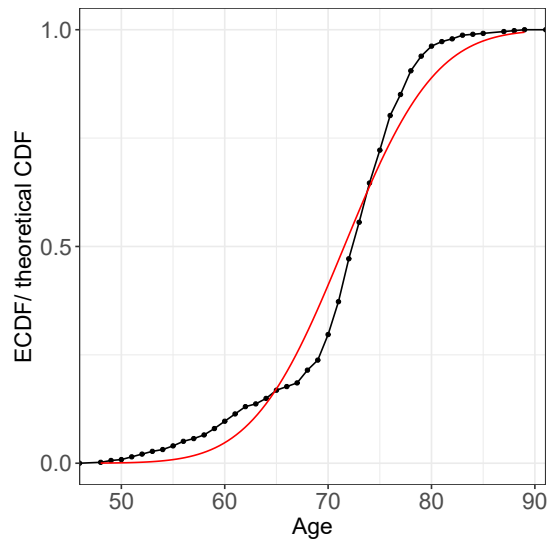
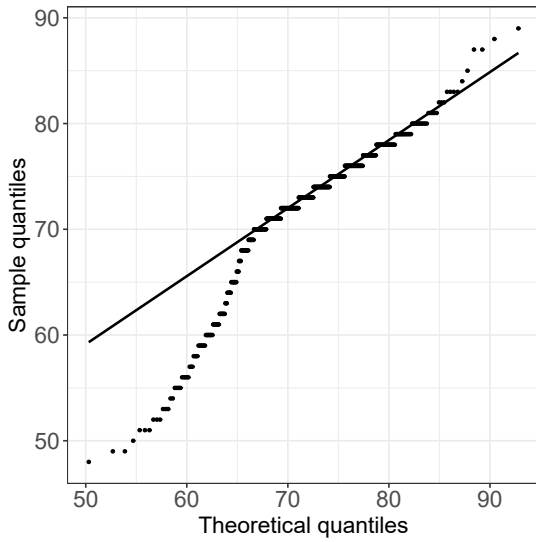


Fig. A.2a Distribution of age compared to the truncated normal distribution with $\mu = 71.56$, and $\sigma = 6.91$.

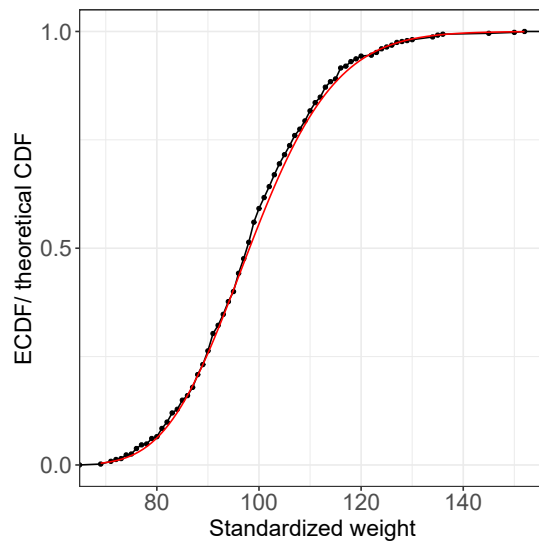
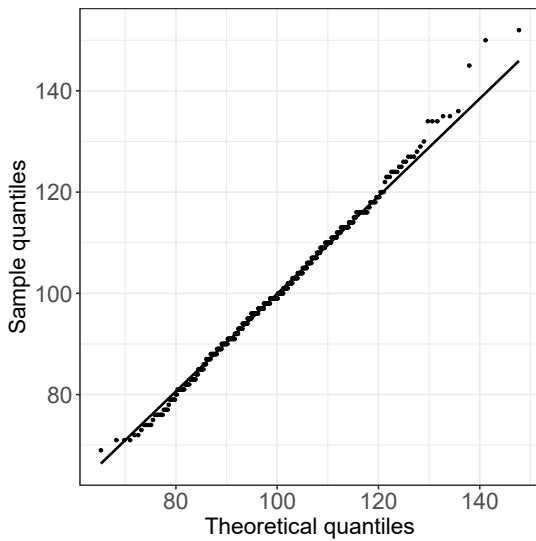


Fig. A.2b Distribution of standardized weight compared to the truncated log-normal distribution with $\log(\mu) = 4.59$, and $\log(\sigma) = 0.13$.

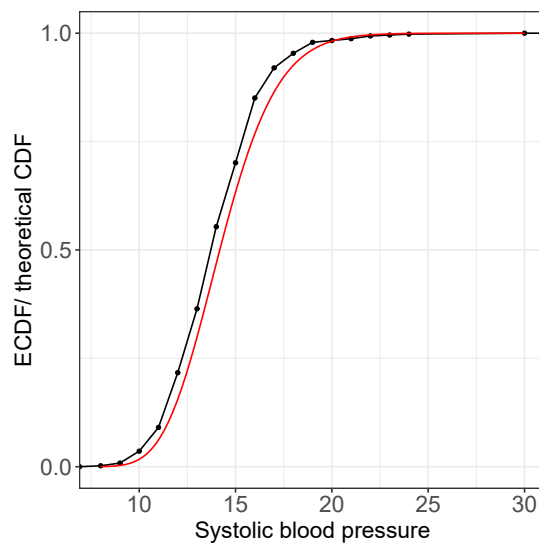
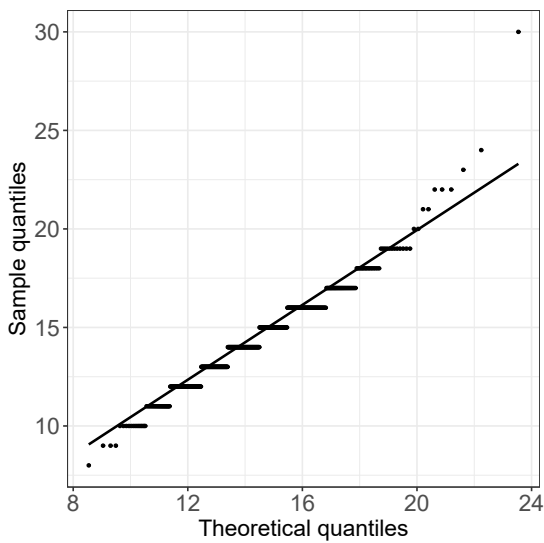


Fig. A.2c Distribution of systolic blood pressure compared to the truncated log-normal distribution with $\log(\mu) = 2.65$, and $\log(\sigma) = 0.16$.

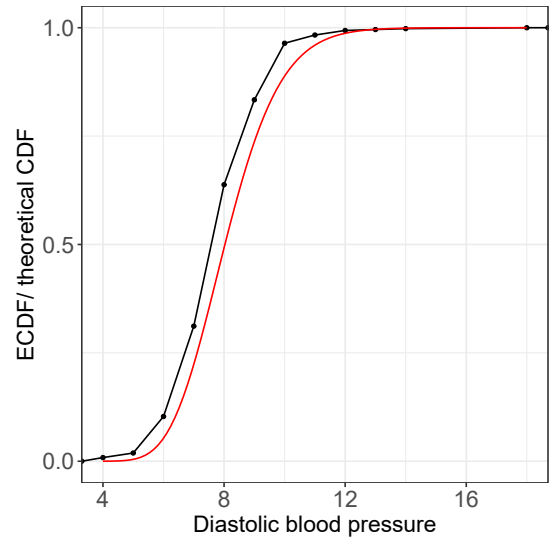
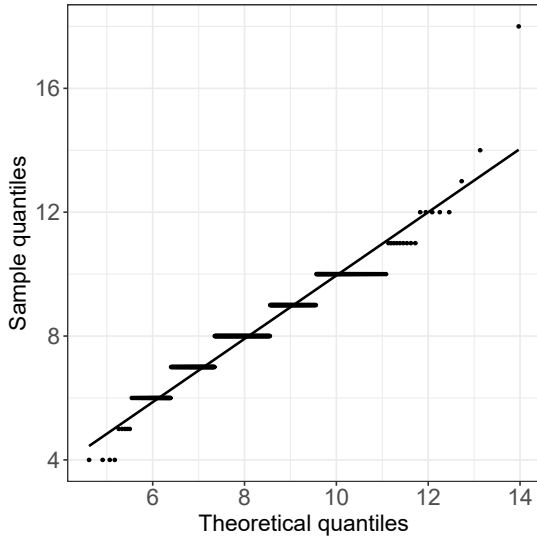


Fig. A.2d Distribution of diastolic blood pressure compared to the truncated log-normal distribution with $\log(\mu) = 2.08$, and $\log(\sigma) = 0.18$.

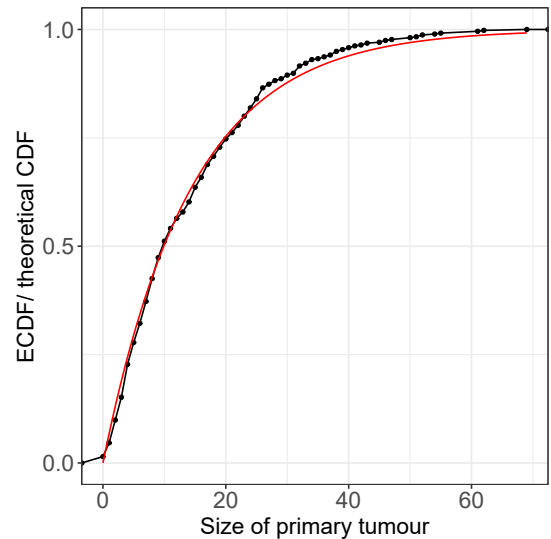
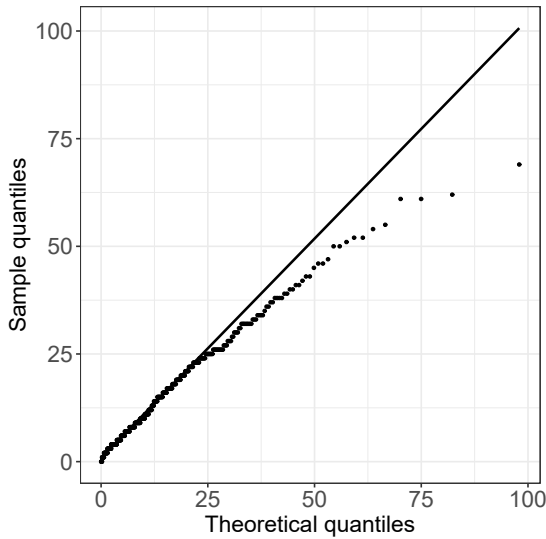


Fig. A.2e Distribution of size of primary tumour compared to the truncated exponential distribution with $\lambda = 0.07$.

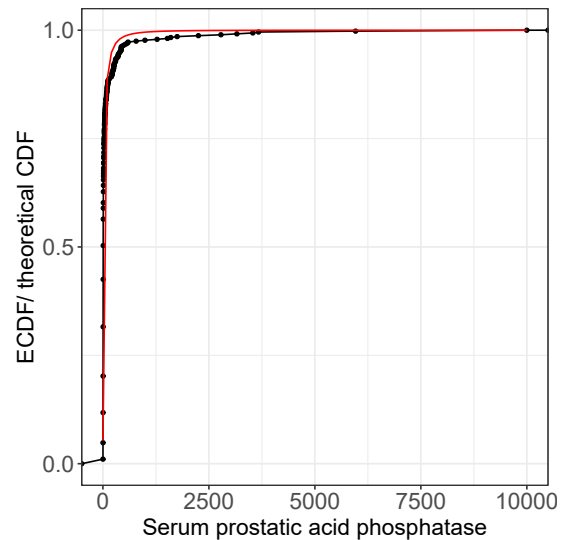
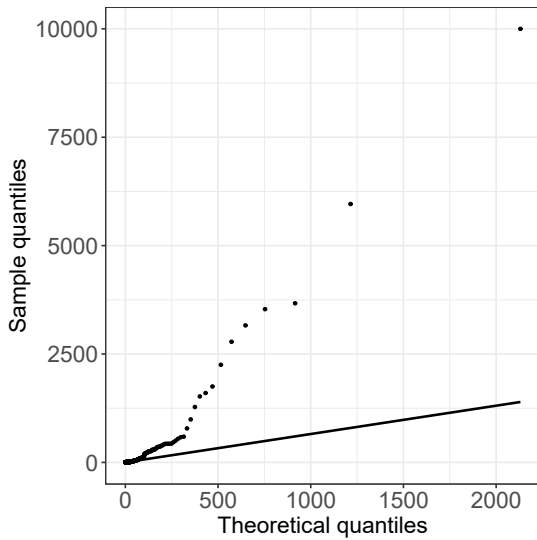


Fig. A.2f Distribution of serum (prostatic) acid phosphatase compared to the truncated log-normal distribution with $\log(\mu) = 2.64$, and $\log(\sigma) = 1.63$.

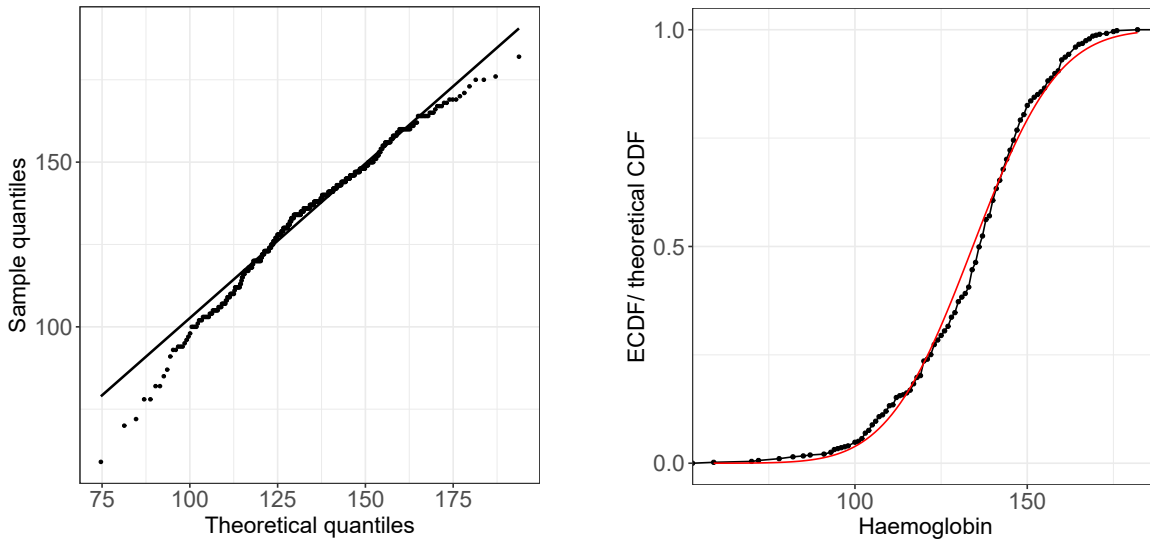


Fig. A.2g Distribution of haemoglobin compared to the truncated normal distribution with $\mu = 134.2$, and $\sigma = 19.36$.

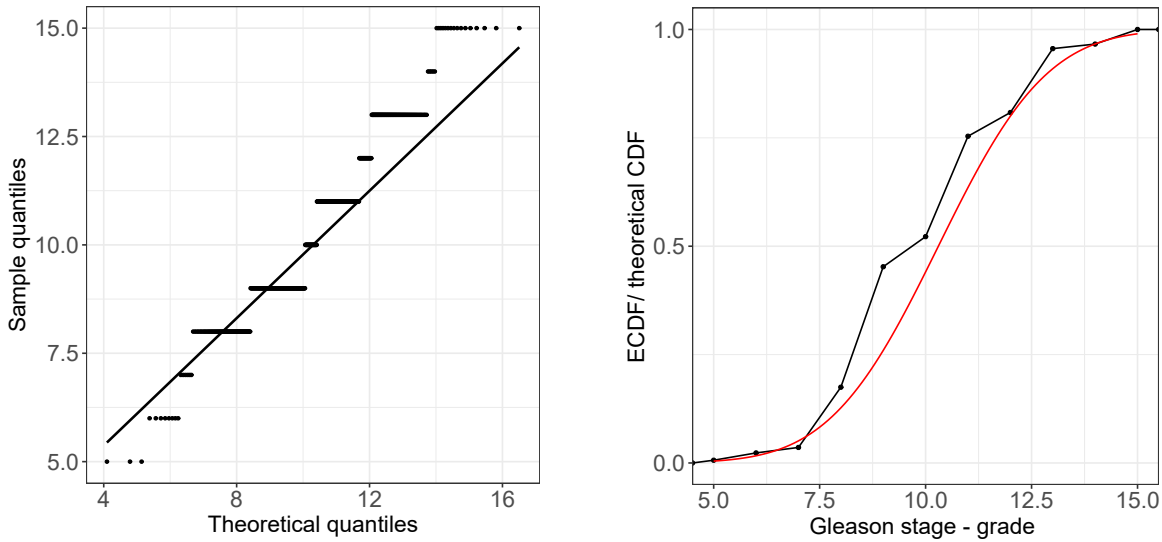


Fig. A.2h Distribution of Gleason stage-grade category compared to the truncated normal distribution with $\mu = 10.3$, and $\sigma = 2.01$.

A.2: Comparison of the true covariate distribution with the distribution used in the copula model (prostate cancer dataset). QQ-plot (left) and plot comparing the theoretical and empirical cumulative distribution functions (right) based on maximum likelihood estimates of the respective distributional parameters for each continuous variable in the prostate cancer dataset. Truncated distributions were fitted with lower and upper limits corresponding to the minimum and maximum value of the variable.

Supplementary Material B: Simulation study results

In this section, full simulation study results of the C index (B.1), Integrated Brier score (B.2), and calibration curves (B.3) are shown, i.e. boxplots of the estimates' distribution and tables of means and standard errors for the 500 simulated datasets per scenario.

B.1: C index

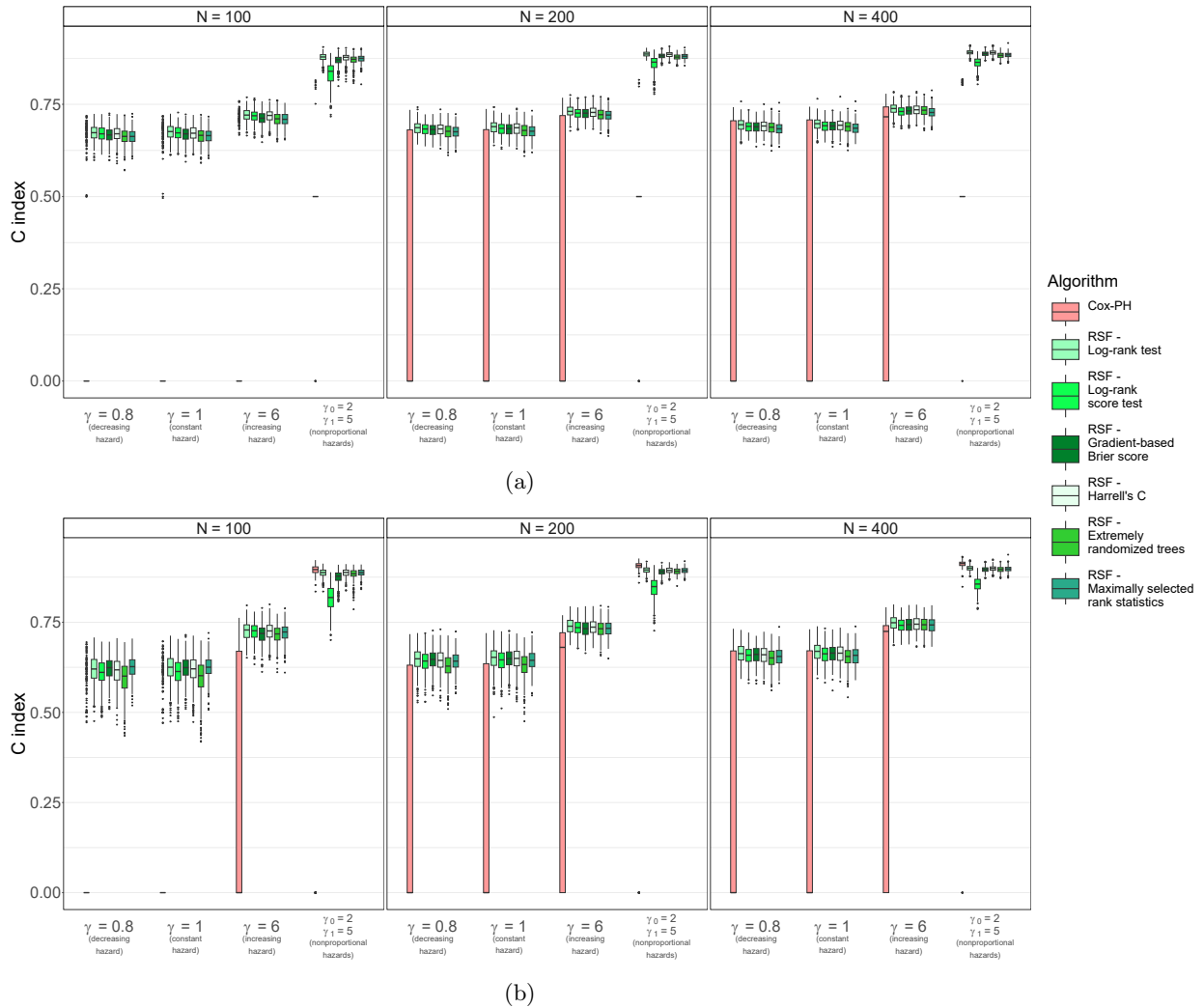


Fig. B.1a: Distribution of C index estimates for the Cox and RSF model when applied to the simulated data (primary biliary cirrhosis dataset, $\beta_{\text{treatment}} = 0$). Boxplots showing the distribution of the C index estimates obtained from 500 simulated datasets based on data without treatment-covariate interactions (primary biliary cirrhosis dataset) for the regression coefficient of the treatment effect $\beta_{\text{treatment}} = 0$. The scale parameter of the Weibull distributed survival times ($\lambda = 2241.74$) is chosen to be constant, shape parameters (γ) vary. Results are shown for different total sample sizes N , and censoring rates (a: 30%, b: 60%).

Abbreviations: Cox-PH - Cox proportional hazards model, RSF - Random survival forest.

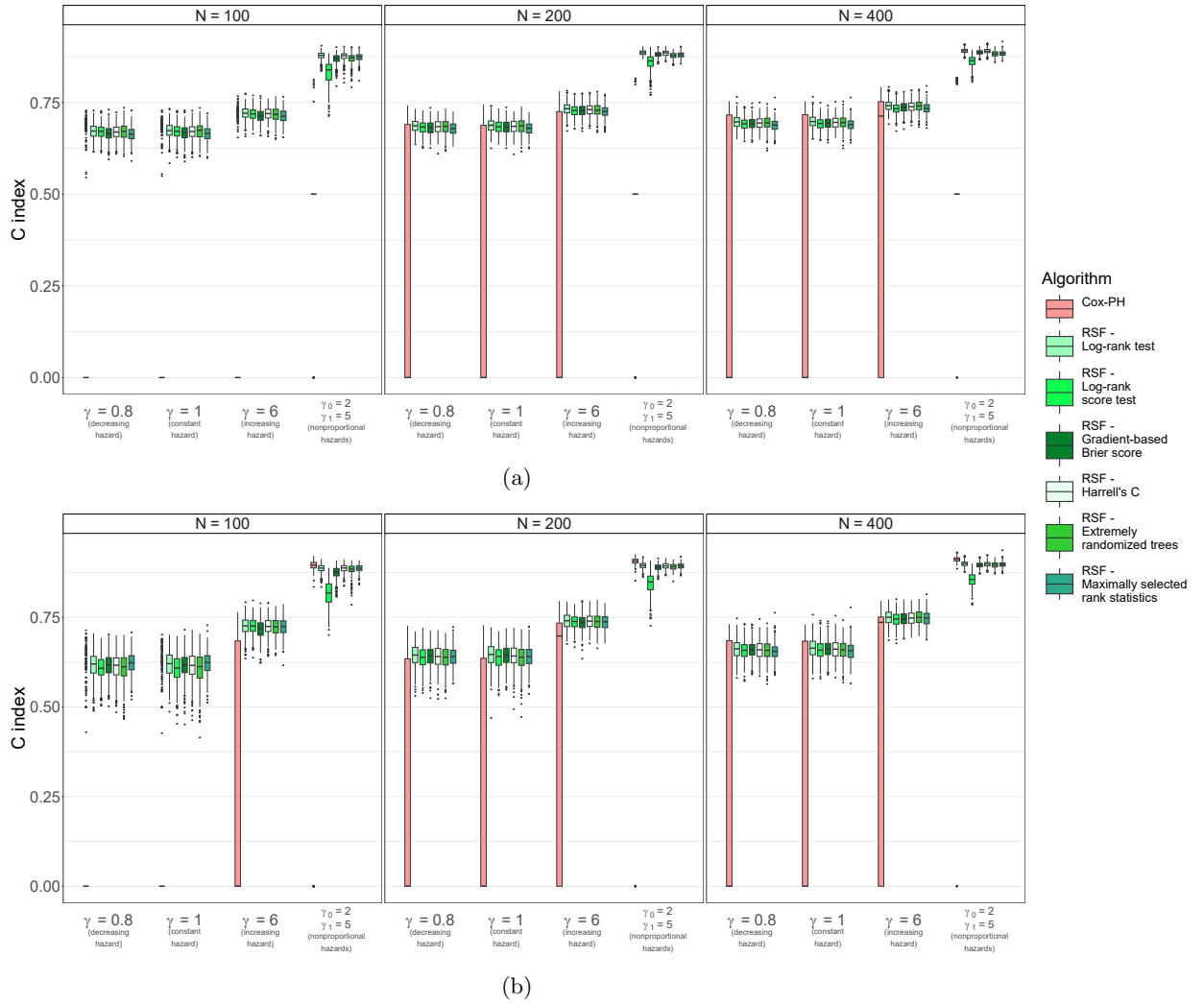


Fig. B.1b: Distribution of C index estimates for the Cox and RSF model when applied to the simulated data (primary biliary cirrhosis dataset, $\beta_{\text{treatment}} = 0.8$). Boxplots showing the distribution of the C index estimates obtained from 500 simulated datasets based on data without treatment-covariate interactions (primary biliary cirrhosis dataset) for the regression coefficient of the treatment effect $\beta_{\text{treatment}} = 0.8$. The scale parameter of the Weibull distributed survival times ($\lambda = 2241.74$) is chosen to be constant, shape parameters (γ) vary. Results are shown for different total sample sizes N , and censoring rates (a: 30%, b: 60%).

Abbreviations: Cox-PH - Cox proportional hazards model, RSF - Random survival forest.

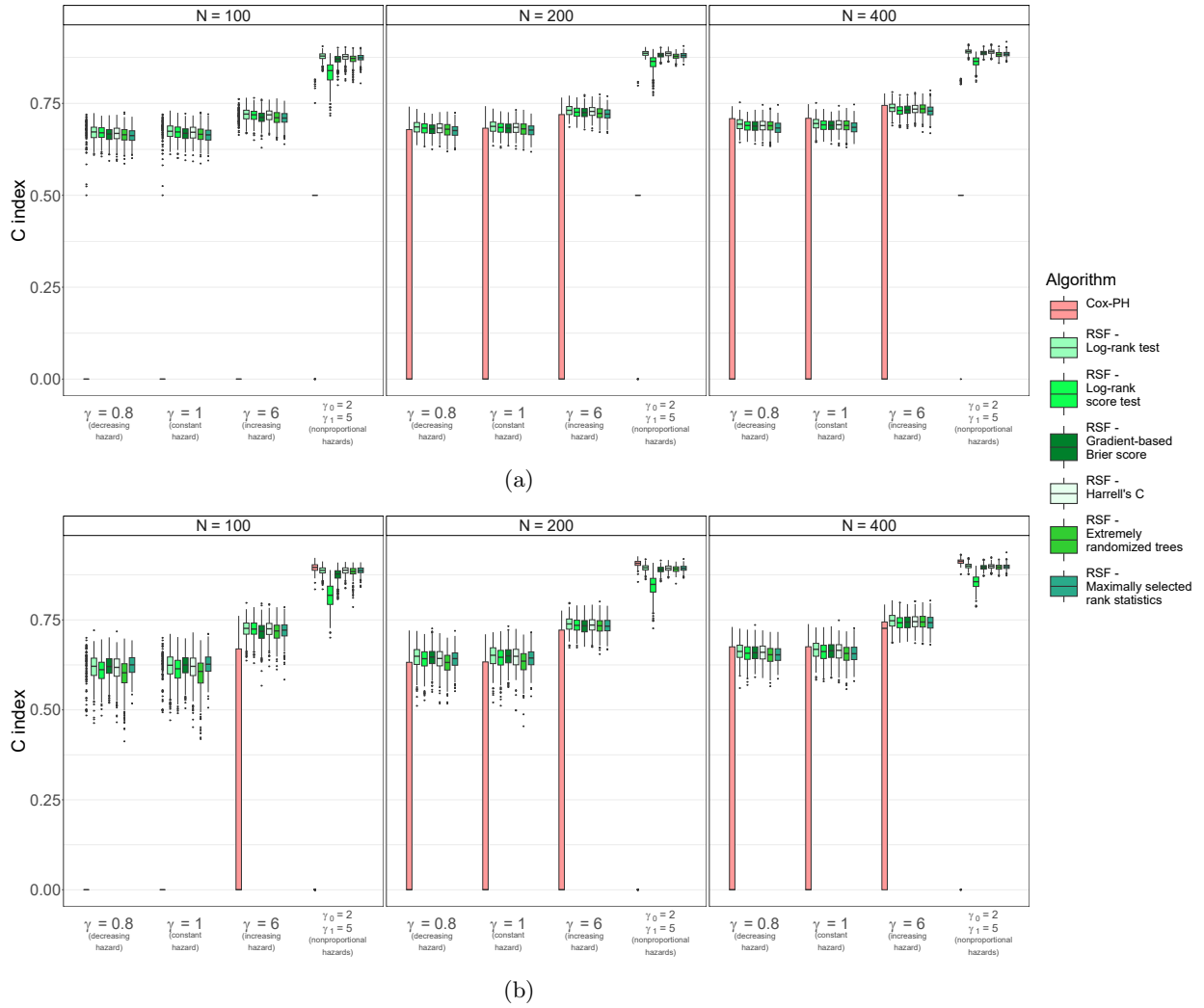


Fig. B.1c: Distribution of C index estimates for the Cox and RSF model when applied to the simulated data (primary biliary cirrhosis dataset, $\beta_{\text{treatment}} = -0.4$). Boxplots showing the distribution of the C index estimates obtained from 500 simulated datasets based on data without treatment-covariate interactions (primary biliary cirrhosis dataset) for the regression coefficient of the treatment effect $\beta_{\text{treatment}} = -0.4$. The scale parameter of the Weibull distributed survival times ($\lambda = 2241.74$) is chosen to be constant, shape parameters (γ) vary. Results are shown for different total sample sizes N , and censoring rates (a: 30%, b: 60%).

Abbreviations: Cox-PH - Cox proportional hazards model, RSF - Random survival forest.

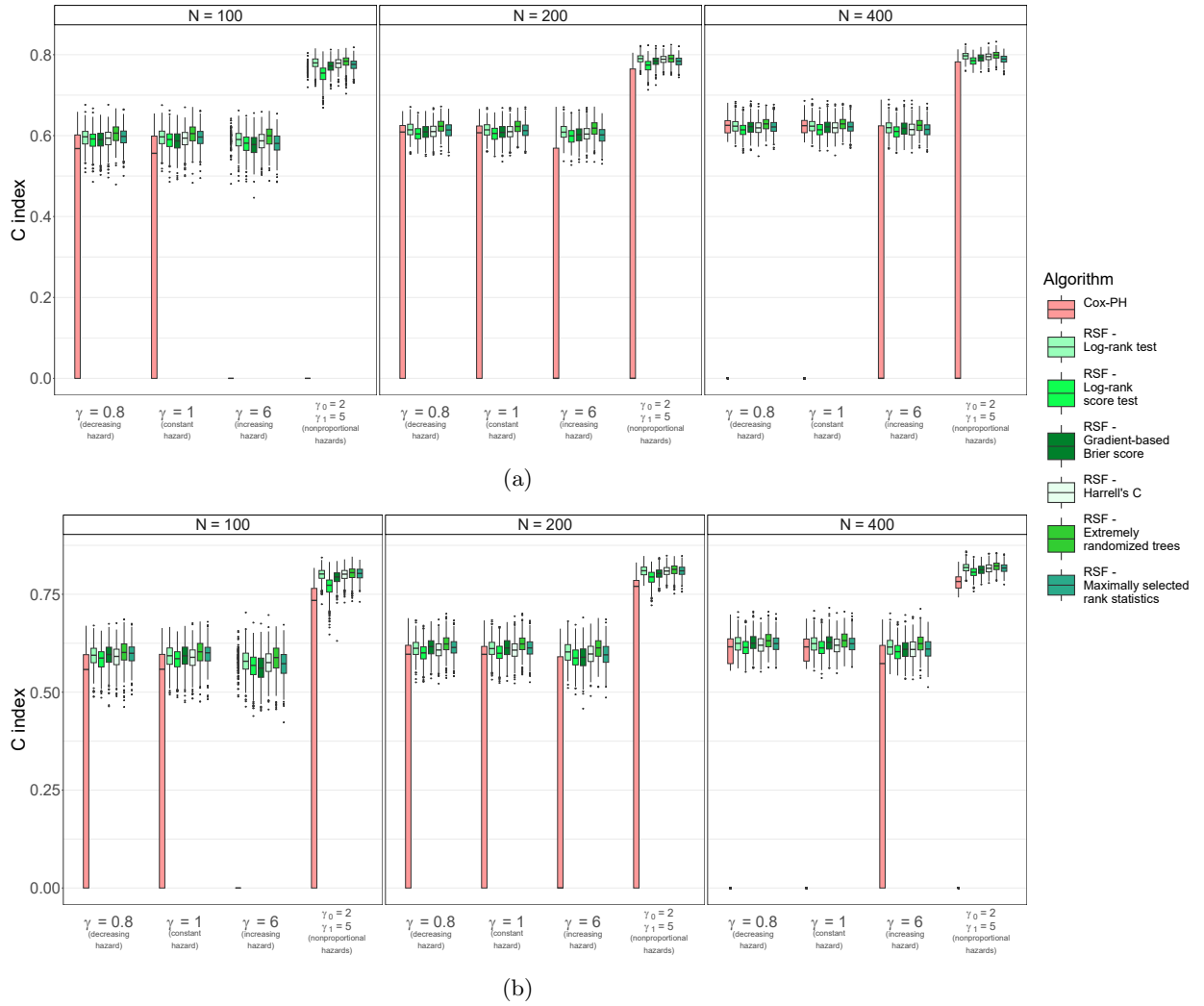


Fig. B.2a: Distribution of C index estimates for the Cox and RSF model when applied to the simulated data (prostate cancer dataset, $\beta_{\text{treatment}} = 0$). Boxplots showing the distribution of the C index estimates obtained from 500 simulated datasets based on data with three treatment-covariate interactions (prostate cancer dataset) for the regression coefficient of the treatment effect $\beta_{\text{treatment}} = 0$. The scale parameter of the Weibull distributed survival times ($\lambda = 39.2$) is chosen to be constant, shape parameters (γ) vary. Results are shown for different total sample sizes N , and censoring rates (a: 30%, b: 60%).

Abbreviations: Cox-PH - Cox proportional hazards model, RSF - Random survival forest.

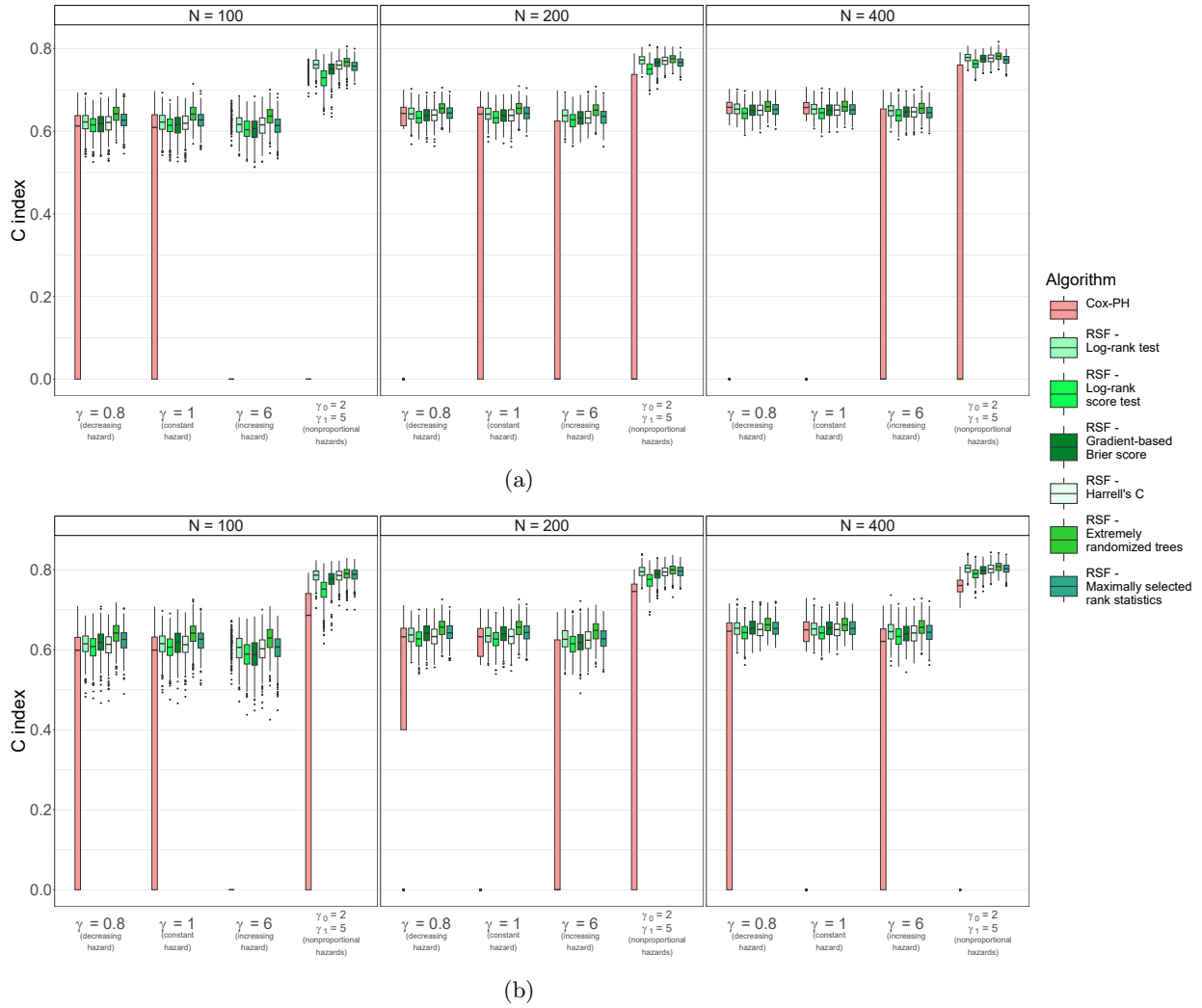


Fig. B.2b: Distribution of C index estimates for the Cox and RSF model when applied to the simulated data (prostate cancer dataset, $\beta_{\text{treatment}} = 0.8$). Boxplots showing the distribution of the C index estimates obtained from 500 simulated datasets based on data with three treatment-covariate interactions (prostate cancer dataset) for the regression coefficient of the treatment effect $\beta_{\text{treatment}} = 0.8$. The scale parameter of the Weibull distributed survival times ($\lambda = 39.2$) is chosen to be constant, shape parameters (γ) vary. Results are shown for different total sample sizes N , and censoring rates (a: 30%, b: 60%).

Abbreviations: Cox-PH - Cox proportional hazards model, RSF - Random survival forest.

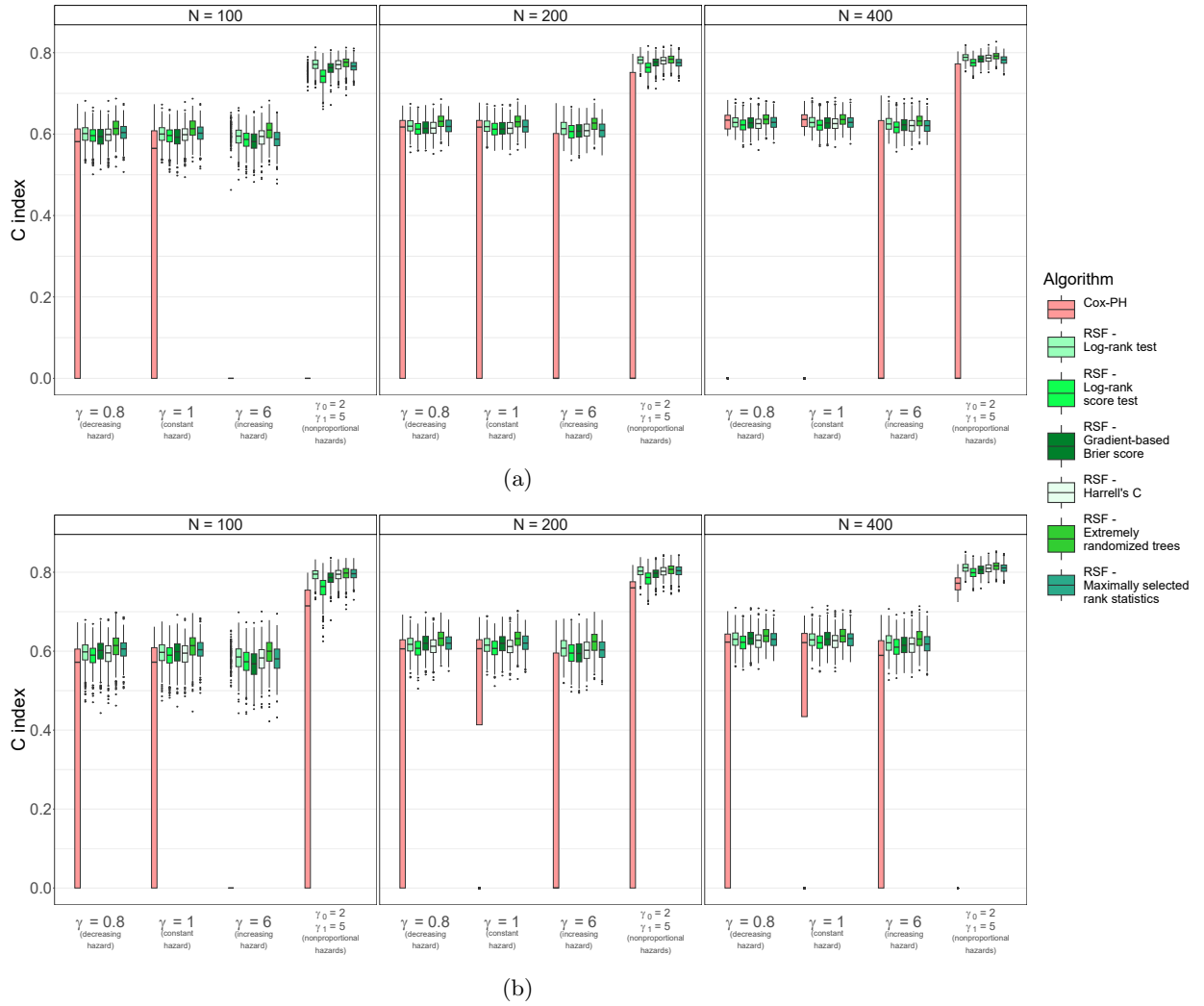


Fig. B.2c: Distribution of C index estimates for the Cox and RSF model when applied to the simulated data (prostate cancer dataset, $\beta_{\text{treatment}} = -0.4$). Boxplots showing the distribution of the C index estimates obtained from 500 simulated datasets based on data with three treatment-covariate interactions (prostate cancer dataset) for the regression coefficient of the treatment effect $\beta_{\text{treatment}} = -0.4$. The scale parameter of the Weibull distributed survival times ($\lambda = 39.2$) is chosen to be constant, shape parameters (γ) vary. Results are shown for different total sample sizes N , and censoring rates (a: 30%, b: 60%).

Abbreviations: Cox-PH - Cox proportional hazards model, RSF - Random survival forest.

B.2: Integrated Brier score (IBS)

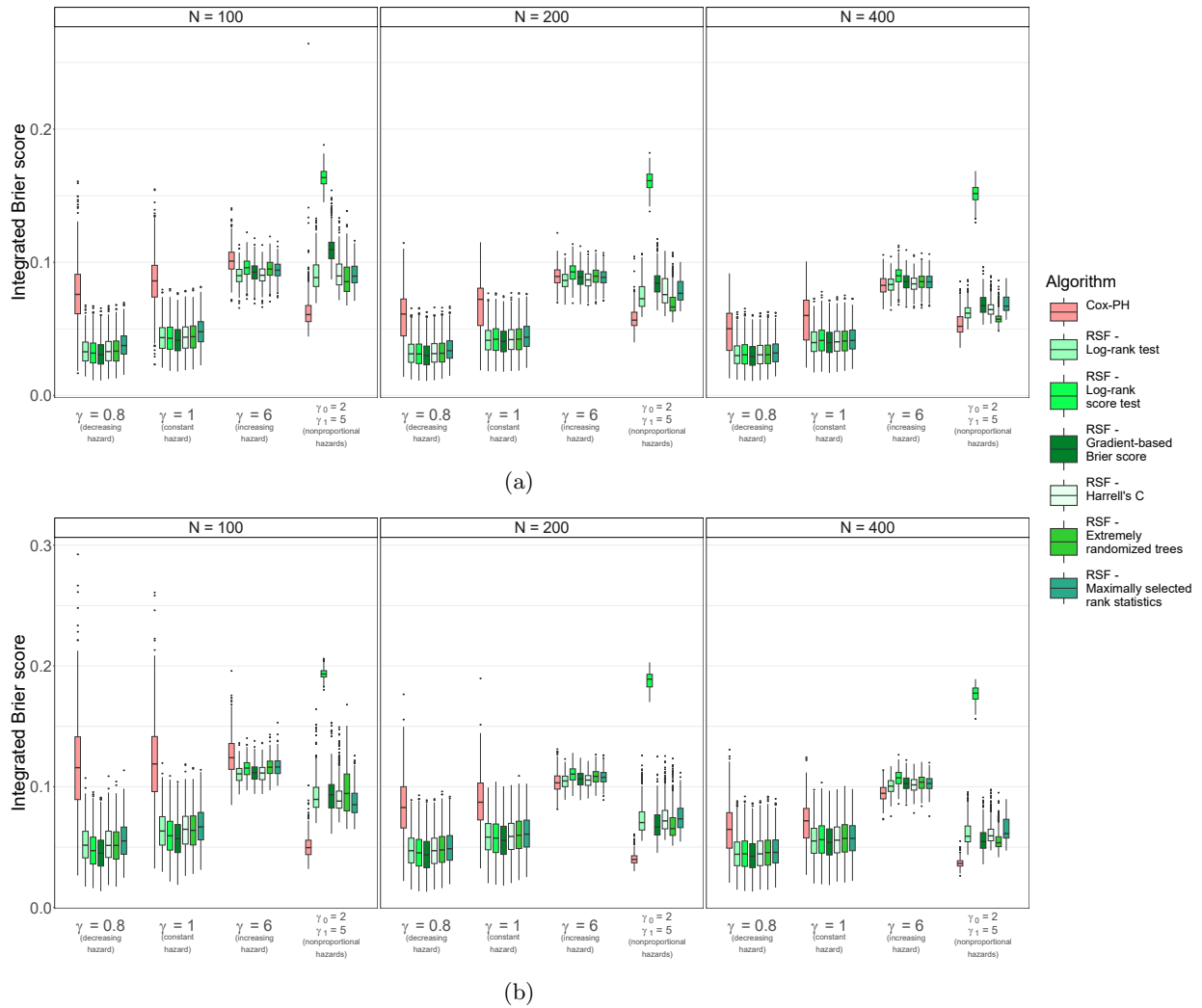


Fig. B.3a: Distribution of Integrated Brier score (IBS) estimates for the Cox and RSF model when applied to the simulated data (primary biliary cirrhosis dataset, $\beta_{\text{treatment}} = 0$). Boxplots showing the distribution of the Integrated Brier score (IBS) estimates obtained from 500 simulated datasets based on data without treatment-covariate interactions (primary biliary cirrhosis dataset) for the regression coefficient of the treatment effect $\beta_{\text{treatment}} = 0$. The scale parameter of the Weibull distributed survival times ($\lambda = 2241.74$) is chosen to be constant, shape parameters (γ) vary. Results are shown for different total sample sizes N , and censoring rates (a: 30%, b: 60%).

Abbreviations: Cox-PH - Cox proportional hazards model, RSF - Random survival forest.

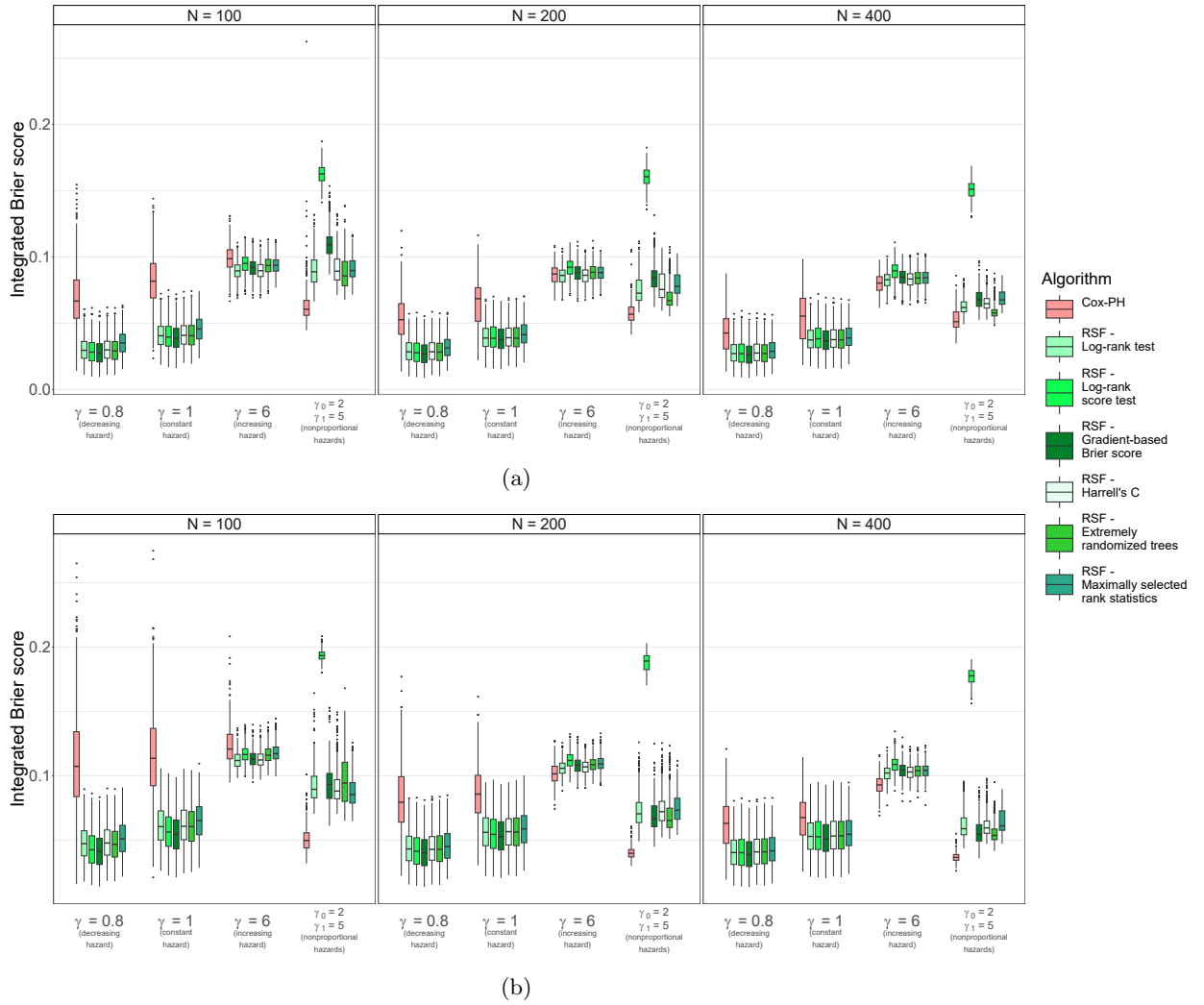


Fig. B.3b: Distribution of Integrated Brier score (IBS) estimates for the Cox and RSF model when applied to the simulated data (primary biliary cirrhosis dataset, $\beta_{\text{treatment}} = 0.8$). Boxplots showing the distribution of the Integrated Brier score (IBS) estimates obtained from 500 simulated datasets based on data without treatment-covariate interactions (primary biliary cirrhosis dataset) for the regression coefficient of the treatment effect $\beta_{\text{treatment}} = 0.8$. The scale parameter of the Weibull distributed survival times ($\lambda = 2241.74$) is chosen to be constant, shape parameters (γ) vary. Results are shown for different total sample sizes N , and censoring rates (a: 30%, b: 60%).

Abbreviations: Cox-PH - Cox proportional hazards model, RSF - Random survival forest.

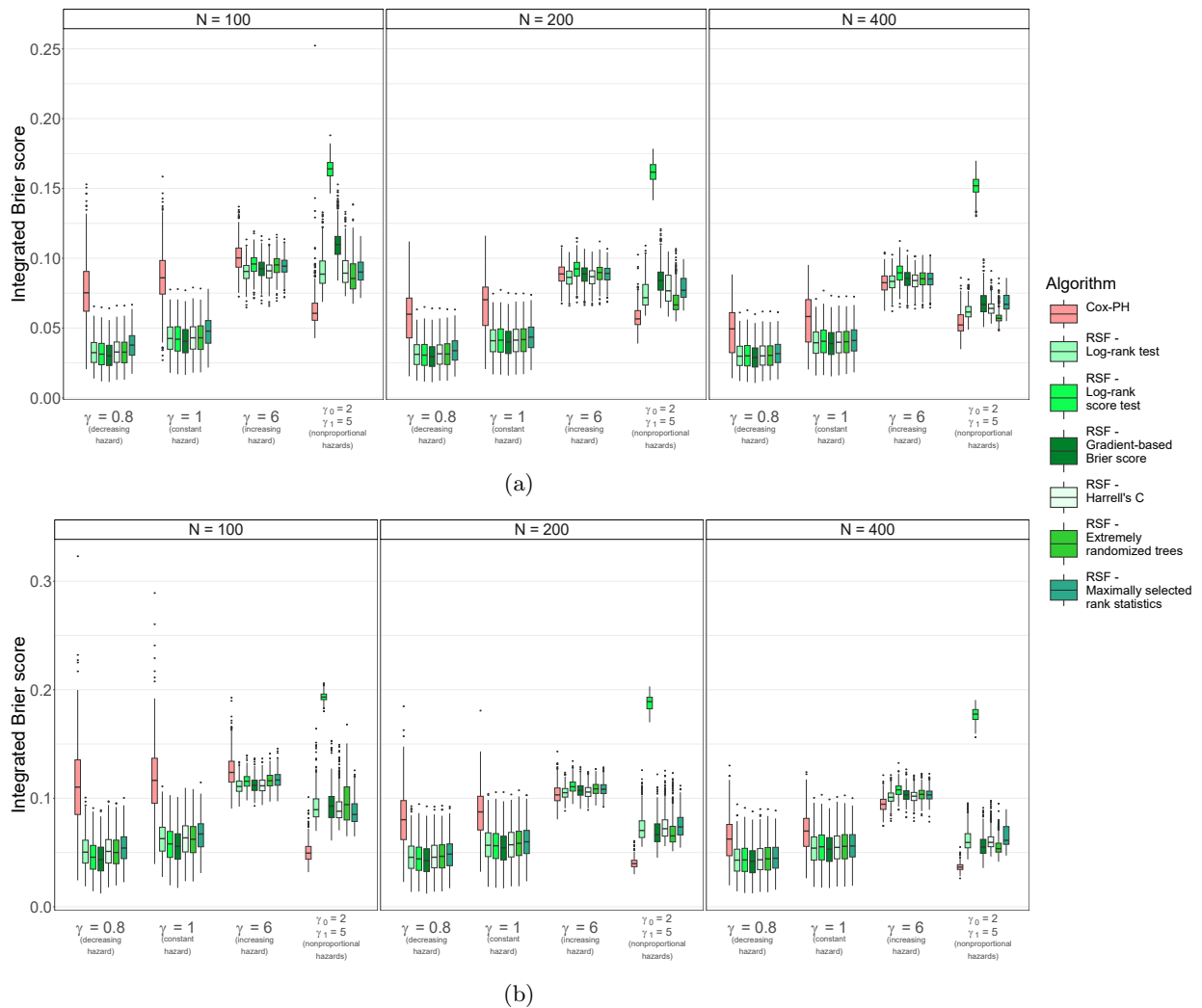


Fig. B.3c: Distribution of Integrated Brier score (IBS) estimates for the Cox and RSF model when applied to the simulated data (primary biliary cirrhosis dataset, $\beta_{\text{treatment}} = -0.4$). Boxplots showing the distribution of the Integrated Brier score (IBS) estimates obtained from 500 simulated datasets based on data without treatment-covariate interactions (primary biliary cirrhosis dataset) for the regression coefficient of the treatment effect $\beta_{\text{treatment}} = -0.4$. The scale parameter of the Weibull distributed survival times ($\lambda = 2241.74$) is chosen to be constant, shape parameters (γ) vary. Results are shown for different total sample sizes N , and censoring rates (a: 30%, b: 60%).

Abbreviations: Cox-PH - Cox proportional hazards model, RSF - Random survival forest.

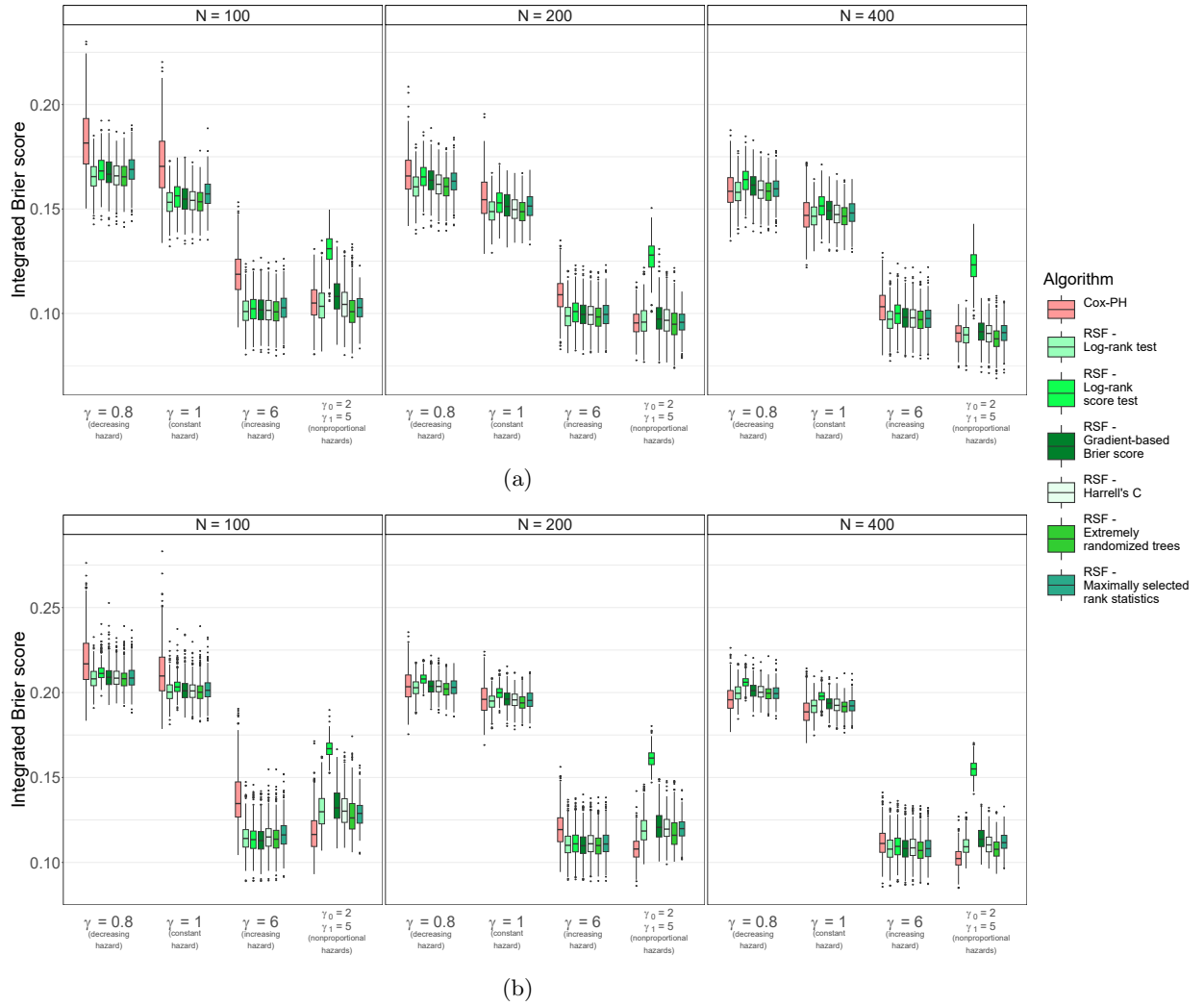


Fig. B.4a: Distribution of Integrated Brier score (IBS) estimates for the Cox and RSF model when applied to the simulated data (prostate cancer dataset, $\beta_{\text{treatment}} = 0$). Boxplots showing the distribution of the Integrated Brier score (IBS) estimates obtained from 500 simulated datasets based on data with three treatment-covariate interactions (prostate cancer dataset) for the regression coefficient of the treatment effect $\beta_{\text{treatment}} = 0$. The scale parameter of the Weibull distributed survival times ($\lambda = 39.2$) is chosen to be constant, shape parameters (γ) vary. Results are shown for different total sample sizes N , and censoring rates (a: 30%, b: 60%).

Abbreviations: Cox-PH - Cox proportional hazards model, RSF - Random survival forest.

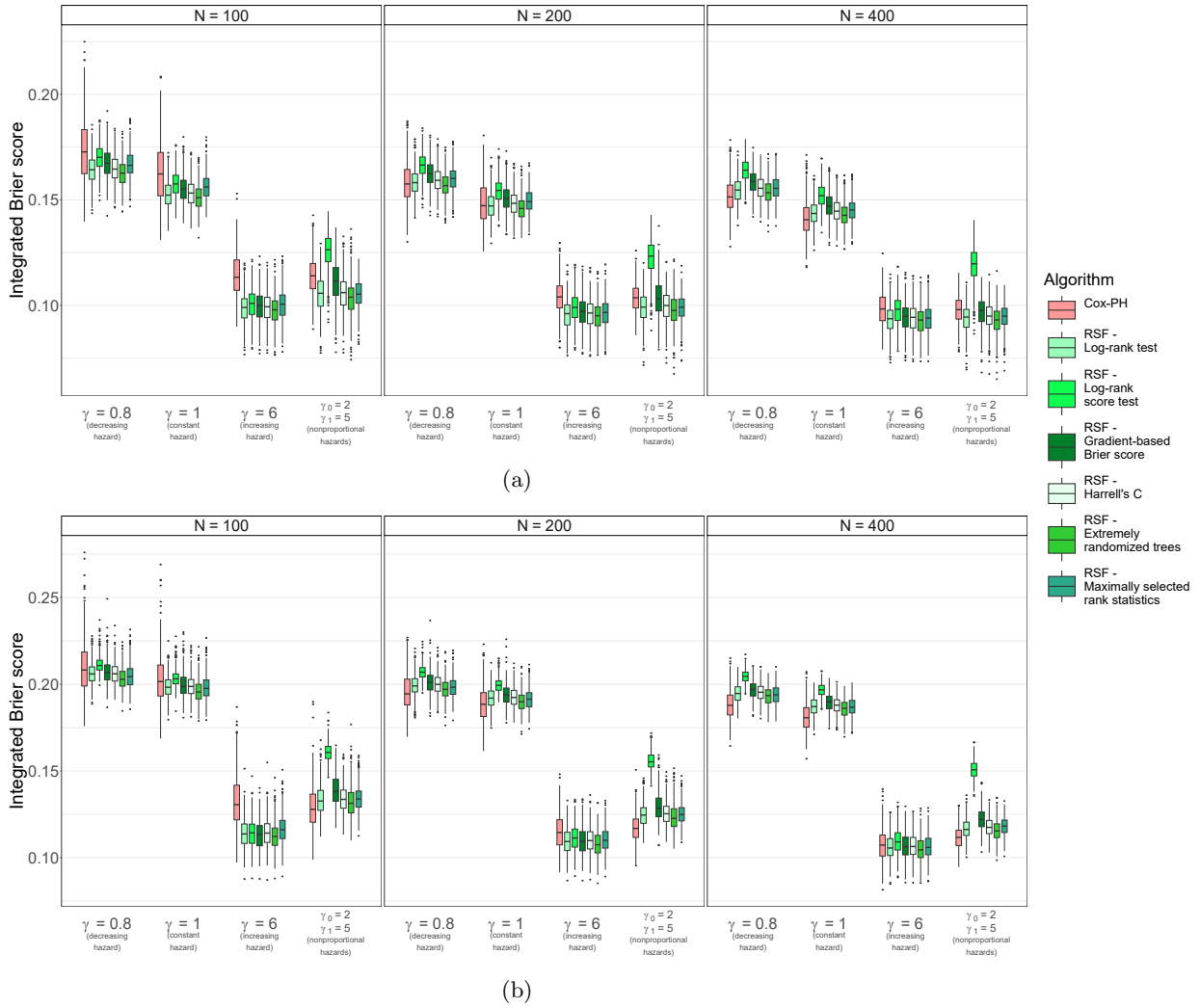


Fig. B.4b: Distribution of Integrated Brier score (IBS) estimates for the Cox and RSF model when applied to the simulated data (prostate cancer dataset, $\beta_{\text{treatment}} = 0.8$). Boxplots showing the distribution of the Integrated Brier score (IBS) estimates obtained from 500 simulated datasets based on data with three treatment-covariate interactions (prostate cancer dataset) for the regression coefficient of the treatment effect $\beta_{\text{treatment}} = 0.8$. The scale parameter of the Weibull distributed survival times ($\lambda = 39.2$) is chosen to be constant, shape parameters (γ) vary. Results are shown for different total sample sizes N , and censoring rates (a: 30%, b: 60%).

Abbreviations: Cox-PH - Cox proportional hazards model, RSF - Random survival forest.

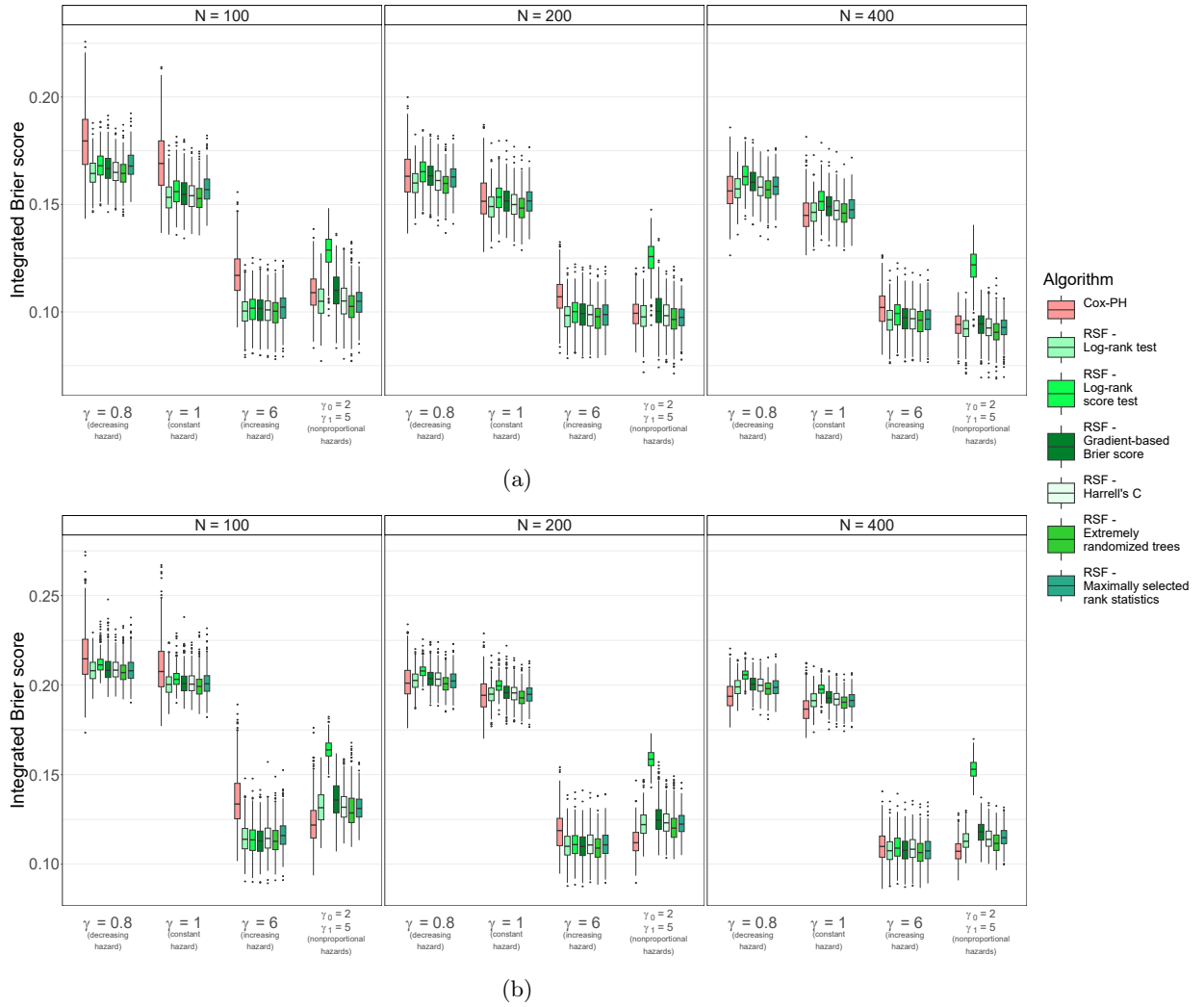


Fig. B.4c: Distribution of Integrated Brier score (IBS) estimates for the Cox and RSF model when applied to the simulated data (prostate cancer dataset, $\beta_{\text{treatment}} = -0.4$). Boxplots showing the distribution of the Integrated Brier score (IBS) estimates obtained from 500 simulated datasets based on data with three treatment-covariate interactions (prostate cancer dataset) for the regression coefficient of the treatment effect $\beta_{\text{treatment}} = -0.4$. The scale parameter of the Weibull distributed survival times ($\lambda = 39.2$) is chosen to be constant, shape parameters (γ) vary. Results are shown for different total sample sizes N , and censoring rates (a: 30%, b: 60%).

Abbreviations: Cox-PH - Cox proportional hazards model, RSF - Random survival forest.

B.3: Calibration curves

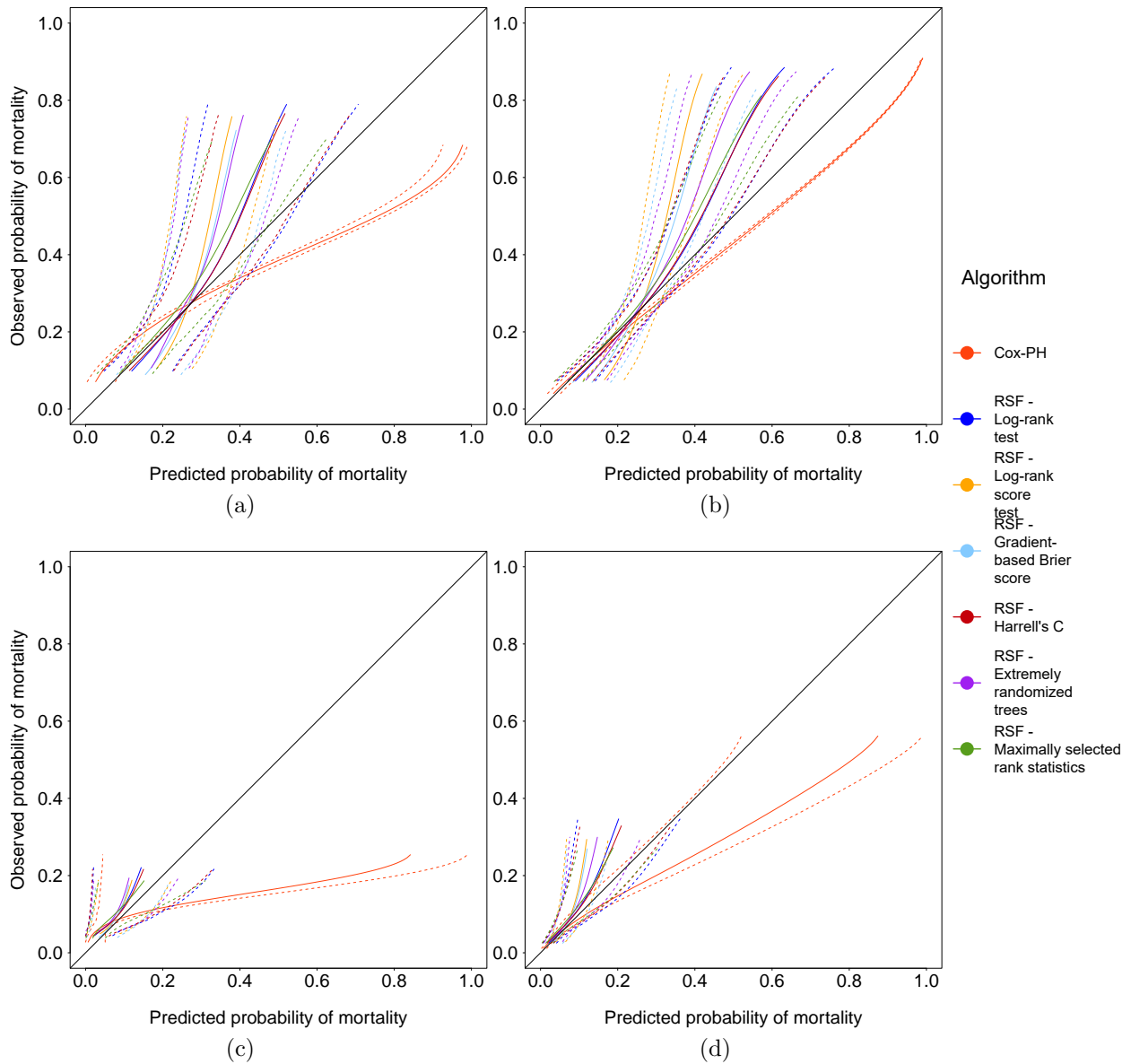


Fig. B.5a: Calibration curves for a proportional hazards scenario (primary biliary cirrhosis dataset). Calibration curves at the median (50% quantile) survival time for a proportional hazards setting (Weibull survival time distribution $W(\lambda = 2241.74, \gamma = 1)$ and $n_{\text{sim}} = 500$ simulated datasets based on data without treatment-covariate interactions (primary biliary cirrhosis dataset)). The solid line represents the mean calibration curve, the outer dotted lines represent the 2.5th and 97.5th percentile of the calibration curve. The black diagonal line corresponds to perfect calibration.

(a) 30% censoring, $N = 100$, (b) 30% censoring, $N = 400$,

(c) 60% censoring, $N = 100$, (d) 60% censoring, $N = 400$.

Abbreviations: Cox-PH - Cox proportional hazards model, RSF - Random survival forest.

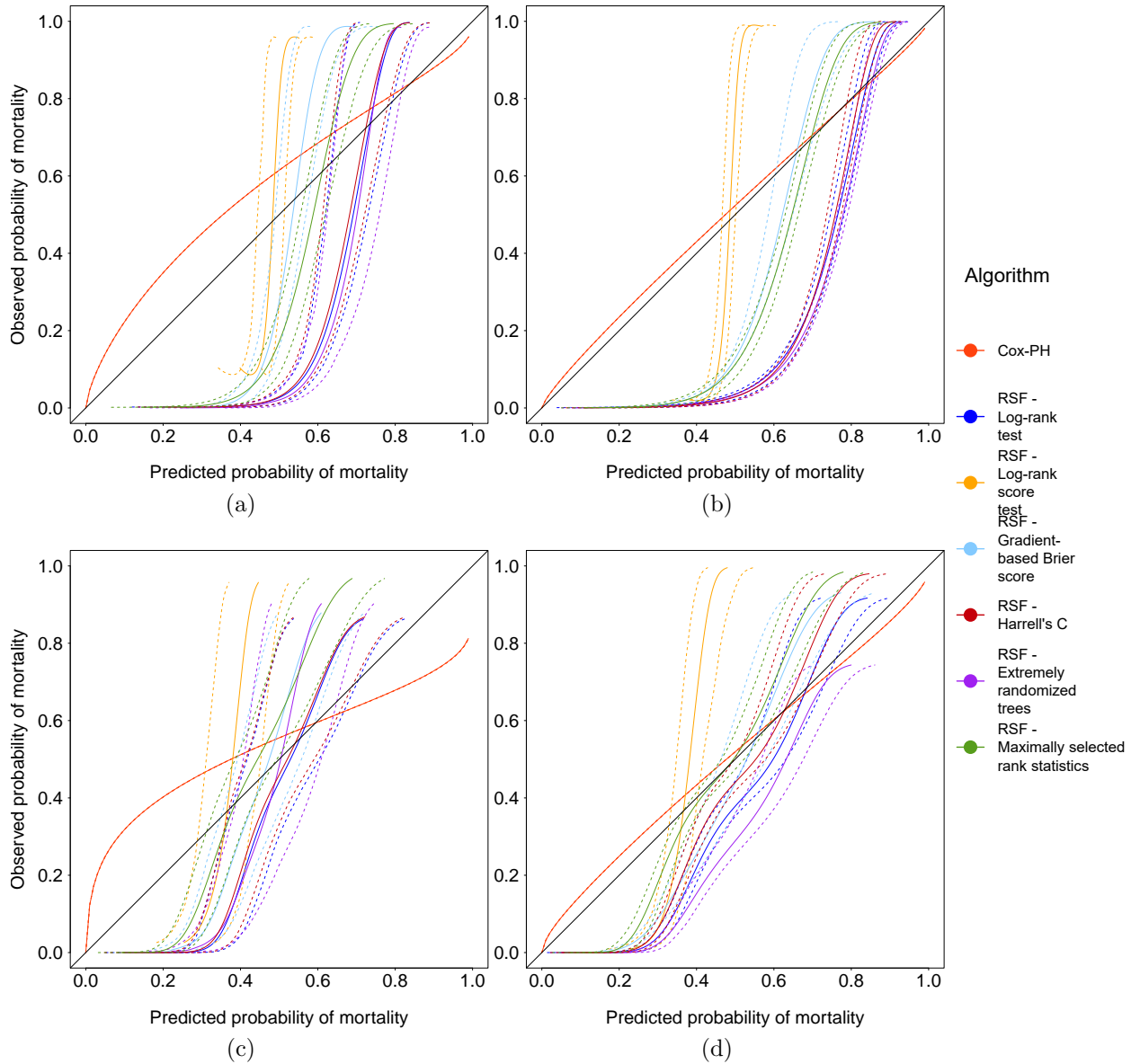


Fig. B.5b: Calibration curves for a nonproportional hazards setting (primary biliary cirrhosis dataset). Calibration curves at the median (50% quantile) survival time for a nonproportional hazards setting (Weibull survival time distribution $W(\lambda = 2241.74, \gamma \in \{2, 5\})$) and $n_{\text{sim}} = 500$ simulated datasets based on data without treatment-covariate interactions (primary biliary cirrhosis dataset). The solid line represents the mean calibration curve, the outer dotted lines represent the 2.5th and 97.5th percentile of the calibration curve. The black diagonal line corresponds to perfect calibration.

(a) 30% censoring, $N = 100$, (b) 30% censoring, $N = 400$,

(c) 60% censoring, $N = 100$, (d) 60% censoring, $N = 400$.

Abbreviations: Cox-PH - Cox proportional hazards model, RSF - Random survival forest.

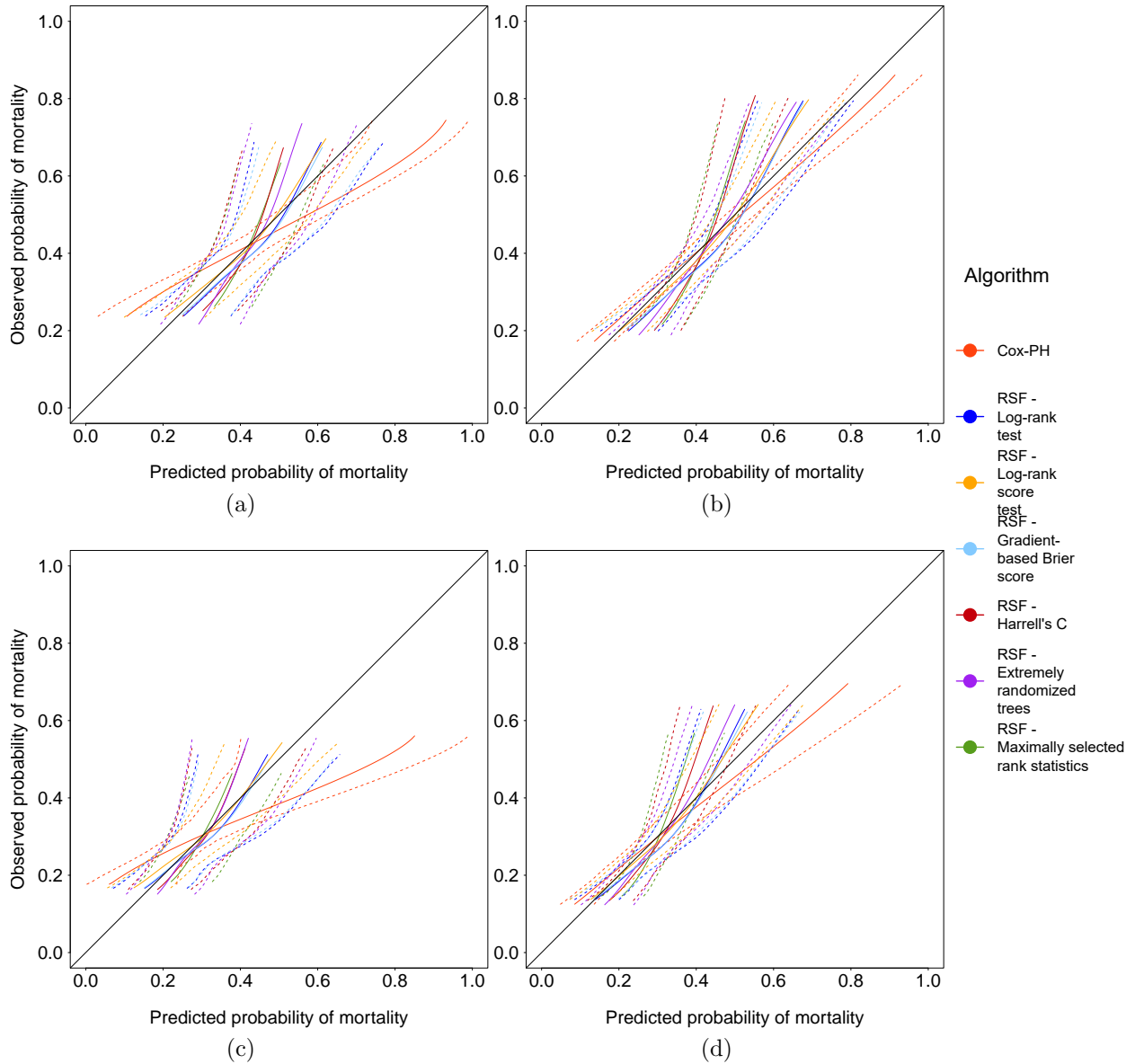


Fig. B.6a: Calibration curves for a proportional hazards setting (prostate cancer dataset). Calibration curves at the median (50% quantile) survival time for a proportional hazards setting (Weibull survival time distribution $W(\lambda = 2241.74, \gamma = 1)$) and $n_{\text{sim}} = 500$ simulated datasets based on data with three treatment-covariate interactions (prostate cancer dataset). The solid line represents the mean calibration curve, the outer dotted lines represent the 2.5th and 97.5th percentile of the calibration curve. The black diagonal line corresponds to perfect calibration.

(a) 30% censoring, $N = 100$, (b) 30% censoring, $N = 400$,

(c) 60% censoring, $N = 100$, (d) 60% censoring, $N = 400$.

Abbreviations: Cox-PH - Cox proportional hazards model, RSF - Random survival forest.

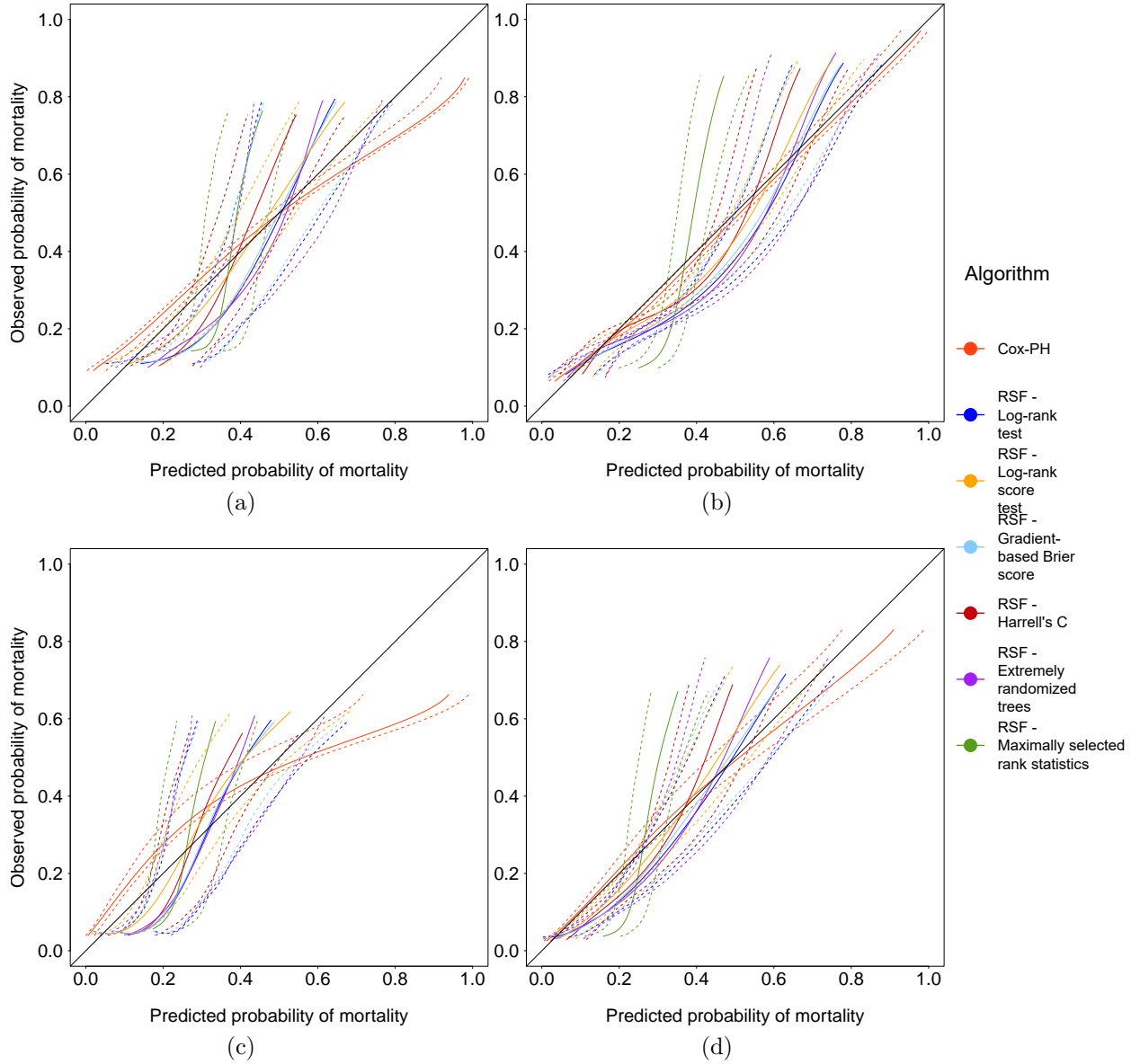


Fig. B.6b: Calibration curves for a nonproportional hazards setting (prostate cancer dataset). Calibration curves at the median (50% quantile) survival time for a nonproportional hazard setting (Weibull survival time distribution $W(\lambda = 39.2, \gamma \in \{2, 5\})$) and $n_{\text{sim}} = 500$ simulated datasets based on data with three treatment-covariate interactions (prostate cancer dataset). The solid line represents the mean calibration curve, the outer dotted lines represent the 2.5th and 97.5th percentile of the calibration curve. The black diagonal line corresponds to perfect calibration. (a) 30% censoring, $N = 100$, (b) 30% censoring, $N = 400$, (c) 60% censoring, $N = 100$, (d) 60% censoring, $N = 400$.

Abbreviations: Cox-PH - Cox proportional hazards model, RSF - Random survival forest.

Table C.1: Overview of currently available splitting rules for the RSF in the R packages `randomForestSRC` (Ishwaran et al., 2008) and `ranger` (Wright et al., 2023) compared in the simulation study.

Splitting rule	Notes	Recommendations/drawbacks	Abbreviation in R package	Availability
Log-rank test	<ul style="list-style-type: none"> • standard split criterion, most widely used 	<ul style="list-style-type: none"> + log-rank and log-rank score splitting almost always have the lowest prediction error but poor performance in data with high censoring rates + stable/preferable in noisy scenarios (Ishwaran et al., 2008; Schmid et al., 2016) – biased, i.e. favors splitting variables with many possible splits (Wright et al., 2016) – preference for more unbalanced splits (“end-cut preference”)(Schmid et al., 2016) – less suitable for small-scale clinical trials and high censoring rates (Schmid et al., 2016) 	logrank	<code>randomForestSRC</code> <code>ranger</code>
Log-rank score (Hothorn and Lausen, 2003)	<ul style="list-style-type: none"> • a standardized log-rank statistic 	<ul style="list-style-type: none"> + log-rank and log-rank score splitting almost always have the lowest prediction error but poor performance in data with high censoring rates, stable in presence of noise variables (Ishwaran et al., 2008) 	logrankscore	<code>randomForestSRC</code>
Gradient-based (global non-quantile) Brier score		<ul style="list-style-type: none"> + preferable to log-rank splitting when censoring depends strongly on the covariates (more robust) (Ishwaran and Lu, 2019) 	bs.gradient	<code>randomForestSRC</code>
Harrell’s C (Schmid et al., 2016)	<ul style="list-style-type: none"> • Harrell’s C (C index) most common performance measure for RSF \rightarrow overcomes discrepancy between node splitting and model evaluation 	<ul style="list-style-type: none"> + recommend it for smaller scale clinical trials and if censoring is high + has a lower end-cut preference than the log-rank statistic – recommend log-rank test for large-scale (omics) studies (Schmid et al., 2016) 	C	<code>ranger</code>
Extremely randomized trees (Geurts et al., 2006)	<ul style="list-style-type: none"> • strong randomization of variable and cut-point choices while splitting 	<ul style="list-style-type: none"> + main strength: computational efficiency (Geurts et al., 2006) 	extratrees	<code>ranger</code>
Maximally selected rank statistics (Wright et al., 2016)	<ul style="list-style-type: none"> • splitting variables are compared on the p-value scale 	<ul style="list-style-type: none"> + unbiased in case of informative dichotomous and uninformative categorical variables with more possible splits 	maxstat	<code>ranger</code>

Supplementary Material C: Additional theoretical information

Computation of the C index for the Cox and Random survival forest model

The C index, a time range measure, can be obtained from the Cox regression and RSF models as follows. For a Cox model

$$h(t) = h_0(t) \exp(\beta_1 x_1 + \dots + \beta_p x_p)$$

with baseline survival function $h_0(t)$ and regression coefficients $\beta \in \mathbb{R}^p$, and unique ordered survival times t_1, \dots, t_m , at each uncensored survival time, the rank of the predicted outcome $\hat{h}_i(t)$ for the considered subject i who experienced the event is compared to all $\hat{h}_j(t), j \neq i$ where individuals j had a longer survival time. The C index can thus be written as:

$$\Pr(\hat{h}_i > \hat{h}_j | t_i < t_j) = \frac{\sum_i (R_i - 1)}{\sum_i (N_i - 1)}, \quad i, j \in \{1, \dots, m\}, i \neq j$$

where R_i is the rank of individual i with survival time t_i , N_i the number at risk at time t_i , and thus $N_i - 1$ the number of individuals who can be compared with i (Kremers and von Liebzig, 2007).

For the RSF model, the C index is computed based on the patient-specific predictions of the ensemble mortality in the terminal nodes of each tree. For this we first consider the out-of-bag (oob) ensemble estimator of the cumulative hazard function (CHF) at time t for patient i , $H_i^{oob}(t)$. It is given by the average prediction of the n_{tree_i} trees for which the sample was not part of the bootstrap sample for building the tree (Ishwaran et al., 2021):

$$H_i^{oob}(t) = \frac{1}{n_{\text{tree}_i}} \sum_{b \in n_{\text{tree}_i}} H_b(t|\mathbf{X})$$

where $H_b(t|\mathbf{X})$ is the CHF predicted in the terminal node of the b th tree for the covariate vector $\mathbf{X} \in \mathbb{R}^p$ of patient i at time t . The out-of-bag ensemble mortality for each patient $i = 1, \dots, n$ is then estimated as the sum of the oob CHF estimates over all unique event times t_1, \dots, t_m in the training data (Ishwaran et al., 2021):

$$M_i^{oob} = \sum_{j=1}^m H_i^{oob}(t_j)$$

The C index is the proportion of concordant pairs among all pairs for which the decision can be made. If $M_{i_1}^{oob} > M_{i_2}^{oob}$ and patient i_1 has the shorter event time compared to patient i_2 or vice versa, the pair is concordant. The closer C index estimates are to 1 the better.

References

- Austin, P., Harrell, F., and Klaveren, D. (2020). Graphical calibration curves and the integrated calibration index (ICI) for survival models. *Statistics in Medicine*, 39:.
- Ballarini, N. M., Thomas, M., Rosenkranz, G. K., and Bornkamp, B. (2021). subtee: An R package for subgroup treatment effect estimation in clinical trials. *Journal of Statistical Software*, 99(14):1–17.
- Baralou, V., Kalpourtzi, N., and Touloumi, G. (2022). Individual risk prediction: comparing Random Forests with Cox proportional-hazards model by a simulation study. *Biometrical Journal*, 65:.
- Bell, E., Pugh, S., McElroy, J., Gilbert, M., Mehta, M., Klimowicz, A., Magliocco, A., Bredel, M., Robe, P., Grosu, A., Stupp, R., Curran, W., Becker, A., Salavaggione, A., Barnholtz-Sloan, J., Aldape, K., Blumenthal, D., Brown, P., Glass, J., Souhami, L., Lee, R., Brachman, D., Flickinger, J., Won, M., and Chakravarti, A. (2017). Molecular-based recursive partitioning analysis model for glioblastoma in the temozolomide era: A correlative analysis based on nrg oncology rtog 0525. *JAMA Oncology*, 3.
- Bender, R., Augustin, T., and Blettner, M. (2005). Generating survival times to simulate Cox proportional hazards models. *Statistics in Medicine*, 24:1713–23.
- Boehmke, B. and Greenwell, B. (2019). *Hands-On Machine Learning with R*. Chapman & Hall/CRC, The R Series, 1 edition.
- Brilleman, S. and Gasparini, A. (2022). simsurv: Simulate Survival Data. CRAN. <https://CRAN.R-project.org/package=simsurv>.
- Byar, D. P. and Green, S. B. (1980). The choice of treatment for cancer patients based on covariate information. *Bulletin du Cancer*, 67(4):477–490.
- Carbone, M., Sharp, S., Flack, S., Paximadas, D., Spiess, K., Adgey, C., Griffiths, L., Lim, R., Trembling, P., Lynch, K., Wareham, N., Aldersley, M., Bathgate, A., Burroughs, A., Heneghan, M., Neuberger, J., D, T., Hirschfield, G., Cordell, H., and Mells, G. (2015). The UK-PBC risk scores: Derivation and validation of a scoring system for long-term prediction of end-stage liver disease in primary biliary cirrhosis. *Hepatology*, 63:.
- Carey, W. D. (1980). Nonhomogeneous copper distribution in primary biliary cirrhosis. *Cleveland Clinic quarterly*, 47(2):101–107.
- Chowdhury, M., Naeem, I., Quan, H., Leung, A., Sikdar, K., O’Beirne, M., and Turin, T. (2022). Prediction of hypertension using traditional regression and machine learning models: a systematic review and meta-analysis. *PLOS ONE*, 17:e0266334.
- Chowdhury, M. Z. I., Leung, A. A., Walker, R., Sikdar, K. C., O’Beirne, M., Quan, H., and Turin, T. C. (2023). A comparison of machine learning algorithms and traditional regression-based statistical modeling for predicting hypertension incidence in a Canadian population. *Scientific Reports*, 13:13.
- Cohen, J. D., Li, L., Wang, Y., Thoburn, C., Afsari, B., Danilova, L., Douville, C., Javed, A. A., Wong, F., Mattox, A., Hruban, R. H., Wolfgang, C. L., Goggins, M. G., Molin, M. D., Wang, T.-L., Roden, R., Klein, A. P., Ptak, J., Dobbryn, L., Schaefer, J., Silliman, N., Popoli, M., Vogelstein, J. T., Browne, J. D., Schoen, R. E., Brand, R. E., Tie, J., Gibbs, P., Wong, H.-L., Mansfield, A. S., Jen, J., Hanash, S. M., Falconi, M., Allen, P. J., Zhou, S., Bettegowda, C., Diaz, L. A., Tomasetti, C., Kinzler, K. W., Vogelstein, B., Lennon, A. M., and Papadopoulos, N. (2018). Detection and localization of surgically resectable cancers with a multi-analyte blood test. *Science*, 359(6378):926–930.
- Collins, G., De Groot, J., Dutton, S., Omar, O., Shanyinde, M., Tajar, A., Voysey, M., Wharton, R., Yu, L.-Y., Moons, K., and Altman, D. (2014). External validation of multivariable prediction models: A systematic review of methodological conduct and reporting. *BMC medical research methodology*, 14:40.
- Collins, G., Mallett, S., Omar, O., and Yu, L. (2011). Developing risk prediction models for type 2 diabetes: a systematic review of methodology and reporting. *BMC Medicine*, 9(1):103.
- Cook, N. (2007). Use and misuse of the receiver operating characteristic curve in risk prediction. *Circulation*, 115:928–35.
- Cox, D. R. (1972). Regression models and life-tables. *Journal of the Royal Statistical Society. Series B (Methodological)*, 34(2):187–220.
- Datema, F., Moya, A., Krause, P., Bäck, T., Willmes, L., Langeveld, T., Baatenburg de Jong, R., and Blom, H. (2012). Novel head and neck cancer survival analysis approach: Random

- Survival Forests versus Cox proportional hazards regression. *Head Neck*, 34:50–8.
- Dickson, E. R., Grambsch, P. M., Fleming, T. R., Fisher, L. D., and Langworthy, A. L. (1989). Prognosis in primary biliary cirrhosis: Model for decision making. *Hepatology*, 10:.
- Du, M., Haag, D., Lynch, J., and Mittinty, M. (2020). Comparison of the tree-based machine learning algorithms to cox regression in predicting the survival of oral and pharyngeal cancers: Analyses based on seer database. *Cancers*, 12(10):2802.
- Efron, B. and Tibshirani, R. (1997). Improvements on cross-validation: The .632+ bootstrap method. *Journal of the American Statistical Association*, 92:548–560.
- Elsevier (2022). ClinicalPath: Evidence-based Oncology Decision Support and Analytics for Cancer Care. Elsevier, January 7, 2025, <https://www.elsevier.com/solutions/clinicalpath>.
- Farhadian, M., Karsidani, S., Mozayanimonfared, A., and Mahjub, H. (2021). Risk factors associated with major adverse cardiac and cerebrovascular events following percutaneous coronary intervention: a 10-year follow-up comparing Random Survival Forest and Cox proportional-hazards model. *BMC Cardiovascular Disorders*, 21(38):.
- Gerds, T. A. pec: Prediction Error Curves for Risk Prediction Models in Survival Analysis. CRAN, September 10, 2024, <https://CRAN.R-project.org/package=pec>.
- Geurts, P., Ernst, D., and Wehenkel, L. (2006). Extremely randomized trees. *Machine Learning*, 63:3–42.
- Goet, J., Perez, C., Harms, M., Floreani, A., Cazzagon, N., Bruns, T., Prechter, F., Dalekos, G., Verhelst, X., Gatselis, N., Lindor, K., Lammers, W., Gulamhusein, A., Reig, A., Carbone, M., Nevens, F., Hirschfield, G., Van der Meer, A., Buuren, H., and Parés, A. (2021). A comparison of prognostic scores (Mayo, UK-PBC, and GLOBE) in primary biliary cholangitis. *American Journal of Gastroenterology*, page .
- Goldstein, B., Navar, A., Pencina, M., and Ioannidis, J. (2017). Opportunities and challenges in developing risk prediction models with electronic health records data: A systematic review. *Journal of the American Medical Informatics Association*, 24(1):198–208.
- Graf, E., Schmoor, C., Sauerbrei, W., and Schumacher, M. (1999). Assessment and comparison of prognostic classification schemes for survival data. *Statistics in Medicine*, 18 17-18:2529–45.
- Grambsch, P. M. and Therneau, T. M. (1994). Proportional hazards tests and diagnostics based on weighted residuals. *Biometrika*, 81(3):515–526.
- Greenberg, B. G. and Sen, P. K. (1985). *Biostatistics: Statistics in Biomedical, Public Health and Environmental Sciences: the Bernard G. Greenberg volume*. Elsevier Science Pub. Co. (North-Holland).
- Guo, Y., Yonamine, S., Ma, C., Stewart, J., Acharya, N., Arnold, B., McCulloch, C., and Sun, C. (2023). Developing and validating models to predict progression to proliferative diabetic retinopathy. *Ophthalmology Science*, 3:100276.
- Harrell, F. E., Califf, R. M., Pryor, D. B., Lee, K. L., and Rosati, R. A. (1982). Evaluating the yield of medical tests. *JAMA*, 247 18:2543–6.
- Harrell, F. E., Lee, K. L., and Mark, D. B. (1996). Multivariable prognostic models: Issues in developing models, evaluating assumptions and adequacy, and measuring and reducing errors. *Statistics in Medicine*, 15(4):361–387.
- Hartman, N., Kim, S., He, K., and Kalbfleisch, J. (2023). Pitfalls of the concordance index for survival outcomes. *Statistics in Medicine*, 42:.
- Hilsenbeck, S. G., Ravdin, P. M., de Moor, C. A., Chamness, G. C., Osborne, C. K., and Clark, G. M. (1998). Time-dependence of hazard ratios for prognostic factors in primary breast cancer. *Breast cancer research and treatment*, 52(1-3):227 – 237.
- Hothorn, T. and Lausen, B. (2003). On the exact distribution of maximally selected rank statistics. *Computational Statistics & Data Analysis*, 43(2):121–137.
- Hueting, T. A., van Maaren, M. C., Hendriks, M. P., Koffijberg, H., and Siesling, S. (2022). The majority of 922 prediction models supporting breast cancer decision-making are at high risk of bias. *Journal of Clinical Epidemiology*, 152:238–247.
- Ishwaran, H., Kogalur, U., Blackstone, E., and Lauer, M. (2008). Random Survival Forests. *Annals of Applied Statistics*, 2:841–60.
- Ishwaran, H. and Kogalur, U. B. (2023). randomForestSRC: Fast Unified Random Forests for Survival, Regression, and Classification (RF-SRC). CRAN. <https://CRAN.R-project.org/package=randomForestSRC>.

- Ishwaran, H., Lauer, M. S., Blackstone, E. H., Lu, M., and Kogalur, U. B. (2021). randomForestSRC: random survival forests vignette. *Random Survival Forests*. <http://randomforestsrc.org/articles/survival.html>.
- Ishwaran, H. and Lu, M. (2019). *Random Survival Forests*, pages 1–13.
- Jiang, B., Zhang, X., and Cai, T. (2008). Estimating the confidence interval for prediction errors of Support Vector Machine classifiers. *Journal of Machine Learning Research*, 9:521–540.
- Kawakami, E., Tabata, J., Yanaihara, N., Ishikawa, T., Koseki, K., Iida, Y., Saito, M., Komazaki, H., Shapiro, J. S., Goto, C., Akiyama, Y., Saito, R., Saito, M., Takano, H., Yamada, K., and Okamoto, A. (2019). Application of artificial intelligence for preoperative diagnostic and prognostic prediction in epithelial ovarian cancer based on blood biomarkers. *Clinical Cancer Research*, 25(10):3006–3015.
- Kim, D. W., Lee, S., Kwon, S., Nam, W., Cha, I.-H., and Kim, H. (2019). Deep learning-based survival prediction of oral cancer patients. *Scientific Reports*, 9:6994.
- Kremers, W. K. and von Liebig, W. J. (2007). Concordance for survival time data: fixed and time-dependent covariates and possible ties in predictor and time. Mayo Foundation for Medical Education and Research, <https://www.mayo.edu/research/documents/biostat-80pdf/DOC-10027891>.
- Lammers, W. J., Hirschfield, G. M., Corpechot, C., Nevens, F., Lindor, K. D., Janssen, H. L., Floreani, A., Ponsioen, C. Y., Mayo, M. J., Invernizzi, P., Battezzati, P. M., Parés, A., Burroughs, A. K., Mason, A. L., Kowdley, K. V., Kumagi, T., Harms, M. H., Trivedi, P. J., Poupon, R., Cheung, A., Lleo, A., Caballeria, L., Hansen, B. E., and van Buuren, H. R. (2015). Development and validation of a scoring system to predict outcomes of patients with primary biliary cirrhosis receiving ursodeoxycholic acid therapy. *Gastroenterology*, 149(7):1804–1812.e4.
- Lin, J., Yin, M., Liu, L., Gao, J., Yu, C., Liu, X., Xu, C., and Zhu, J. (2022). The development of a prediction model based on random survival forest for the postoperative prognosis of pancreatic cancer: A seer-based study. *Cancers*, 14(19).
- Mahar, A., Compton, C., Halabi, S., Hess, K., Weiser, M., and Groome, P. (2017). Personalizing prognosis in colorectal cancer: A systematic review of the quality and nature of clinical prognostic tools for survival outcomes. *Journal of Surgical Oncology*, 116:969–982.
- Mallett, S., Royston, P., Waters, R., Dutton, S., and Altman, D. (2010). Reporting performance of prognostic models in cancer: A review. *BMC Medicine*, 8:21.
- McLernon, D. J., Giardiello, D., Van Calster, B., Wynants, L., van Geloven, N., van Smeden, M., Therneau, T., Steyerberg, E. W., and topic groups 6 and 8 of the STRATOS Initiative (2023). Assessing performance and clinical usefulness in prediction models with survival outcomes: practical guidance for Cox proportional hazards models. *Annals of Internal Medicine*, 176(1):105–114.
- Miao, F., Cai, Y., Zhang, Y.-X., Li, Y., and Zhang, Y. (2015). Risk prediction of one-year mortality in patients with cardiac arrhythmias using Random Survival Forest. *Computational and Mathematical Methods in Medicine*, page .
- Miller, M., Shih, L., and Kolachalama, V. (2023). Machine learning in clinical trials: a primer with applications to neurology. *Neurotherapeutics*, 20(4):1066–1080.
- Moncada-Torres, A., van Maaren, M., Hendriks, M., Siesling, S., and Geleijnse, G. (2021). Explainable machine learning can outperform Cox regression predictions and provide insights in breast cancer survival. *Scientific Reports*, 11:1–13.
- Moons, K. G. M., Altman, D. G., Reitsma, J. B., Ioannidis, J. P. A., Macaskill, P., Steyerberg, E. W., Vickers, A. J., Ransohoff, D. F., and Collins, G. S. (2015). Transparent reporting of a multivariable prediction model for individual prognosis or diagnosis (TRIPOD): Explanation and elaboration. *Annals of Internal Medicine*, 162(1):W1–W73.
- Moons, K. G. M., Kengne, A. P., Woodward, M., Royston, P., Vergouwe, Y., Altman, D. G., and Grobbee, D. E. (2012). Risk prediction models: I. development, internal validation, and assessing the incremental value of a new (bio)marker. *Heart*, 98(9):683–690.
- Morris, T. P., White, I. R., and Crowther, M. J. (2019). Using simulation studies to evaluate statistical methods. *Statistics in Medicine*, 38:2074 – 2102.
- Murmu, A. and Györfy, B. (2024). Artificial intelligence methods available for cancer research. *Frontiers of Medicine*, 18:778–797.
- Nguyen, K. D., Sundaram, V., and Ayoub, W. S. (2014). Atypical causes of cholestasis. *World Journal of Gastroenterology*, 20(28):9418–9426.

- Omurlu, I., Ture, M., and Tokatli, F. (2009). The comparisons of Random Survival Forests and Cox regression analysis with simulation and an application related to breast cancer. *Expert Systems with Applications*, 36:8582–8588.
- Peduzzi, P., Concato, J., Feinstein, A. R., and Holford, T. R. (1995). Importance of events per independent variable in proportional hazards analysis i. background, goals, and general strategy. *Journal of Clinical Epidemiology*, 48(12):1503–1510.
- Phung, M. T., Tin, S. T., and Elwood, J. M. (2019). Prognostic models for breast cancer: a systematic review. *BMC Cancer*, 19(230).
- Poupon, R. (1991). La cirrhose biliaire primitive [primary biliary cirrhosis]. *Schweizerische medizinische Wochenschrift*, 121(20):727–732.
- Qiu, X., Gao, J., Yang, J., Hu, J., Hu, W., Kong, L., and Lu, J. (2020). A comparison study of machine learning (Random Survival Forest) and classic statistic (Cox proportional hazards) for predicting progression in high-grade glioma after proton and carbon ion radiotherapy. *Frontiers in Oncology*, 10:551420.
- Ramos, P., Fuentes Guzman, D., Mota, A., Saavedra, D., Rodrigues, F., and Louzada, F. (2024). Sampling with censored data: a practical guide. arXiv. <https://arxiv.org/abs/2011.08417>.
- fedesoriano. Cirrhosis prediction dataset. kaggle, September 10, 2024, <https://www.kaggle.com/datasets/fedesoriano/cirrhosis-prediction-dataset>.
- Fleming, Thomas R. and Harrington, David P. (2005). *Counting processes and survival analysis*. Wiley.
- University of Massachusetts (1980). Primary biliary cirrhosis study. UMASS, September 10, 2024, <https://www.umass.edu/statdata/statdata/stat-survival.html>.
- Vanderbilt Department of Biostatistics. Mayo Clinic primary biliary cirrhosis data. Vanderbilt Biostatistics Datasets, September 10, 2024, <https://hbiostat.org/data/>.
- Ripley, B., Venables, B., Bates, D. M., Hornik, K., Gebhardt, A., and Firth, D. (2024). MASS: Support Functions and Datasets for Venables and Ripley’s MASS. CRAN. <https://CRAN.R-project.org/package=MASS>.
- Royston, P. and Sauerbrei, W. (2004). A new approach to modelling interaction between treatment and continuous covariates in clinical trials by using fractional polynomials. *Statistics in Medicine*, 23:2509–25.
- Ruyssinck, J., van der Hertten, J., Houthoofd, R., Ongenae, F., Couckuyt, I., Gadeyne, B., Colpaert, K., Decruyenaere, J., De Turck, F., and Dhaene, T. (2016). Random survival forests for predicting the bed occupancy in the intensive care unit. *Computational and Mathematical Methods in Medicine*, 2016.
- Salaspuro, M., Pikkarainen, P., Sipponen, P., Vuori, E., and Miettinen, T. (1981). Hepatic copper in primary biliary cirrhosis: biliary excretion and response to penicillamine treatment. *Gut*, 22(11):901–6.
- Sarica, A., Aracri, F., Bianco, M. G., Arcuri, F., Quattrone, A., and Quattrone, A. (2023). Explainability of Random Survival Forests in predicting conversion risk from mild cognitive impairment to Alzheimer’s disease. *Brain Informatics*, 10:31.
- Scheuer, P. (1989). Primary biliary cirrhosis. *Proceedings of the Royal Society of Medicine*, 60(12):1257–1260.
- Schmid, M., Wright, M. N., and Ziegler, A. (2016). On the use of Harrell’s C for clinical risk prediction via Random Survival Forests. *Expert Systems with Applications*, 63:450–459.
- Sebastiani, G. and Alberti, A. (2006). Non invasive fibrosis biomarkers reduce but not substitute the need for liver biopsy. *World Journal of Gastroenterology*, 12:3682–94.
- Spooner, A., Chen, E., Sowmya, A., Sachdev, P., Kochan, N., Trollor, J., and Brodaty, H. (2020). A comparison of machine learning methods for survival analysis of high-dimensional clinical data for dementia prediction. *Scientific Reports*, 10:.
- Spytek, M., Krzyzinski, M., Langbein, S., Baniecki, H., Kapsner, L., and Biecek, P. (2024). survex: Explainable Machine Learning in Survival Analysis. CRAN. <https://CRAN.R-project.org/package=survex>.
- Steyerberg, E., Moons, K., van der Windt, D., Hayden, J., Perel, P., Schroter, S., Riley, R., Hemingway, H., and Altman, D. (2013). Prognosis research strategy (progress) 3: Prognostic model research. *PLoS medicine*, 10:e1001381.
- Steyerberg, E., Vickers, A., Cook, N., Gerds, T., Gonen, M., Obuchowski, N., Pencina, M., and Kattan, M. (2010). Assessing the performance of prediction models a framework for traditional and novel measures. *Epidemiology*, 21:128–38.

- Therneau, T. and Grambsch, P. (2000). *Modeling Survival Data: Extending the Cox Model*, volume 48. Springer.
- Therneau, T. M. and Lumley, T. (2024). survival: Survival Analysis. CRAN. <https://CRAN.R-project.org/package=survival>.
- Van Calster, B., McLernon, D., van Smeden, M., Wynants, L., and Steyerberg, E. (2019). Calibration: the achilles heel of predictive analytics. *BMC Medicine*, 17(1):230.
- Vickers, A. J. and Cronin, A. M. (2010). Traditional statistical methods for evaluating prediction models are uninformative as to clinical value: towards a decision analytic framework. *Seminars in Oncology*, 37(1):31–38.
- Vittinghoff, E. and McCulloch, C. E. (2006). Relaxing the rule of ten events per variable in logistic and cox regression. *American Journal of Epidemiology*, 165(6):710–718.
- Wahl, S., Boulesteix, A.-L., Zierer, A., Thorand, B., and Wiel, M. (2016). Assessment of predictive performance in incomplete data by combining internal validation and multiple imputation. *BMC Medical Research Methodology*, 16:144.
- Weber, L., Saelens, W., Cannoodt, R., Sonesson, C., Hapfelmeier, A., Gardner, P., Boulesteix, A.-L., Saeys, Y., and Robinson, M. (2019). Essential guidelines for computational method benchmarking. *Genome Biology*, 20(1):125.
- Weissler, E. H., Naumann, T., Andersson, T., Ranganath, R., Elemento, O., Luo, Y., Freitag, D. F., Benoit, J., Hughes, M. C., Khan, F. M., Slater, P., Shameer, K., Roe, M., Hutchison, E. R., Kollins, S. H., Broedl, U. C., Meng, Z., Wong, J. L., Curtis, L., Huang, E., and Ghassemi, M. (2021). The role of machine learning in clinical research: transforming the future of evidence generation. *Trials*, 22(1):537.
- Wilson, P. W. F., D’Agostino, R. B., Levy, D., Belanger, A. M., Silbershatz, H., and Kannel, W. B. (1998). Prediction of coronary heart disease using risk factor categories. *Circulation*, 97(18):1837–1847.
- Wright, M. N., Dankowski, T., and Ziegler, A. (2016). Unbiased split variable selection for Random Survival Forests using maximally selected rank statistics. *Statistics in Medicine*, 36:1272 – 1284.
- Wright, M. N., Wager, S., and Probst, P. (2023). ranger: A Fast Implementation of Random Forests. CRAN. <https://CRAN.R-project.org/package=ranger>.
- Wynants, L., Kent, D., Timmerman, D., Lundquist, C., and Van Calster, B. (2019). Untapped potential of multicenter studies: a review of cardiovascular risk prediction models revealed inappropriate analyses and wide variation in reporting. *Diagnostic and Prognostic Research*, 3.
- Zhang, F., Jia, J., Cui, R., Wang, B., and Wang, H. (2002). Clinical features of forty patients with primary biliary cirrhosis. *Chinese Medical Journal*, 115(6):904–908.
- Zhang, Z., Li, J., He, T., and Ding, J. (2020). Bioinformatics identified 17 immune genes as prognostic biomarkers for breast cancer: Application study based on artificial intelligence algorithms. *Frontiers in Oncology*, 10.
- Zhou, Y. and Mcardle, J. J. (2015). Rationale and applications of survival tree and survival ensemble methods. *Psychometrika*, 80(3):811 – 833.